Electrochemical characterization of platinum based catalysts for fuel cell applications

By

Adonisi Thobeka

A thesis submitted in fulfilment of the requirements for the degree of Magister Scientiae in the Department of Chemistry, University of the Western Cape.

Supervisor: Dr L. Khotseng

November 2012

DECLARATION

I declare that "Electrochemical characterization of platinum based catalysts for fuel cell applications" is my own work, that is has not been submitted for any degree or examination in any other university, and that all the sources I have used or quoted have been indicated and acknowledged by complete references.

Adonisi Thobeka November 2012

Signed:……

ABSTRACT

Fuel cells convert chemical energy from a fuel into electricity through chemical reaction with oxygen. This possesses some challenges like slow oxygen reduction reaction (ORR), overpotential, and methanol fuel cross over in a direct methanol fuel cell (DMFC). These challenges cause inefficiency and use of higher amounts of the expensive platinum catalyst. Several binary catalysts with better ORR activity have been reported. In this study we investigate the best catalyst with better ORR and MOR performances and lower over-potentials for PEMFC and DMFC applications by comparing the in-house catalysts (10%Pt/C, 20%Pt/C, 30%Pt15%Ru/C, 40%Pt20%Ru/C, 30%PtCo/C, 20%Pt20%Cu/C and 20%PtSn/C) with the commercial platinum based catalysts (10%Pt/C, 20%Pt/C, 20%Pt10%Ru/C, 20%PtCo/C, 20%PtCu/C and 20%PtSn/C) using the cyclic voltammetry and the rotating disk electrode to determine their oxygen reduction reaction and methanol tolerance. HRTEM and XRD techniques were used to determine their particle size, arrangement and the atomic composition. It was observed that the 20%Pt/C in-house catalyst gave the best ORR activity and higher methanol oxidation current peaks compared to others catalysts followed by 20%Pt10%Ru/C commercial catalyst. The 20%PtCo/C commercial, 30%PtCo/C in-house and 20%PtSn/C in-house catalysts were found to be the most methanol tolerant catalysts making them the best catalysts for ORR in DMFC. It was observed that the ORR activity of 20%PtCo/C commercial and 30%PtCo/C in-house catalysts were enhanced when heat treated at 350 ^{0}C. From XRD and HRTEM studies, the particle sizes were between 2.72nm to 5.02nm with little agglomeration but after the heat treatment, the particles were nicely dispersed on the carbon support.

ACKNOWLEDGEMENTS

I would like to thank God for giving me the strength to continue with my work and finish, it is all because of His grace that I am where I am today.

Greatest thanks to my mother for the love, support and encouragement throughout my studies, I don't know where I would be if it wasn't for her.

Huge thanks to Prof. V.M. Linkov, Dr L. Khotseng and the staff of the South African Institute for Advanced materials for giving me the opportunity to conduct my research in the institute.

Mr A Josephs and Miss S. Botha (Electron microscopy unit, Department of physics, University of the Western Cape) for helping me with the High resolution transmission electron microscopy.

Dr R. Bucher (Materials Research Group, iThemba Labs) for helping me with the X-ray diffraction.

I would like to express my gratitude to the Laboratory technician Stanford for assisting me in the Lab.

NRF and TESP for their financial support

Lastly, Lynwill Martins for the help with the Rotating disk electrode and support throughout my studies not forgetting my colleagues for the support and encouragements.

TABLE OF CONTENTS

LIST OF FIGURES

LIST OF TABLES

ABBREVIATIONS

PEMFC	Proton Exchange Membrane fuel cell
DMFC	Direct methanol fuel cell
AFC	Alkaline fuel cell
PAFC	Phosphoric acid fuel cell
MCFC	Molten carbonate fuel cell
ORR	Oxygen reduction reaction
MOR	Methanol oxidation reaction
XRD	X-ray diffraction
HRTEM	Higher resolution transmission microscopy
CV	Cyclic voltammetry
RDE	Rotating disk electrode
ECSA	Electrochemical surface area
MA	Mass activity
SA	Specific activity
C	Coulomb

CHAPTER 1

INTRODUCTION: MOTIVATION AND OBJECTIVES OF THE STUDY

1.1. Background to fuel cell technology

The world energy demand is increasing every day as households, transportation and industries that use these energy increases. 86% of the energy sources that are used are fossil fuels and they are not environmental friendly [1]. Examples of such fossil fuels are coal, petroleum, and natural gases. These fossil fuels are available worldwide in one form or another. They release oxide gases into the atmosphere that causes ozone layer depletion and consequently global warming, rising sea levels, spills, leaks, and strip mining. Therefore there is a need to focus on renewable energy sources that do not pollute the environment, and reduce or stop the use of fossil fuels as energy source. Fuel cells have been found to be one of the technologies that are environmentally friendly as it produces only water and carbon dioxide as by-product and this is not poisonous to the environment because any carbon dioxide released is taken from the atmosphere by photosynthetic plants [1].

The use of fuel cells has a number of benefits including:

Clean Electricity –Fuel cells uses pure hydrogen and oxygen, as a result pure water is produced as a by-product. In some fuel cells carbon dioxide is produced but it is concentrated and can be readily recaptured, as opposed to being emitted into the atmosphere.

Distributed generation – Fuel cells are compatible and come in small sizes and can be placed in places where electricity is needed such as, commercial, industrial, and even transportation settings.

Dependability – Fuel cells have no moving parts or complicated machinery and so they are a source of electricity capable of operating for thousands of hours. In addition, they are very quiet and safe sources of electricity.

Efficiency – Fuel cells convert the energy stored within fossil fuels into electricity much more efficiently than traditional generation of electricity using combustion. This means that less fuel is required to produce the same amount of electricity [2].

Reliability & Maintenance – When compared to internal combustion engines, there are considerably less moving parts and these require less maintenance (no oil changes every 150 hours).

Very low noise and vibrations – few moving parts means all you will ever hear of a fuel cell is a compressor, blower or pump (think of the fan in a desktop computer).

Fuel flexibility – Different types of fuel cells can operate on a range of different fuels, e.g. Direct methanol fuel cell which uses methanol as the fuel.

Safety – Hydrogen is a safe fuel as long as appropriate safety procedures are followed, as they should with any fuel, [3].

The generation of energy is a challenge but if new energy sources can be investigated the energy generation is expected to change dramatically in the next twenty years. Fuel cells are the best energy devices for energy generation.

1.2. Rational for the research

The energy demand is increasing and fuel cells are found to be one of the devices that can help resolve the energy crisis and are environmental friendly [1]. However, there are some problems that are encountered in the use of fuel cells such as the high content of the expensive platinum (Pt) catalyst that is used for the fuel cell cathode electrodes due to the slowness of the reaction at the cathode side which results in overpotential losses of 0.3-0.4V under typical operating conditions. Pt supported on carbon black is widely used as an electro-catalyst for the ORR in fuel cells due to its high catalytic activity, selectivity, excellent durability and excellent chemical stability in the fuel cell environment. The cathode catalysts, also suffer from serious intermediate tolerance, anode crossover, poor stability in an electrochemical environment and the slow kinetics of oxygen reduction reaction on the best available Pt-based catalysts.

Fuel cells use a variety of fuels that are oxidized at the anode, such as hydrogen, methanol etc. Oxygen from air is used as an oxidant. They consist of three basic components namely the anode, cathode and the membrane. At the anode a fuel is oxidized to produce protons and electrons. The electrons migrate through the external circuit towards the cathode and the protons pass through the membrane towards the cathode. At the cathode oxygen adsorbs onto the Pt surface (see reaction 1.1) and is reduced. Oxygen adsorption breaks the O=O bond following the consecutive step (see reaction 1.2) on the Pt surface and forms adsorbed atomic O (see reaction 1.3), which further gains electrons in the consecutive steps (see reaction 1.4 and 1.5) forming water.

$$O_2 + Pt \rightarrow Pt(O_2) \qquad (1.1)$$

$$Pt(O_2) + H^+ + e^- \rightarrow Pt(HO_2) \quad (1.2)$$

$$Pt(HO_2) + H^+ + e^- \rightarrow H_2O + Pt(O) \quad (1.3)$$

$$Pt(O) + H^+ + e^- \rightarrow Pt(OH) \quad (1.4)$$

$$Pt(OH) + H^+ + e^- \rightarrow H_2O + Pt \quad (1.5)$$

The O=O bond may not be broken in the steps above, resulting in the formation of H_2O_2 as shown in reaction 1.6. The H_2O_2 could further be reduced to water or be a final product [4].

$$Pt(HO_2) + H^+ + e^- \rightarrow H_2O_2 + Pt \quad (1.6)$$

There are two possible reactions that can occur as follows; the four-electron transfer which is the electro-reduction of oxygen to water (see reaction 1.7), and the two-electron transfer, which is the electro-reduction of oxygen to hydrogen peroxide (see reaction 1.8). The two-electron transfer is less desirable because it is low in efficiency and generates hydrogen peroxide that is corrosive.

$$O_2 + 4e^- + 4H^+ \leftrightarrow 2H_2O \qquad E^0 = 1.23V \quad (1.7)$$

$$O_2 + 2e^- + 2H^+ \leftrightarrow 2H_2O_2 \qquad E^0 = 0.67V \quad (1.8)$$

The reduction potential of the four-electron transfer is higher than that of the two-electron transfer and this provides a thermodynamic driving force for the four-electron reaction. Even though the reduction potential of the four-electron transfer reaction is higher, the reaction is kinetically slow. The sluggish kinetics of the oxygen reduction reaction (ORR) are typically attributed to the strength of the O=O bond (498kJ/mol) that must be broken in the course of the reaction. Thus, a catalyst must be used, as it will lower the activation energy giving higher current densities at lower overpotentials increasing the ORR kinetics. It has been stated earlier that the formation of H_2O_2 is not desirable for the oxygen reduction reaction since it is low in efficiency and it is corrosive. Therefore, new catalysts are needed that will give higher ORR performances and reduce the platinum (Pt) amount used in order to reduce the cost associated with it. It is necessary to develop ORR catalysts more active than Pt to deal with the cost of Pt as well as the voltage losses. Platinum binary catalysts, Pt-M/C (M being the metal supported on C i.e. carbon black) for cathode catalysts have to be investigated for ORR. Incorporating a second metal to the Pt could contribute to the decreasing of the cost of Pt and also give better ORR activities.

1.3 Objectives for the study

The main objective of this study is to investigate the best cathode catalyst for ORR that will give better performances and activity as well as to study the catalysts of a PEMFC and DMFC, looking at the effect of fuel crossover on the activity of the catalysts.

The aims of this study include:

- Studying the effect of heat treatment on the morphology of the catalysts using the TEM and XRD physical characterization techniques.
- Studying the effect of alloying on the activity and fuel tolerance of the catalysts using the electrochemical means of characterization such as cyclic voltammetry and Rotating disk electrode.

1.4. Research outline

Chapter 2: Literature review

This chapter focuses on fuel cells as renewable energy devices. The types of fuel cells are discussed. It also gives emphasis on the oxygen reduction reaction occurring at the cathode and the electro-catalysts for ORR. The preparation and supports for these electro-catalysts is also reviewed.

Chapter 3: Methodology

This chapter describes the methods and materials used in this study. It describes in detail the physical and electrochemical characterization methods used in this study.

Chapter 4: Results and discussion

The physical and electrochemical characterizations of the catalysts focusing on the ORR activity of the catalysts are discussed in this chapter. The results for direct methanol fuel cells (DMFC) electro-catalysts as anode and cathode are also discussed.

Chapter 5: Conclusions and recommendations

This chapter concludes the overall work and gives future recommendations for the fuel cell catalysts.

CHAPTER 2

LITERATURE REVIEW

2.1 Overview of fuel cells

In 1838 Sir William Robert Grove developed a device which would combine hydrogen and oxygen to produce electricity called a fuel cell [5]. This device converts chemical energy from a fuel into electricity through a chemical reaction with oxygen as an oxidizing agent and will continue to produce electricity for as long as the fuel and an oxidant inputs are supplied. The fuel cells are classified according to the name of the fuel they use. The hydrogen fuel is the widely used fuel in fuel cells.

The fuel cell consists of three basic components, the anode which oxidizes the fuel into protons and electrons, cathode where oxygen is reduced and an electrolyte or membrane that allows charges to move between the two sides of the fuel cell. The electrons and protons are drawn from the anode to the cathode, producing direct current electricity, pure water and very small amounts of carbon dioxide. Fuel cells come in a variety of sizes and produce very small amounts of electricity, about 0.7 volt and so are placed in a series or parallel circuits called stacks, to increase the voltage and current output to meet an application's power generation requirements [6]. The energy efficiency of a fuel cell is generally between 40-60%, or up to 85% efficient if waste heat is captured for use. Figure 2.1 shows a schematic diagram of a fuel cell.

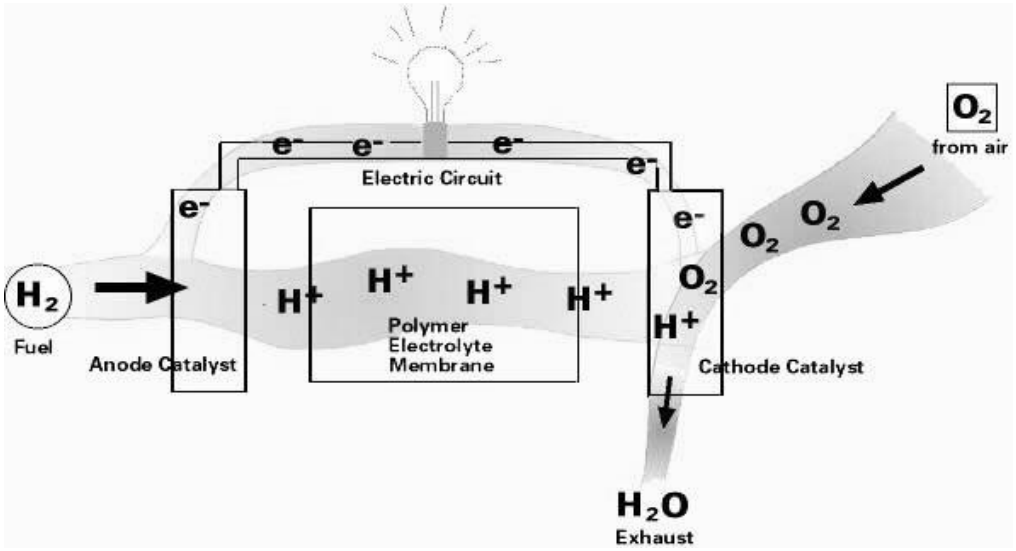

Figure 2.1: Basic fuel cell operation

There are different types of fuel cells. They are divided into low temperature fuel cell systems (Proton Exchange Membrane Fuel cell, Direct Methanol Fuel Cell, Alkaline Fuel Cell) and high temperature fuel cell systems (Molten Carbonate Fuel Cell, Solid Oxide Fuel Cell, Phosphoric acid fuel cell). Given below are the names and brief description of the types of fuel cells. This research focuses mainly on two different types of low temperature fuel cells namely; proton exchange membrane fuel cell (PEMFC) and direct methanol fuel cell (DMFC).

2.2 High temperature fuel cells

Solid Oxide Fuel Cell (SOFC): The SOFCs were first developed by Emil Baur and H Preis in 1930. They used zirconium, yttrium, cerium, lanthanum, and tungsten oxide as the preparation material [7]. The SOFC uses hydrogen and hydrocarbons such as natural gas and carbon monoxide as the fuel and uses air as an oxidant [8].Water is produced as the by-product in this fuel cell which means that it meets the requirements of an environmental friendly energy source. The SOFC operates at temperatures between 700 and 1000 ^{0}C. The high temperature of these fuel cells results in the use of solid materials for this fuel cell not liquid, more especially the electrolyte as it separates the two electrodes, ceramics are used. SOFC have a power output from 1kW to 2MW. The large amount of heat generated by the SOFC is usually utilized to drive secondary gas turbine in order to increase the efficiency. This fuel cell reaches efficiencies of up to 70% [9]. One of the challenge for the use of this fuel cell is the hydrogen storage which is a problem because hydrogen is a light gas and the hydrogen storage is still under research.

Molten Carbonate Fuel Cell (MCFC): The use of coal is no longer supported as it is not good for the environment but in the 1960s it was found that the fuel cells from coal are capable of working successfully. MCFCs are prepared directly on coal. Like the SOFC, MCFCs operate at high temperatures and due to that non-precious metals can be used as cathode and anode electro-catalysts [10]. The fuel that is used in this fuel cell is a ceramic due to the high temperatures. MCFCs have efficiencies reaching up to 50-60%. Because MCFCs operate at higher temperatures, around 650 ^{0}C, they are candidates for combined cycle applications, in which the exhaust heat is used to generate additional electricity. When waste heat is used, total thermal efficiencies can approach 85% [11].

Phosphoric Acid Fuel Cell (PAFC): This fuel cell uses Pt electro-catalysts as the anode and cathode catalysts. The fuel that this fuel cell uses is phosphoric acid which is contained in

Teflon-bonded silicon carbide matrix and porous carbon electrodes containing the platinum catalyst. This fuel cell is a high temperature fuel cell and it operates at temperatures in the range of 205 ^{0}C. PAFCs are used mainly for stationary power generation, but some have been applied in large vehicles such as city buses. It is said to be the first fuel cell to be commercially available [12]. PAFCs give 40% efficiency. The steam produced by this fuel cell is used for co-generation. These fuel cells are typically large and heavy and as a result are less powerful compared to other fuel cells and are expensive. The use of the Pt catalyst is a problem for this fuel cell because the catalyst is expensive.

2.3 Low temperature fuel cells

Alkaline Fuel Cell (AFC): There are three types of AFCs namely, mobile electrolyte, static electrolyte and dissolved fuel. The mobile and the static electrolyte are being used in the space programme. This fuel cell uses an alkaline solution as a fuel (OH^- ion moving across the electrolyte). This fuel cell has several advantages such as the low activation overpotential at the cathode, high operating voltage (0.875), the use of non-precious metals, do not need bipolar plates and there is not much water management problem as compared to the Proton exchange membrane fuel cell (PEMFC). The major disadvantages of the AFCs are, low power density, and CO_2 is poison to the fuel cell. The first real application of the fuel cells started with the space program. The mobile electrolyte system was used in the first AFCs in 1940s and is used in terrestrial systems. The shuttle orbiter uses a static electrolyte system [13].

Proton exchange membrane fuel cell (PEMFC): A Proton Exchange Membrane Fuel Cell (PEMFC) is a fuel cell that uses a thin ion conducting solid electrolyte, a polymer electrolyte membrane (PEM). The PEM is a proton permeable but electrical insulator barrier. This barrier allows the transport of the protons from the anode to the cathode through the membrane but forces the electrons to travel around the conductive path to the cathode. A solid electrolyte, the Polymer Electrolyte Membrane has its advantages over liquid electrolytes in that it has high power density and reduced corrosion. This fuel cell uses hydrogen as the fuel and oxygen as the oxidant. It is a low temperature fuel cell which operates at 70-80 ^{0}C. Because of the low temperature, noble metal catalysts can be used. The use of the Pt catalyst hinders the use of this fuel cell because of the cost of this catalyst [14]. PEMFCs are used for transport because they can start quickly due to a low operating temperature. Also there are no corrosive fluid hazards and the fuel cell can work in any

orientation. This fuel cell produces zero emissions and so is an environmental friendly energy source. The problem encountered in the use of a PEMFC is the use of a contaminated hydrogen gas stream that enters the anode, the carbon monoxide (CO) then adsorbs onto the active sites of the Pt thus blocking them and this decreases the performance of the PEMFC [15]. Figure 2.2 shows a schematic diagram of a PEMFC.

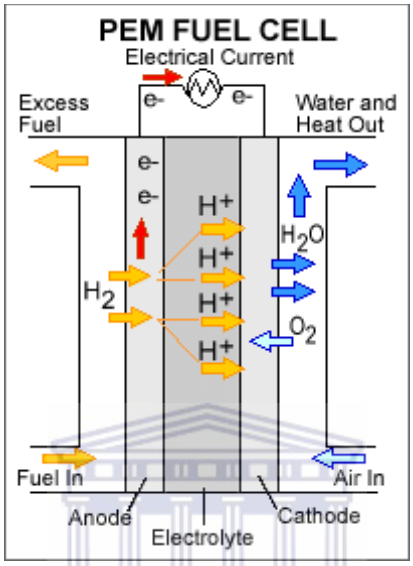

Figure 2.2: Diagram of a proton exchange membrane fuel cell (PEMFC)

Direct methanol fuel cell (DMFC): The use of a hydrogen fuel is a challenge for fuel cell applications because it is difficult to store and handle since it is a light metal. The DMFC uses methanol as its fuel without a reformer. It produces power by direct conversion of liquid methanol to hydrogen ions on the anode side of the fuel cell. The DMFC has all fuel cell components such as the anode, cathode, membrane and catalysts the same as those of a PEMFC. The anode catalyst oxidizes the methanol fuel and at the cathode oxygen reduction occurs, carbon dioxide gas, water and heat are produced as the by-products in the course of the reaction at the cathode [16]. The low temperature fuel cells have higher energy density compared to conventional energy sources such as batteries or combustion engines [17, 18]. Figure 2.3 gives a schematic diagram of a DMFC.

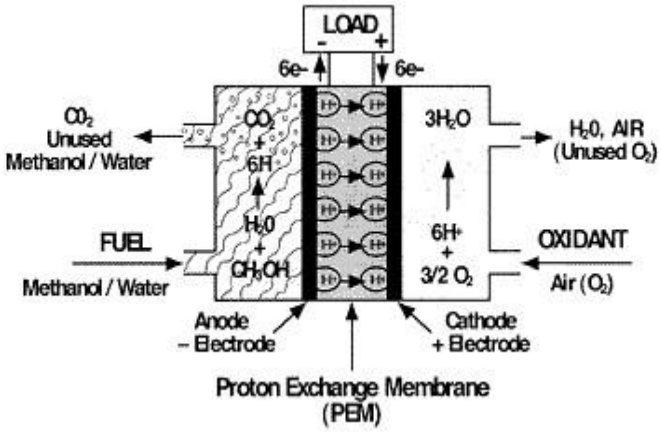

Figure 2.3: Diagram of a direct methanol fuel cell (DMFC)

Challenges facing the use of direct methanol fuel cells

This fuel cell faces major challenges such as the cost of the platinum (Pt) catalyst that it uses and the poor kinetics of the anode and cathode reactions associated with it.

The electrochemical oxidation of methanol on the Pt at the anode involves the methanol dehydrogenation, chemisorption of methanol residues (such as CO) and the dissociative chemisorption of water [19, 20].

$$Pt + CH_3OH \rightarrow Pt\text{-}(CH_3OH)_{ads} \quad (2.1)$$

$$Pt\text{-}(CH_3OH)_{ads} \rightarrow Pt\text{-}(CO)_{ads} + 4H^+ + 4e^- \quad (2.2)$$

$$Pt + H_2O \rightarrow Pt(OH)_{ads} + H^+ + e^- \quad (2.3)$$

$$Pt\text{-}(CO)_{ads} + Pt(OH)_{ads} \rightarrow CO_2 + 2Pt + H^+ + e^- \quad (2.4)$$

Methanol is electrochemically oxidised on the Pt surface at the anode (see reaction 2.1). The carbon monoxide (CO) which is by-product of the methanol oxidation strongly adsorbs onto Pt (see reaction 2.2) and occupies all the active sites of the catalyst, resulting in Pt poisoning and this can be solved by oxidising the CO to carbon dioxide (CO_2) as shown in reaction 2.3 and 2.4. The electrochemical potential of reaction 2.4 is high (0.7V) and this is a problem. It is thus essential to develop a catalyst that can easily form $M(OH)_{ads}$ (M being the metal) species at a low electrode potential. A more active catalyst than Pt for methanol oxidation should result in H_2O discharging to form $M(OH)_{ads}$ (see reaction 2.5 and 2.6) species at low

potentials and then weaken CO chemisorption or catalyse the oxidation of adsorbed CO (see reaction 2.7) [21].

$$M + H_2O \rightarrow M\text{-}(H_2O)_{ads} \quad (2.5)$$

$$M\text{-}(H_2O)_{ads} \rightarrow M\text{-}(OH)_{ads} + H^+ + e^- \quad (2.6)$$

$$Pt\text{-}(CO)_{ads} + M\text{-}(OH)_{ads} \rightarrow Pt + M + CO_2 + H^+ + e^- \quad (2.7)$$

PtRu/C has been proved to be a better anode catalyst than Pt alone [22].

Another problem facing the use of a direct methanol fuel cell is when methanol crosses over from the anode towards the cathode and at the cathode it interferes with the oxygen reduction reaction giving mixed potentials [23] as shown in Figure 2.4. Catalysts that can be methanol tolerant, reduce the cost of Pt or find other alternative catalysts and most importantly giving higher current densities have to be investigated [1].

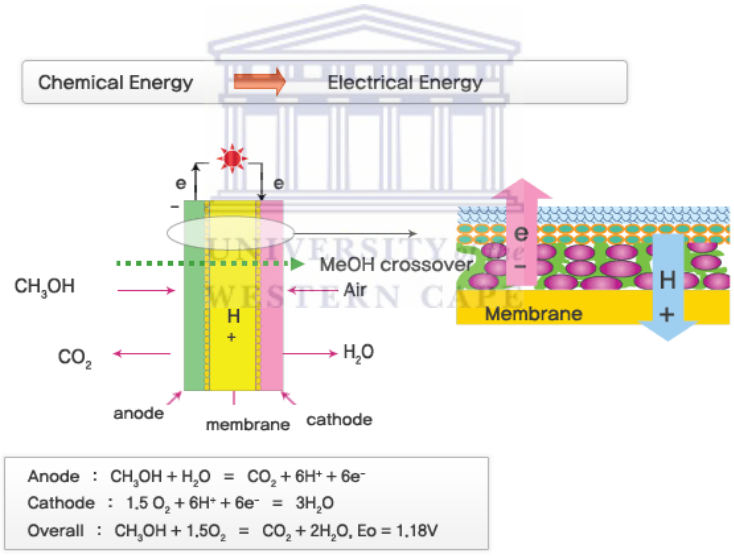

Figure 2.4: Methanol crossover phenomenon

2.4 Catalysts

A catalyst is a compound that increases the rate of a reaction but is not consumed during the overall reaction. The catalyst's role in a reaction is to make the rate of the reaction fast such as to lower the energy needed for the reaction place, this will be explained more thoroughly later on. Catalysts are classified as heterogeneous and homogeneous. A heterogeneous catalyst does not dissolve in the solution, and hence the catalysis takes place in a phase

separate from the solution (typically the surface of the catalyst). A homogeneous catalyst dissolves in the solution, and hence normal spectroscopic and chromatographic techniques can be employed to explore the mechanism and identify intermediates. Acids, bases, enzymes and most organometallic species are used as homogeneous catalysts. The energy that is needed by a reaction to take place is called activation energy and reactions need this activation energy in the course of the reactions. A catalyst can lower the activation energy without itself being changed or consumed during the reaction. All catalysts operate by the same general principle, that is, the activation energy of the rate-determining step must be lowered in order for a rate enhancement to occur [24]. Figure 2.5 shows the activation plots of a catalysed and an un-catalysed reaction.

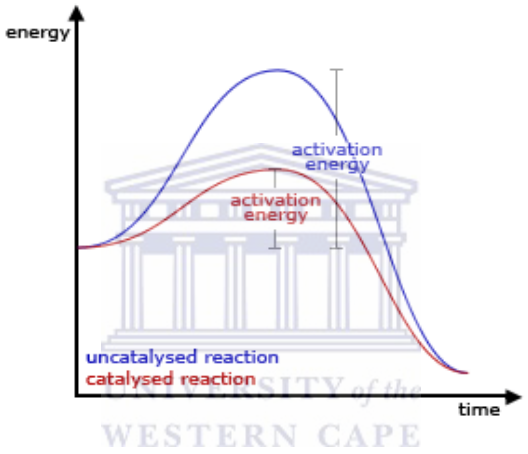

Figure 2.5: Diagram displaying the activation energy pathways for a catalysed reaction and an un-catalysed reaction

The blue plot (the un-catalysed reaction) and the red plot (the catalysed reaction) indicate the higher activation energy and lower activation energy, respectively. The catalyst reaction (the red plot) lowers the activation energy by providing an alternative pathway for the reaction to occur. The catalyst makes the rate of the reaction faster [25].

2.4.1 Preparation methods of catalysts

Different methods are used for catalyst synthesis, and they include impregnation method, Pt precursor and precipitation method, colloidal method, sol-gel method, Bonnemann method and micro-emulsion method. A good method for making electro-catalysts should provide:

- Highly dispersed catalyst on support
- Narrow particle size distribution

- Uniform particle composition
- Multi-metal catalyst structure with preferred atomic ratio
- Preferred crystallite structure

The synthesis methods of catalysts are discussed below and the Bonnemann method was used for this study.

Impregnation reduction method: The impregnation method is widely used for the preparation of the Pt-based catalyst. In the Impregnation method the metallic catalyst precursor is soaked into a support before it is reduced into metallic nanoparticles. There are two possible reduction steps such as chemical and electrochemical reduction and these reduction steps can be conducted in a liquid phase or gas phase. The metallic catalyst precursors used in this method are chloride salts (H_2PtCl_6 and $RuCl_3$) because they are easily available. The hydrogen (H_2) flowing at high temperatures greater than 300 ^{0}C is used for gas-phase reduction and the reducing agents such as $Na_2S_2O_3$, $Na_4S_2O_5$, N_2H_4, $NaBH_4$, HCOOH, ethylene glycol and formaldehyde are used for liquid-phase reduction [26]. The catalyst precursor is mixed with the catalyst support (porous or nanostructured carbon), and penetrates into pores, the catalyst support helps in penetration and wetting of the precursor and during the reduction step the carbon support confines the growth of the particle size. The challenge about this method is the use of the chloride precursors that might lead to chloride poisoning, resulting in lower catalytic activity and stability of the chloride-salt derived catalyst. Impregnation methods that could use chloride free precursors have been investigated using metal nitrate/nitrite salts such as $Pt(NH_3)_2(NO_2)_2$ and $RuNO(NO_3)x$ [27], carbonyl complexes such as $Ru_3(CO)_{12}$ [28] and metal sulphite salts such as $Na_6Pt\ (SO_3)_4$ and $Na_6Ru(SO_3)_4$ [29] as metal precursors in the impregnation method, respectively. These chloride-free routes give higher dispersion and better catalytic activity as compared to the conventional Cl-containing route.

Pt precursor and precipitation method: This method uses a chemical precipitation route at low temperatures. In this method the reducing agent is added to a metal precursor salt solution. Metal precursor salts such as Pt (H_2PtCl_6) and Ru ($RuCl_3$) are used and hydrogen is used as the reducing agent. The metal precursor salt is reduced to the metallic state and precipitates out of the solution, forming unsupported electro-catalysts that can be filtered and washed. The problem that is encountered in this preparation method is the use of the chloride metal precursors and so the use of carbonyl precursors that decompose at low temperatures

has been under investigation and has been reported to be good for the method [30, 31]. The carbonyl precursors are used by bubbling a CO gas through a solution of e.g. Platinic acid (H_2PtCl_6) and this results in the formation of a $Pt(CO)_2$ precipitate that can be washed, filtered and dried [31].

The catalyst is then supported before the reduction step to enhance the surface area of the catalysts giving a possibility to good activity and stability of the catalyst [32].

Sol gel method: The sol gel method uses an aged gel, metal salts and a reducing agent. In this method the gel is formed and then calcified to change the physical and chemical properties of the gel. After calcification a mesoporous solid or powder is formed [33]. Metal salts are added during gel formation or after the mesoporous structure has formed followed by the reduction step [34]. Metallic nanocatalysts can be incorporated into the mesoporous structure by a variety of methods. The challenge facing this method is that the catalytic nanoparticles may be buried within the structure rather than near the pores. If the particles are not located near the pores they will not be efficient catalysts but adding nanoparticles after the mesoporous structure has formed, i.e. after calcination, ensures that the particles forms in the pores provided that the particle size or pore ratio is suitable. The aging and calcination steps allow for fine control of the pore size distribution and volume by controlling experimental parameters like time, temperature, heating rate, and pore liquid composition.

The colloidal method: This method uses a metal colloids followed by the reduction step. The synthesis occurs in an organic or aqueous medium where the metal precursor is reduced chemically in the presence of a protective agent (i.e. NR41, PPh_3, PVP, SB12 or PVA).The catalyst is supported with a catalyst support to enhance the surface area and the dispersion of the catalyst. The colloidal metal nanoparticles are stabilized by steric hindrance or by electrostatic charges to obtain a narrow size distribution. . Steric stabilization can be provided by coating the metal core with organic chain molecules [35, 36]. The electrostatic repulsion of like charges limits the agglomeration of charged colloids or adsorbed ions. The challenge facing this method is the use of protecting agents, which may affect the catalytic activity of the nanoparticles and it may be removed by washing in an appropriate solvent or by decomposition at temperatures in an inert atmosphere. There are some other challenges facing this method such as its complexity, time consuming and high cost, which will bring difficulty for scaling up. The colloidal method prepares catalysts with nanoparticle size and a narrow size distribution

Microemulsion method: This method has been widely used for the preparation of Pt and PtRu nanoparticles as electro-catalysts for fuel cells [37, 38]. In this method a reducing agent is added to the micro-emulsion system to reduce the metal salt or the microemulsion system that contains a reducing agent can be added with a microemulsion system that contains a metal salt [39, 40]. A carbon support powder with tetrahydrofuran solvent is added to the microemulsion system to support the catalyst nanoparticles [40]. The role of the solvent is to destabilize the microemulsion system by competing with a surfactant such as (sodium 2-bis (2-ethylbexyl) sulfosuccinate (Na(AOT)) to adsorb onto the particles, and in the destabilized system the particles will adsorb onto the support. There is another route used that does not involve the solvent for the deposition of the support material, the emulsion and the support material are simply mixed and stirred [37, 38]. After deposition, residual surfactant molecules are typically removed by heat treatment [39]. Emulsion systems are very sensitive to temperature and therefore the oil and surfactant must be carefully selected [40].

Bonnemann method: This method is one of the colloidal methods. The synthesis process is carried out under anhydrous and inert gas conditions. The anhydrous metal chlorides, $MeCl_n$, are dissolved in tetrahdrofuran (THF) based on the metallic atomic ratio in total. The tetraoctylammonium triethylhydroborate $N(Oct)_4HB(Et)_3$ is then added drop wise to the dissolved metal chloride(s) in THF to produce metal colloids (Me*). The obtained colloid solution is then added to carbon paper suspension (Vulcan carbon XC-72R form Cabot corp) in THF. The supported metal colloid suspension is filtered and washed with ethanol and dried under high vacuum. Excess protective surfactants surrounding the catalyst surface are eliminated by placing the product into a Lindberg tube furnace and heat treated at 350 ^{0}C with the flow of Nitrogen. The catalyst synthesized by this method has the advantages of small average particle size and narrow particle distribution. Moreover, this method is very suitable to produce metal alloys with any atomic ratios as long as the physical solubility is allowed for the prototype of metal chloride(s) in solution [41].

2.4.2 Catalysts used in fuel cells

Fuel cells consist of two electrodes. These electrodes contain catalysts so as to speed up the electrochemical reaction that takes place on these electrode surfaces. The most widely used catalyst is platinum and research on platinum alloys and other noble metals has been done. There are many factors that affect the rate of the reaction such as bigger particle size, lower

surface area, low temperature, low pH etc. which necessitate the use of a catalyst. In a fuel cell the anode catalyst oxidises the fuel and the cathode catalyst reduces the oxygen which is the oxidant and this results in the formation of water and carbon dioxide. The oxygen reduction reaction which is catalysed by a cathode catalyst is a slow reaction due to the higher energy that is needed for the reaction to occur and so the use of a catalyst is needed to lower the activation energy and give good ORR performance [42]. In a DMFC the cathode catalyst is poisoned by the methanol fuel which crosses over from the anode to the cathode and the catalysts of this fuel cell has to be methanol resistant and not allow their performance to be affected by the methanol crossover.

The platinum (Pt) catalyst has the best activity for both the anode and the cathode electrodes of a fuel cell however, this catalyst is expensive. In this study the ways of reducing the amount of the Pt catalyst used were investigated. The Pt catalysts use catalysts supports so as to lower the amount of the catalyst that is used and also to provide with higher surface area and give higher catalyst performances [43]. Incorporating another metal with Pt helps reduce the amount of Pt that is used and so Pt binary catalysts are used as ORR catalysts nowadays.

Oxygen reduction reaction

A fuel cell consists of two electrodes, the anode and the cathode. At the cathode oxygen from air is reduced and the reaction is named oxygen reduction reaction (ORR). The electrochemical reaction at the cathode involving oxygen is a kinetically slow reaction. The overall reaction for the oxygen reduction reaction is given below:

$$O_2 + 4H^+ + 4e^- \rightarrow 2H_2O \qquad (2.8)$$

The oxygen reduction reaction can take place through two pathways, that is the four-electron pathway which is the electro-reduction of oxygen to water and there's also the two-electron transfer which is the electro-reduction of oxygen to hydrogen peroxide [44-46]. The first pathway is the direct four-electron pathway and it takes place via the reaction pathway above (see reaction 2.8). The second pathway is the peroxide pathway, which is a two-step process involving the two-electron electrochemical reaction creating hydrogen peroxide (see reaction 2.9) and then the subsequent two-electron decomposition (see reaction 2.11) or reduction (see reaction 2.10) of peroxide to water or hydroxide ions. These steps follow the reaction pathway below:

$$O_2 + 2H^+ + 2e^- = H_2O_2 \qquad E= 0.67V \qquad (2.9)$$

Reduction of peroxide:

$H_2O_2 + 2H^+ + 2e^- = 2H_2O$ E= 1.77V (2.10)

Or decomposition of peroxide:

$2H_2O_2 = 2H_2O + O_2$ (2.11)

This pathway results in the presence of hydrogen peroxide in the solution, before it is either reduced or decomposed into hydroxide ions or water. Nonetheless, the overall reaction is still the four-electron pathway [44]. The peroxide that is produced in this path is low in efficiency and is also corrosive and the reaction itself is a slow reaction.

Due to the slow kinetics of the oxygen reduction reaction, catalysts have been investigated and it has been found that platinum has the highest catalytic activity for oxygen reduction reaction more especially when the catalyst is supported with a catalyst support material [47]. The Pt catalyst is the widely used catalyst for ORR but it is expensive. Higher amounts of the catalyst are being used because the reaction is kinetically slow and so ways to lower the amount and the cost of Pt have been investigated and the Pt binary catalysts have been reported as ORR catalysts. The fuel cell also suffers from anode crossover which leads to mixed potentials at the cathode, resulting from the oxygen reduction reaction and the fuel oxidation occurring simultaneously and this reduces the cell voltage. These problems ultimately results in instability as well as a reduction in cell performance. These problems could be solved by developing new cathode catalysts with higher activity for the ORR than Pt.

2.5 Catalysts for Oxygen reduction reaction

2.5.1 Platinum a catalyst for fuel cell

Platinum is a silvery-white, lustrous, ductile, and malleable pure metal [48]. It is more ductile than gold, silver and copper, thus being the most ductile of pure metals, but gold is still more malleable than platinum [49-50]. Platinum does not oxidize at any temperature, although it is corroded by halogens, cyanides, sulfur, and caustic alkalis. It is insoluble in hydrochloric acid, but dissolves in hot aqua regia to form chloroplatinic acid, H_2PtCl_6 [51]. The metal has an excellent resistance to corrosion and high temperature and has stable electrical properties. It has been used for industrial applications [52].Platinum is mostly used as a catalyst in chemical reactions, as platinum black. This metal also catalyses the decomposition of hydrogen peroxide into water and oxygen gas [53]. Pt is used as a catalyst in fuel cells for both electrodes. The reaction occurring at the anode, hydrogen oxidation is faster but the oxygen reduction occurring at the cathode is very slow and so higher amounts of Pt at the

cathode are used. The Pt catalyst is supported with a catalyst support for the oxygen reduction catalysts giving good catalyst dispersion on the catalyst support and also high surface area, which results in reasonable cell performances. Research is being done to find ways of reducing the cost of Pt. The move from platinum black to carbon supported platinum catalysts has significantly cut platinum requirements. Typical loadings in the electrode today are about 0.4-0.8mg platinum/cm^2, which is significantly lower than 25mg/cm^2 with early platinum black catalysts [54].

2.5.2 Platinum binary catalysts as cathode catalysts for fuel cells

In this fuel cells electrodes (i.e. the anode and the cathode), platinum (Pt) is used as the catalyst. In the case of the anode the reaction is so fast that the amount of Pt catalyst, and hence the cost, is still a concern but not as so as in the case with cathode catalysts. In the case of cathode, where O_2 is reduced (ORR), the ORR reduction kinetics are sluggish, so the amount of Pt and hence the cathode catalyst costs are high. Another problem experienced in ORR is the fuel crossover in a DMFC, in this fuel cell methanol crosses through the membrane from the anode towards the cathode and this interferes with the ORR activity giving mixed potentials as a result of methanol oxidation and oxygen reduction occurring simultaneously. There is a need to look at a catalyst that will reduce the amount of Pt that is used at the same time reducing the cost but giving good activity, as well as a catalyst that will not be affected by the fuel crossover. Incorporating Pt with another metal would be a solution as it would reduce the amount of Pt used and the cost. Much research has been done on the Pt binary catalysts and they have been found to give enhanced catalytic activity [55]. PtCr/C electro-catalysts were prepared using the colloidal method from the Bonnemann method. The catalyst gave better ORR activity than the Pt/C catalyst. It was observed that the addition of chromium to Pt does not alter the mechanism of ORR which involves four-electrons [56]. The use of Pt binary catalysts was further investigated and Pt-Pd/C catalyst was synthesized for the ORR studies. The effect of Pt-Pd atomic ratio in this catalyst coated membrane on the activity of ORR was also studied, the results demonstrated that the atomic ratios had an effect on the electro-catalyst and performance in a fuel cell. The particle size was increased due to the decrease in Pt:Pd atomic ratio and the particle dispersion, electro-active surface area, current density, activity and mass activity decreased [57]. The Pt:Pd atomic ratio of 1:2 exhibited maximum activity towards ORR and RDE studies showed that the electro-catalyst involved a four-electron pathway [57].

It has been found that the metallic character has an effect on the electro-catalytic activity of ORR and this was proved by preparing a Pt_3Co/C catalyst by the colloidal method and studied the catalyst for the ORR in a DMFC. The catalyst showed good ORR activity but was not methanol tolerant, this was attributed to the enhanced metallic character of Pt in the Pt_3Co catalyst due to an intra-alloy electron transfer from Co to Pt, and to the adsorption of oxygen species on the more electropositive element (Co) that promotes methanol oxidation according to the bi-functional theory [58]. It was also reported that Pt-WC/C catalyst gives enhanced ORR activity compared to the commercial Pt/C catalyst. He also noted that catalyst dispersion on the support and particle size distribution plays a huge role in the activity enhancement [59]. This was further proved by the preparation of $Pt_{70}Co_{30}$/C nanoparticles by a polyol method, the nanoparticles were found to have very small particle and narrow distribution homogeneously dispersed on the carbon support and having a high degree of alloying. The catalyst showed enhanced catalytic activity giving mass activity higher than that of commercial catalyst. The catalyst showed to be a better cathode electro-catalyst than Pt/C [55].

An ethylene glycol method was modified for the preparation of nanostructured Pt-Fe/C catalyst with varying Pt:Fe ratio. It was observed that the electro-active surface area increased with increasing atomic percentages of Fe from 0 to ca. 50%, and decreased with more Fe in the Pt-Fe/C catalyst. RDE studies showed that the Pt-Fe/C catalyst with a Pt:Fe ratio 1.2:1.0 showed high mass activity and specific activity to ORR [60]. Carbon supported Polypyrrole modified with Cobalt and/or Platinum catalyst was also studied for ORR and the results showed that the catalysts have better electro-catalytic activity for ORR. When C-PPy was added this resulted in more positive potentials for ORR than when Co was added alone, but when both metals were added the results were similar to the catalyst where only Pt was added (C-Ppy-Pt). The C-Ppy-Co-Pt catalyst showed the highest exchange current density, it is assumed that the presence of the metallic particles play an important role in the high electro-catalytic activity [61].

PtCo/C catalyst was also reported to have shown better ORR kinetics than commercial Pt/C catalyst and it was found that these catalysts were undergoing a four-electron pathway [62]. Pt-Fe/C, PtRh/C, and PWA-Pt/C catalysts were studied as cathode catalysts for DMFC. The catalyst exhibited high ORR activity than Pt/C and it showed resistance towards methanol while the Pt/C was poisoned by methanol [63-65].

It has been found that electron transfer from Pt to M (metal) within an alloy is responsible for the synergistic promotion of the ORR on a Pt-M electrode. Varying compositions of an alloy

catalyst were prepared to investigate the ORR activity of this catalyst. It was then concluded that the electron transfer form Pt to Au within the alloy is responsible for the synergistic promotion of the ORR on a Pt-Au electrode [66]. Tungsten carbide nanocrystal and tungsten carbide nanocrystal modified Pt electro-catalysts were prepared by the IMH method for the ORR study. It was found that these catalysts were both active for ORR [67].The Pt-decorated with PdFe nanoparticles were also investigated as ORR catalysts. The catalyst was compared with the Pt/C catalyst and it was found that the Pt-decorated PdFe catalyst has an activity four times better than that of Pt/C in-terms of ORR, cost and methanol tolerance [68].

The nanostructured platinum-bismuth catalysts supported on carbon (Pt_3Bi/C, PtBi/C and $PtBi_3$/C) were synthesized by the micro-emulsion method to study them as cathode catalysts in a DMFC. The catalysts showed higher ORR activity and methanol tolerance than Pt/C. The platinum-bismuth catalysts showed higher mass activities for ORR, 1-1.5 times better than Pt/C [69].

2.6 Heat treatment effect on catalysts

The heat treatment process has been reported to have an effect on the activity of electro-catalysts and thus it is called thermal activation. Heat treatment is considered a necessary step for fuel cell electro-catalysts as it removes undesirable impurities from the preparation stages and the heat treatment allows better metal particle size, size distribution, particle surface morphology and metal dispersion on the support [70]. These effects help to increase the electrochemical surface area (ECSA) of the catalytic metal and generally improve the performance of these types of catalysts. There are different types of heat treatment methods used such as the oven/furnace heating, microwave heating, plasma thermal heating, and ultrasonic spray pyrolysis. Among all these the oven/furnace heating method is widely used. Catalysts using carbon black as support for the catalytic metal, the heat treatment process is understood to provide two main functions for the stability, the removal of oxygenated functional groups and graphitization of the carbon support surface. The carbon surface of most carbon blacks is functionalized with various oxygen-containing functionalities which affect the surface chemistry of the carbon support [71].

The carbon black (Vulcan XC72R)-supported palladium–vanadium electro-catalysts were heat treated at a range of temperatures in 10% H_2 in Ar and the effect of heat treatment on particle morphology was studied and the results showed that the particle size increased at high temperatures. It was also found that the catalyst showed enhancement in the electro-catalytic activity after heat treatment [72]. The polyol reduction process was employed to

synthesize the Pt–Sn/C catalyst for the ORR study. It was observed that the size of the particles obtained was very small but the size slightly increased with the temperature of heat-treatment and the particles were found to be well distributed on the carbon support. XRD confirmed the alloying of Sn with Pt and as the temperature of heat-treatment increased. Lattice parameter value of Pt–Sn/C electro-catalysts increased from that of Pt indicating the increasing Pt–Pt distance on increasing heat-treatment. The increased Pt–Pt bond distance creates unfavourable situation for adsorption/dehydrogenation of methanol. The catalysts showed increased ORR activity and methanol resistance as the heat temperature increased [73]. It is considered that the specific crystalline structure and work function have an influence on the catalytic activity for the ORR.

Ti oxide catalysts were heat treated from 600-1000 ^{0}C under various conditions for the ORR study as cathode catalysts. The catalysts heat treated at 900 ^{0}C showed higher electro-catalytic activity. It was found that the heat-treatment condition changed the oxidation state, crystalline structure and work function of the catalysts. In particular, the crystalline structure of the Ti oxide catalysts changed with the heat-treatment temperature and the catalytic activity for the ORR increased with the TiO_2 (rutile) (1 1 0) plane [74]. Fe1Co1–TPTZ complex and Fe-TPTZ complexes were also heat-treated to optimize ORR activity. It was found that 700 ^{0}C heat-treatment yielded the most activeFe1Co1–N/C catalyst for the ORR and 800 ^{0}C for the (Fe-N/C) catalyst [75, 76].

2.7 Particle size and structural effects on the electro-catalytic activity

Fuel oxidation and oxygen reduction reactions are both affected by the particle size of electro-catalysts. If the particle size of the electro-catalyst is smaller than 3 nm, the catalyst activity for ORR will be lower [77]. Thus, the best compromise is to control the structure and the particle size in order to increase ORR [77]. Studies show that the particle size has an effect on the kinetics of ORR and MOR [78-85].The kinetics of methanol oxidation on Pt is not only affected by the particle size but also by the particle shape which may modify the distribution of methanol adsorption sites on the Pt surface [86, 87]. ORR kinetics of a Pt/C catalyst were investigated to study the effect of particle size on the ORR activity. The results showed that the utilization of the catalyst with narrow size distribution provided evidence for a particle size effect on the ORR activity and methanol tolerance. It was found that the mass activity for ORR increased with a decrease in particle size. An addition of a second metal was also investigated, based on the particle size PtCr/C catalyst appeared to be more active than Pt/C alone for both ORR and MOR [88]. The crucial electro-sorption properties of the metal

electro-catalysts were observed to be dependent on the particle size [89]. It was suggested that the change in the fraction of surface atoms on the (100) and (111) crystal faces of Pt particles, which are assumed to be cubo-octahedral structures, can be correlated to the mass activity (A/g Pt) and specific activity(~AJcm 2 Pt) of highly dispersed Pt catalysts. The maximum in mass activity that is observed at 3.5 nm in several studies is attributed to the maximum in the surface fraction of Pt atoms on the (100) and (111) crystal faces, which results from the change in surface coordination number with a change in the average particle size. The reduction of oxygen on supported Pt particles in acid electrolytes is classified as a demanding or structure-sensitive reaction; the specific activity increases with an increase in particle size [90].

Carbon-supported Pt-based binary alloy catalysts (Pt-Co, Pt-Cr and Pt-Ni) were prepared and compared with Pt for ORR study. Pt-alone and Pt-based alloy electro-catalysts showed increasing specific activities with decreasing surface area. This indicates that oxygen reduction on platinum surface is a structure-sensitive reaction and the Pt-based alloy catalysts showed significantly higher specific activities than Pt-alone catalysts with the same surface area. This comes from the reduced Pt–Pt neighbouring distance as the catalysts were alloyed. The reduced Pt–Pt neighbouring distance is favourable for the adsorption of oxygen [91].

2.8 Supports for catalysts

Platinum based catalysts are deposited on catalyst supports to enhance their surface area [92]. The catalyst supports prevent the electro-catalysts from aggregation but also play a significant role in transporting the electrons generated from and consumed by the electrical reactions [93]. It has been reported that catalyst supports have great influence on the performance and durability of electro-catalysts. An ideal catalyst support should meet these requirements:

- High surface area to improve the catalytic dispersion
- Low combustion reactivity
- High conductivity
- High electrochemical and thermal stability

Currently, the most popular support material is porous carbon black (XC-72) but there are various studies conducted on other types of carbon support material, e.g. carbon nanotubes and non-carbon materials e.g. metal oxides etc.

2.8.1 Carbon black as the support material

The catalyst supports plays a huge role in the performance of the electro-catalysts used in the fuel cells in terms of the activity and reducing the amount of the catalyst that is used in order to reduce the cost. The widely used catalyst material is carbon black. There are different types of carbon blacks, such as Acetylene black, Vulcan XC-72, and Ketjen black. The physical and chemical properties, such as specific surface area, porosity, electrical conductivity and surface functionality are reported to have an effect on the performance of the carbon black supported catalysts but the parameter that has a major effect on the catalytic performance is the specific surface area [94, 95]. Ketjen blacks provides higher surface area and thus provides high catalyst dispersion but this high surface area results in high ohmic and mass transport limitations for fuel cell catalysts [95]. The vulcan XC-72 carbon black has a specific surface area around 230 m^2/g and thus is the most widely used carbon support for the preparation of fuel cell catalysts because of its good compromise between electronic conductivity and the BET surface area [96, 97]. The Carbon blacks are now commercially available at low costs. Pt or other Pt based alloy electro-catalysts are prepared by using Vulcan XC-72 carbon black as support.

There are some drawbacks concerning the use of Vulcan XC-72 carbon. Vulcan XC-72 carbon have pores which are too small to be filled by the electrolyte polymer and, thus, many Pt particles are trapped in the micropores (less than 1 nm) of the carbon black are not involved in the electrochemical reactions on electrodes due to the absence of the triple-phase boundaries (gas-electrolyte-electrode). There are other factors that affect the preparation and performance of carbon-black-supported catalysts, such as pore size and distribution and surface functional groups of carbon blacks [98-102]. The metal catalyst utilization is determined by an electrochemical accessible active area rather than carbon specific surface area. Because of the low cost and availability the carbon blacks are still the most widely used catalyst support materials.

The next chapter will be discussing the methods that were used in this study.

CHAPTER 3

METHODOLOGY

This chapter provides a detailed description of the preparation methods used in this study and the physical and electrochemical characterization techniques used. Various physical characterization techniques and electrochemical characterization techniques are used and will be further discussed in this chapter.

3.1 MATERIALS AND METHODS

3.1.1 Materials

Table 3.1 gives the catalysts that were used in this study. In-house catalysts used, are the catalysts that were prepared using the Bonnemann method. The commercial catalysts were also studied to compare with the in-house catalyst. The 20%PtCo/C commercial and 20%PtCo/C and 30%PtCo/C both in-house catalysts were characterized with and without heat treatment at 800 ^{0}C and compared.

Table 3.1: In-house and commercial Platinum based catalysts used in this study

Catalysts	Supplier
10%Pt/C	In-house
20%Pt/C	In-house
30%Pt15%Ru/C	In-house
40%Pt20%Ru/C	In-house
30%PtCo/C	In-house
20%PtCo/C Sintered at 800^{0}C	In-house
20%Pt20%Cu/C	In-house
20%PtSn/C	In-house
10%Pt/C	Johnson Matthey™
20%Pt/C	Johnson Matthey™
20%Pt10%Ru/C	Johnson Matthey™
20%PtCo/C	BASF
20%PtCu/C	BASF
20%PtSn/C	BASF

Table 3.2: Material used for preparing the electrode

Chemical	Supplier
Nafion®	Aldrich
Iso-2-propanol	Johnson Matthey™
Carbon paper	Carbot

The materials which were used to prepare the electrode are shown in Table 3.2. In addition, other equipments that were used include; the analytical weighing balance, the ultra-sonicating bath, spraying gun, puncher, tube furnace, an oven and the Zeener power water purification system.

3.1.2 Heat treatment of catalysts

The 30%PtCo/C In-house catalyst was heat treated at different temperatures under controlled temperature. The heat treatment of the catalysts affects the morphology of the catalysts and the activity of the catalysts and allows uniform dispersion on the catalyst support. The tube furnace was pre-purged with dry nitrogen gas flowing at 500 ml/min for 45 min to suppress possible surface oxidation of Pt particles due to the remaining oxygen within the tube during the heat treatment. The tube furnace was pre-heated to the target temperature. An alumina boat was loaded with the catalyst and inserted into the centre of the tube furnace. The catalyst was heated at several target temperatures such as 350 ^{0}C, 650 ^{0}C and 800 ^{0}C for 3 hours under nitrogen flowing simultaneously at a rate of 5ml/min. When the heating time was over, the tube was cooled down with the nitrogen gas still constantly flowing at a rate of 5ml/min and the catalyst was taken out of the furnace after it had cooled down.

3.2 PHYSICAL CHARACTERIZATION OF CATALYSTS

3.2.1 High Resolution Transmission electron microscopy (HRTEM)

The transmission electron microscopy was developed in 1932 by Max Knoll and Ernst Ruska in Germany, 35 years after J.J. Thompson's discovered an electron. It was discovered that the technique improved the light transmission microscope because in this technique a focused beam of electrons is used unlike in a light transmission microscope that uses a light to see through the specimen. This technique offers increased magnification and resolution. The main use of the HRTEM is to examine the structure, comparison, or properties of a specimen in sub-microscopic detail. One can see objects to the order of a few Angstroms (10^{-10} m). The

instrument was first commercialized in 1938 by the Siemens-Halske Company in Berlin [103].

An accelerated beam of electrons passes through a sample (50-300Å) and some of the electrons are scattered by the atoms in the sample. An image is created as a result of a phase distortion that is formed or created which results in a phase contrast that is used to create the image. As it has been stated earlier that electrons pass through a sample so those electrons that pass through form the image, while those that are stopped or deflected by dense atoms in the specimen are subtracted from the image. In this way a black and white image is formed. The much lower wavelength of electrons makes it possible to achieve a resolution a thousand times better than that of a light microscope. In HRTEM the operator sees inside the sample not the surface.

The HRTEM analysis was done by first preparing the sample. A very small amount of the sample was added into a vial containing about 5ml of ethanol and the solution was put in a sonic bath for about 10minutes until the sample was nicely sonicated. A drop of the solution was then deposited on the copper grid which was copper coated carbon or formvar® mesh with a diameter of about 3mm. The sample was then left at room temperature for about 10 minutes to allow the ethanol to evaporate and then the grid was placed in the sample holder and introduced in the shaft for analysis (HRTEM Technai G2F20X-Twin MAT 200kV Field emission Transmission electron microscope). The metal surface area can be obtained from TEM data by using the equation below:

$$SA_{Pt} = 6 \times 10^3 (d\rho) \qquad (3.1)$$

where d=density of Pt (21.4g/cm^3) and ρ=particle size in nanometers (nm).

The experimental parameters are given as follows: accelerating voltage (200 kV), current (20 μA), condenser aperture (1), objective aperture (3) and exposure time (3 s).

3.2.2 X-ray diffraction (XRD)

X-ray diffraction is a technique that is used to physically characterize materials and it gives information about the chemical composition and crystallographic structure of natural and manufactured material. Wilhelm Conred Röntgen discovered X-rays in 1895. X-rays interact with electrons in matter and these electrons scatter the X-rays in various directions. Each crystalline substance has a characteristic arrangement of atoms which diffracts X-rays in unique patterns. X-rays reflections takes place from lattice planes according to Bragg's Law:

$$n\lambda = 2d \sin \alpha \ (n=1, 2, 3\ldots..) \qquad (3.2)$$

where λ is the wavelength of the X-rays, d is the lattice spacing, α is the half value of the diffraction angle and n is the order of the reflection and can be any whole number. The wavelength (λ) is determined by the type of X-ray tube, typical wavelengths used for X-ray experiments lie between 0.6 and 1.9Å [24]. A detector is used to scan a range of angles of reflections and this therefore gives a pattern of peaks with certain spacings and intensities. Planes with high electron density will yield strongly intensities whereas planes with low electron density will yield weak intensities. Due to the presence of polycrystalline diffracting domain aggregates, crystallite size may be the same thing as particle size. Scherrer first observed that small crystallite size would give rise to peak broadening. He derived a well-known equation for relating the crystallite size to the peak width, which is called the Scherrer formular:

$$D = \frac{k\lambda}{\beta Cos\theta} \tag{3.3}$$

where D is the average dimension of crystallites; k is the Scherrer constant, a somewhat arbitrary value that falls in the range 0.17-1.0 (and is usually assumed to be 1); λ is the wavelength of the X-rays; and β is the intergral breadth of a reflection (in radians). β is often calculated relative to a reference solid (with crystallite size 7500 nm) added to the sample, $\beta^2 = \beta^2_s - \beta^2_r$ (Where β^2_s and β^2_r are peak widths of the sample and standard in radians). Several factors could change XRD reflections, eg crystallite size, ovelap of peaks, microstrain, lattice structure, and stacking faults [104].

In addition to the information provided, the lattice parameter (α) can be calculated by the following equation:

$$\alpha_0 = d\,(h^2+k^2+l^2)^{1/2} \tag{3.4}$$

where h, k, and l constitutes the Miller indices of a crystal facet, and *d* is the interplanar spacing determined by Bragg's Law.

In XRD analysis, the dry electro-catalyst samples were mounted in plastic sample holders and the surface was flattened to allow maximum X-rays exposure. XRD analysis was done at iThemba LABS, diffractograms were recorded using Bruker AXS D8 Advance measurements X-ray diffractometer.

The XRD parameters for the analysis are given as follows: tube (copper), detector (sodium iodide), monochromator (graphite), generator operation (40kV and 40mA), electron intensity (40 kV), X-ray source (Cu K_α (λ=1.5418Å)), current (30mA), scan range-$2\theta^0$ (5-100) and scan rate-^{0}/min (0.05).

3.3 ELECTROCHEMICAL CHARACTERIZATION OF SUPPORTED ELECTRO-CATALYSTS

3.3.1 Cyclic Voltammetry (CV)

Cyclic voltammetry is the most widely used technique in electrochemistry. It provides information about catalysts and electrochemical reactions, such as the electrochemical response of catalysts and the catalytic activity of the catalysts with respect to some electrochemical reactions [105]. It offers a rapid location of redox potentials of the electro-active species. In cyclic voltammetry the voltage is swept between two values at a fixed rate, resulting in a forward and reverse scan (anodic and cathodic, respectively) however now when the voltage reaches the forward scan (anodic), the scan is reversed and the voltage is swept back to where the scan started (cathodic). The solution contains only a single electrochemical reactant. The electrolysis product is converted back to the reactant when the scan is reversed. The current flow occurs in the opposite way to the forward sweep, it is now from the solution species back to the electrode but otherwise the behaviour can be said to be identical [106].

The platinum active surface area Ar (in cm^2) is estimated by integrating the charge Q_H in the adsorption-desorption region of hydrogen in the potentials range between -0.2 and 0.1V/SCE. Then, the adsorption charge is evaluated as follows:

$$Q_H = \frac{(Q_{adsorption} + Q_{desorption})}{2} \qquad (3.5)$$

where $Q_{adsorption}$ and $Q_{desorption}$ are the absolute values of the charge corresponding to the anodic and cathodic parts of hydrogen region expressed in C (coulomb). Electrochemical surface area measurements (ECSA) of platinum are calculated from both integration of the hydrogen adsorption and desorption peaks. Assuming a correlation value of 210μC/cm^2 [107, 108].

$$A_r = \frac{Q_H}{210\mu C / cm^2} \qquad (3.6)$$

where A_r is the real or electro-active in surface area cm^2, Q_H ($Q_H=(Q_{ad}+Q_{des})/2$) is the hydrogen adsorption/desorption peak, 210μC/cm^2 is the theoretical charge for full monolayer coverage of hydrogen adsorption/desorption on platinum.

The evaluation of the platinum surface area available for the electrochemical reaction allows the total platinum surface area/geometric surface area ratio to be obtained. Since the Pt

loading is known, it is possible to estimate the electro-chemical surface area of Pt. The electro-chemical surface area is calculated from the real surface area and the platinum loading [109, 110].

$$S_{ECSA} = \frac{100A_r}{mAg} \tag{3.7}$$

where A_r is the real surface area, m is the platinum loading, and Ag is the geometric surface area.

In an electrochemical reaction, the exchange current density defines the activity of a catalyst and is given by:

$$i_{0.45V} = \frac{i}{Ag} \tag{3.8}$$

where I is the current and Ag is the geometric surface area.

Alternative ways of defining catalyst activity have emerged, the parameters for determining the activity include mass activity and specific activity. All current densities were calculated from the geometric disk area. Mass activity was calculated from the equation below:

$$MA = \frac{i_{0.45V}}{m} \tag{3.9}$$

where MA is the mass activity in A/g, $i_{0.45V}$ is the current density in A/cm^2 at 0.45V, and m is the loading of Pt in mg/cm^2. The value of 0.45V is chosen to avoid inclusion of any concentration polarization [111]. The specific activity (A/cm^2) is defined as:

$$SA = \frac{MA}{m} \tag{3.10}$$

where SA is specific activity of the catalyst, MA mass activity and m is the loading of Pt in mg/cm^2 [111].

In this study Cyclic voltammetry, was used to evaluate the electrochemical activity of the electro-catalysts at room temperature using the Autolab PGSTAT 30. The experiments were conducted in a three electrode cell with a gas diffusion electrode as a working electrode. The platinum basket and a saturated calomel electrode (SCE) were used as counter and reference electrodes, respectively. 0.5M H_2SO_4 was used as the electrolyte in all experiments. For the preparation of the electrode 75mg of Nafion® and 75mg of ultra-pure water were added to 25mg of the catalyst and the mixture was sonicated for 30minutes, and after that time has elapsed 10ml of Iso-2-propanol was added and the solution was sonicated for a further one and a half hour. The solution was then sprayed using a spray gun onto a 4x2 cm^2 area carbon

paper until the calculated amount of 0.25mg/cm^2 Pt loading was reached. A 12mm puncher was used to cut the gas diffusion electrode which was then assembled in a half cell system. Prior to the measurements the 0.5M H_2SO_4 electrolyte solution was purged with nitrogen for an hour to remove dissolved oxygen. The working electrode potential was cycled for 20 cycles between -0.2 and 1.2V vs. SCE at 50mV/s scan rate to remove all contaminants that may be on the electrode surface and to obtain a stable cyclic voltammogram. For oxygen reduction reaction experiments the electrolyte was bubbled with oxygen for 30minutes and after that the electrode was purged with oxygen while the experiment was running. Then the electrode was screened between 1.2 and -0.2V at 20mV/s. This technique was also used to study the behaviour of the electro-catalysts in the presence of methanol. 0.5M of methanol was used to monitor which of these catalysts tolerated the poison in a better way. The 0.5M of methanol and 0.5M H_2SO_4 solution was purged with nitrogen and the working electrode potential was cycled between -0.2 and 1.2V vs. SCE at 20mV/s scan rate. All the gases used were from Afrox Company. The specifications were as follows: Voltammetric assemble AUTO LAB (Metrohm (Eco Chemie BV, Netherlands)), Working electrode: (Gas diffusion electrode (Pt)), Reference electrode (Saturated calomel electrode) and Counter electrode (Platinum wire mesh).

3.3.2 Rotating disk electrode (RDE)

The Rotating disk electrode is the most common hydrodynamic technique for the evaluation of electro-catalysts. The oxygen reduction reaction is a complex combination of charge and mass transport processes by which the low concentration of oxygen in acid environment is usually studied under hydrodynamic conditions [110]. The RDE technique has been used extensively to study electrode kinetics of oxidation and reduction reactions. The variation of the mass transport can be analysed as a function of the rotation speed. This was first solved mathematically by Levich who showed a relationship between current and the rotation speed, for a reversible electron transfer reaction. Analysis of data from the RDE is commonly done by applying the Koutecky-Levich equation [112]. However, the current measured in an electrochemical environment contains kinetic and diffusion limited components according to the Koutecky-Levich equation [113]:

$$\frac{1}{j} = \frac{1}{j_K} + \frac{1}{j_D} = \frac{1}{j} + \frac{1}{B\omega^{1/2}} \qquad (3.11)$$

where j is the limiting current produced by the oxidation or reduction of electro-active species at the electrode surface. For an RDE, j_D can also be expressed in terms of the Levich slope, B by the following equation:

$$j_D = 0.62nFA\, C_{o2}\, D_{o2}^{2/3} \upsilon^{-1/6} \omega^{1/2} = B\omega^{1/2} \quad (3.12)$$

K-L method substituting equation 3.11 and 3.12 gives a useful form of the K-L equation for the RDE experiments:

$$\frac{1}{j} = \frac{1}{j_K} + \frac{1}{0.062nFA[C]_{BULK} D^{2/3} \upsilon^{-1/6} \omega^{1/2}} \quad (3.13)$$

where j is the limiting current produced by the oxidation or reduction of electro-active species at the electrode surface, n is the number of electrons transferred per O_2 molecule, F is the Faraday constant, ω is the disk rotation speed, Co_2 is the bulk O_2 concentration, Do_2 is the O_2 diffussion coefficient, and υ is the solution kinematic viscosity [114]. For cathodic reactions governed by mixed transport-kinetic controls, plots of 1/j vs $1/\omega^{1/2}$ are predicted to generate straight lines having slopes proportional to 1/n [114]. The slope of the straight lines in K-L plot, allows the evaluation of the number of electrons involved in ORR. Values lower than 4.0 are attributed to the formation of hydrogen peroxide. The four-electron transfer is critical for the development of practical PEMFCs. Note that the slopes of the plots are independent of applied overpotential, but the rate constant may be dependent on potential.

According to electrode kinetic theory [115], the kinetic current density (i_K) can be expressed as a Tafel form:

$$\eta = a - \frac{2.3RT}{\alpha nF} \log j_K \quad (3.14)$$

where η is the overpotential, a is an exchange current density related constant, R is the gas constant, T is the temperature, F is the faraday constant, n is the electron transfer number in the determining step of the ORR, and α is the electron transfer coefficient. The plot of η and log j_K gives a linear relationship, and the slope is 2.303RT/αnF. This slope is called the Tafel slope. The higher the Tafel slope, the faster the overpotential increases with the current density. Thus, for an electrochemical reaction to obtain a high current density at low overpotentials, the reaction should exhibit a low Tafel slope. For ORR usually two Tafel slopes are obtained, 60mV/dec and 120mV/dec, respectively, depending on the electrode materials used and on the potential range. The transfer coefficient is a key factor determining the Tafel slope. For ORR, the transfer coefficient depends on temperature. The Tafel slope can be used to calculate the exchange current from the y-intercept of the Tafel regions.

According to the relationship of η and log (j_K) at different potentials, the Tafel slopes can be calculated.

All electrochemical measurements were conducted on an AUTOLAB PGSTAT 30 with a rotating disk electrode, in a standard three-electrode cell at room temperature, adopting a saturated calomel electrode (SCE) and a platinum mesh as the reference electrode and the counter electrode, respectively. A glassy carbon (GC) disk electrode, polished to a mirror-finish with a 0.05μm alumina suspension before each experiment, was used as substrate for the electro-catalyst thin film in the electrochemical measurements. The thin film catalyst layer as the working electrode was prepared by adding 10mg of catalyst in 4ml of water mixed with 5w/o Nafion solution (DuPont) followed by sonication for five minutes. The electrode was dried at room temperature (~25 ^{0}C) for about 15 minutes [116]. 10 μl of the catalyst ink was then quantitatively transferred onto the surface of the glass carbon electrode by using a micropipette, and dried in an oven for about 15minutes to obtain a catalyst thin film. An aqueous solution containing 0.5M H_2SO_4 was used as the electrolyte for ORR studies and the same solution containing 0.5M methanol was used as the electrolyte for the study of methanol tolerance of the catalysts. For the experiments, the electrolyte was saturated with oxygen for 30minutes. Hydrodynamic voltammograms (at rotation speed varied from 500 to 2500 in 0.5M H_2SO_4 solution saturated with O_2 for about 30 minutes) for ORR were recorded between 1.0 and 0.0V versus SCE and vise versa for methanol tolerance studies, at a scan rate of 5mV/s.

The next chapter will be discussing the results from the analysis of the catalysts employing the methods discussed in this chapter.

CHAPTER 4

RESULTS AND DISCUSSION: STRUCTURAL AND ELECTROCHEMICAL CHARACTERIZATION OF NANOPHASE ELECTRO-CATALYSTS

In this chapter the results of the platinum based catalysts physical characterization will be presented. This chapter evaluates the investigation of structural and electrochemical properties of such catalysts by using the experimental tasks formulated in the literature review and the methodologies given in chapter 3. The results in this section start with morphological characterization of the platinum based catalysts using optical microscopy such as, high resolution transmission electron microscopy followed by crystallinity and graphitization characterization using X-ray diffraction.

The electrochemical characterization of the catalysts is also presented in this chapter. The electrochemical characterization will be done using the cyclic voltammetry (CV) and Rotating disk electrode (RDE) techniques introduced in section 3.3.1 and section 3.3.2, respectively. The RDE and CV will be used to investigate cathode catalysts which have enhanced or better activity for ORR in a PEMFC and DMFC. For a DMFC a better cathode catalyst is a catalyst that its ORR activity will not be affected by the methanol crossover and this will be studied using the RDE. The CV will also be used to study the methanol oxidation reaction of the catalysts as anode catalysts for a DMFC.

4.1 PARTICLE SIZE AND PARTICLE DISTRIBUTION STUDY OF SUPPORTED CATALYSTS (HRTEM)

HRTEM was used to study the morphology of the catalysts. It was also used to determine the particle size and the particle distribution of the catalysts on the carbon support. The carbon support is observed in the HRTEM images as large grey particles with small black Pt particles distributed upon them. Micrographs of HRTEM analysis for the platinum based catalysts are presented in the Figures below.

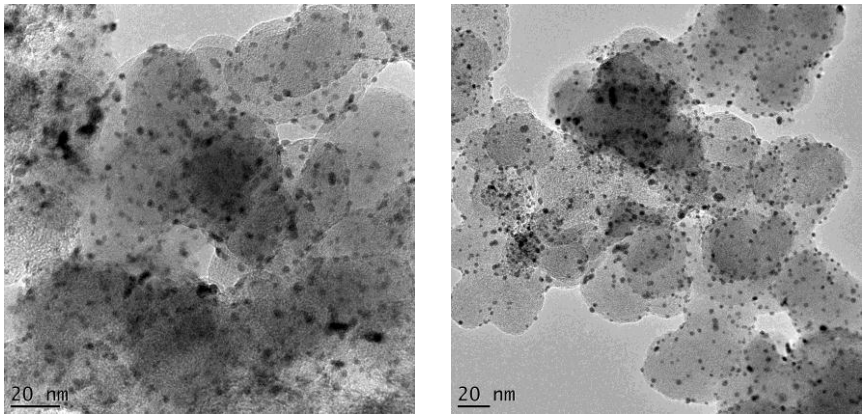

(a) (b)

Figure 4.1: HRTEM images of a) 10%Pt/C Commercial and b) 10%Pt/C In-house electro-catalysts

Figure 4.1 compares the HRTEM images of 10%Pt/C commercial and in-house catalysts and the particle distribution on the catalyst support. As it can be seen, the particles are nicely dispersed on the catalyst support showing no agglomeration. The average particle sizes of the 10%Pt/C commercial and in-house catalyst were found to be 3.54 nm and 3.11 nm, respectively as shown in Table 4.1. The 10%Pt/C in-house catalysts was observed to have smaller particle size than the 10%Pt/C commercial catalyst.

Table 4.1: Particle sizes of 10%Pt/C electro-catalysts

Catalysts	**10%Pt/C Commercial**	**10%Pt/C In-house**
Particle size (nm)	3.54	3.11

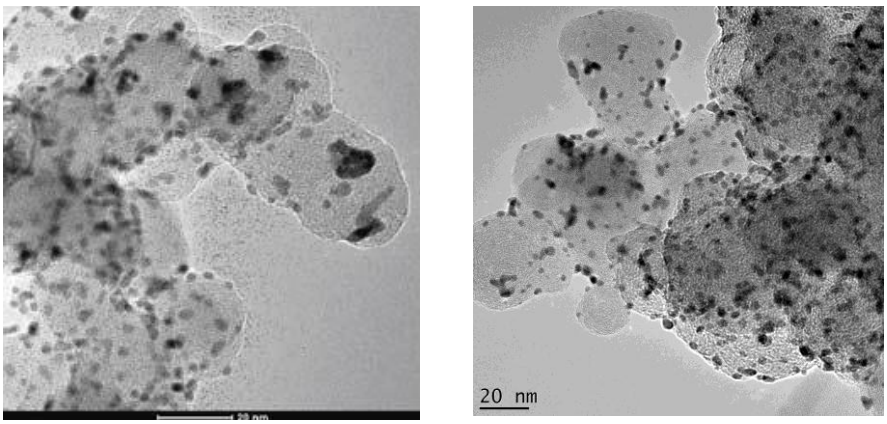

(a) (b)

Figure 4.2: HRTEM images of a) 20%Pt/C Commercial and b) 20%Pt/C In-house electro-catalysts

The HRTEM images in Figure 4.2 show that the particles are homogeneously dispersed on the surface of the carbon support with less agglomeration on some parts of the image. The average particle sizes of these catalysts were found to be 3.43 nm for the 20%Pt/C commercial catalyst and 3.02 nm for the 20%Pt/C in-house catalyst (see Table 4.2).

Table 4.2: Particle sizes of 20%Pt/C electro-catalysts

Catalysts	**20%Pt/C Commercial**	**20%Pt/C In-house**
Particle size (nm)	3.43	3.02

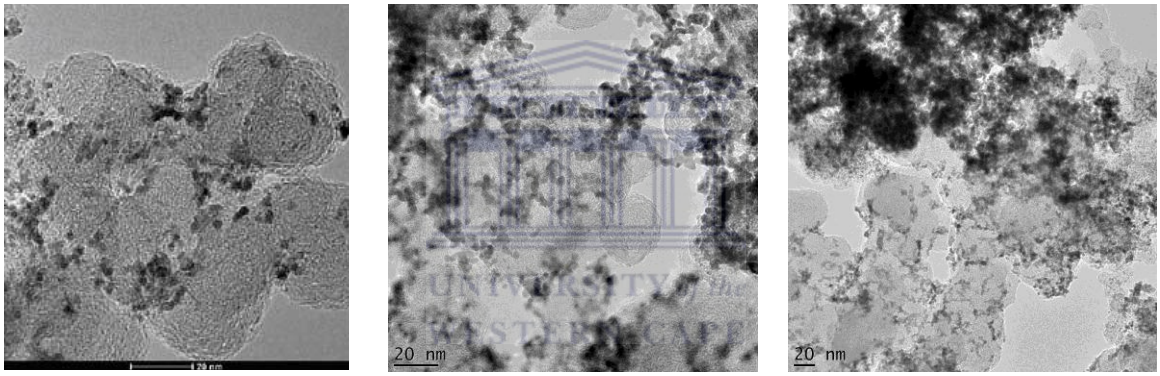

(a) (b) (c)

Figure 4.3: HRTEM images of a) 20%Pt10%Ru/C Commercial, b) 30%Pt15%Ru/C In-house and c) 40%Pt20%Ru/C In-house electro-catalysts

Representative HRTEM images of the catalysts in Figure 4.3 shows less agglomeration in some parts of the 20%Pt10%Ru/C commercial catalyst but the 30%Pt20%Ru/C and 40%Pt20%Ru/C in-house catalysts show very much agglomeration, the particles are very much agglomerated compared to the commercial catalyst. The average particle sizes of the 20%Pt10%Ru/C commercial, 30%Pt15%Ru/C in-house and 40%Pt20%Ru/C in-house catalysts were found to be 2.75 nm, 2.98 nm and 2.96 nm, respectively as shown in Table 4.3 and this shows that there is no particle size growth of PtRu/C catalysts.

Table 4.3: Particle sizes of PtRu/C electro-catalysts

Catalysts	20%Pt10%Ru/C Commercial	30%Pt15%Ru/C In-house	40%Pt20%Ru/C In-house
Particle size (nm)	2.75	2.98	2.96

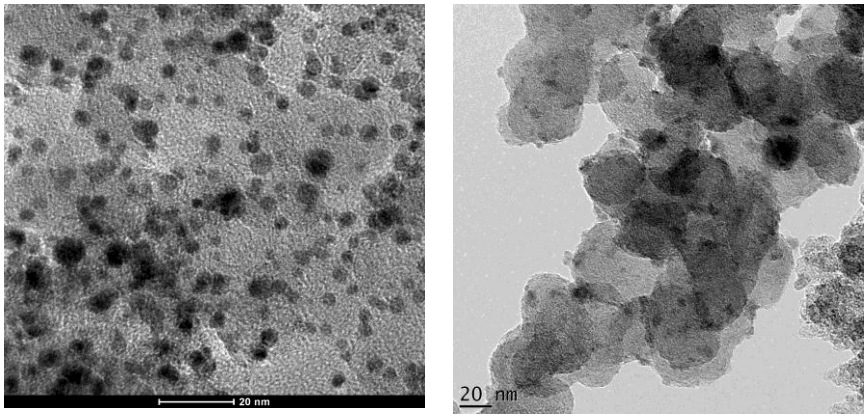

(a) (b)

Figure 4.4: HRTEM images of a) 20%PtCo/C Commercial and b) 30%PtCo/C In-house electro-catalysts

Figure 4.4 shows typical images of 20%PtCo/C commercial catalyst and 30%PtCo/C in-house catalyst. The particles of the 20%PtCo/C commercial catalyst are well dispersed on the catalyst support in a good uniformity and the particles show spherical shape and the particles are well defined and easy to identify. The particles of the 30%PtCo/C in-house catalyst are observed to be very much agglomerated so much that it is very much difficult to identify the particles. The average particle size for the 20%PtCo/C commercial catalyst was obtained as 3.14 nm and that of the 30%PtCo/C in-house catalyst was obtained as 3.89 nm as shown in Table 4.4.

Table 4.4: Particle sizes of PtCo/C electro-catalysts

Catalysts	20%PtCo/C Commercial	30%PtCo/C In-house
Particle size (nm)	3.14	3.89

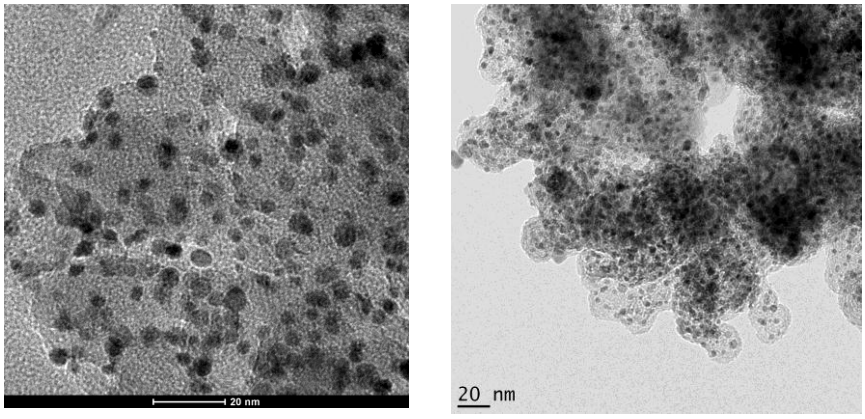

(a) (b)

Figure 4.5: HRTEM images of a) 20%PtCu/C Commercial and b) 20%Pt20%Cu/C In-house electro-catalysts

The HRTEM micrographs of 20%PtCu/C commercial catalyst and 20%Pt20%Cu/C in-house catalyst are presented in Figure 4.5. It is observed that the particles are well dispersed on the support of the 20%PtCu/C commercial catalyst and well separated spherical fringes are observed. The particles are well defined and easy to identity with no agglomeration observed. In Figure 4.5b it is noted that the 20%Pt20%Cu/C in-house catalyst particles are nicely dispersed on the catalyst support with less agglomeration on some portion of the image but, though there particles are less agglomerated. The average particle size of the 20%PtCu/C commercial catalyst was found to be 2.88 nm and that of the 20%Pt20%Cu/C in-house catalyst was found to be 4.18 nm as shown in Table 4.5.

Table 4.5: Particle sizes of PtCu/C electro-catalysts

Catalysts	**20%PtCu/C Commercial**	**20%Pt20%Cu/C In-house**
Particle size (nm)	2.88	4.18

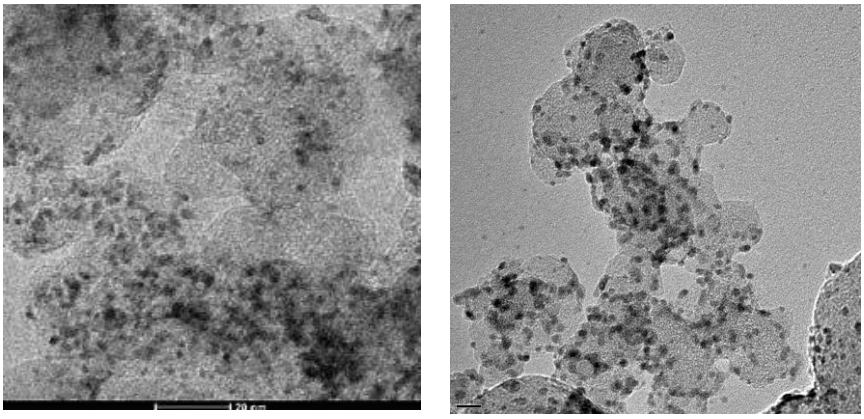

(a) (b)

Figure 4.6: HRTEM images of a) 20%PtSn/C Commercial and b) 20%PtSn/C In-house electro-catalysts

In Figure 4.6 HRTEM images of 20PtSn/C commercial and in-house electro-catalysts are given. Figure 4.6a shows the TEM image of the 20%PtSn/C commercial catalyst and in this image it is observed that the particles are nicely dispersed on the carbon support and the particles are agglomerated on some parts of the image. With the in-house catalyst, the particles are nicely dispersed onto the carbon support and the image doesn't seem to show any agglomeration. The particles size of the 20%PtSn/C commercial and in-house catalysts were found to be 3.42 nm and 4.72 nm, respectively as shown by Table 4.6.

Table 4.6: Particle sizes of PtSn/C electro-catalysts

Catalysts	**20%PtSn/C Commercial**	**20%PtSn/C In-house**
Particle size (nm)	3.42	4.72

(a) Effect of heat treatment on the morphology of the 20%PtCo/C commercial and 30%PtCo/C in-house electro-catalysts

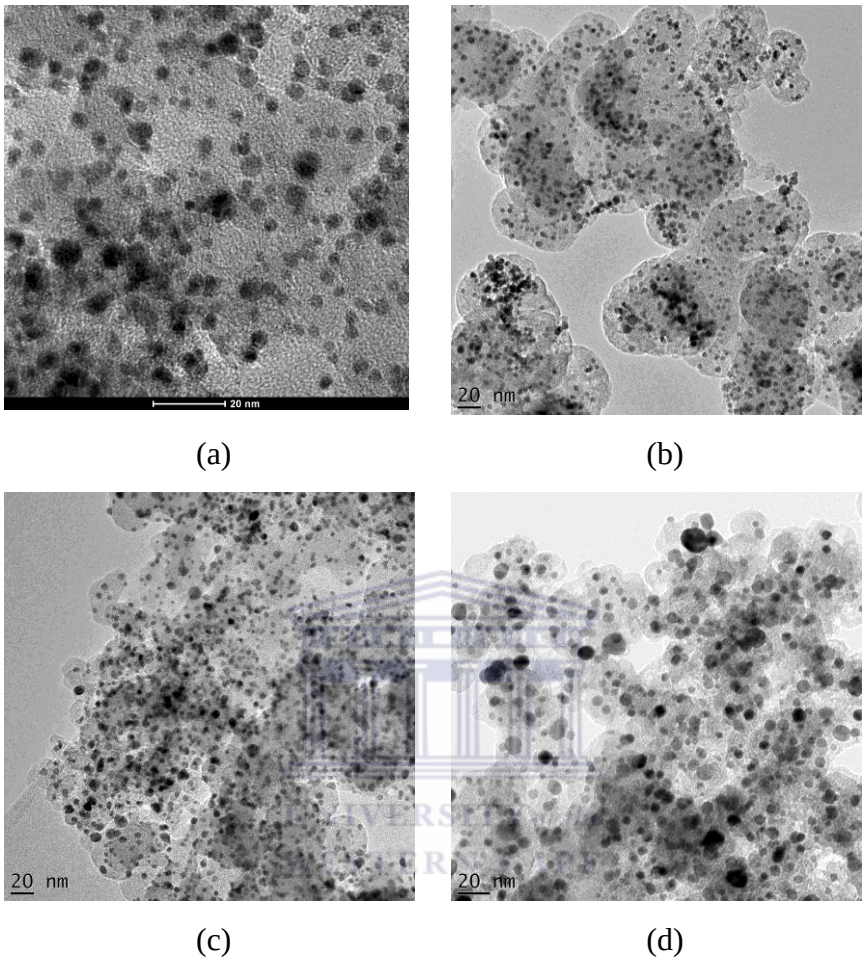

(a) (b)

(c) (d)

Figure 4.7: HRTEM images of a) 20%PtCo/C Commercial (un-sintered), b) 20%PtCo/C Commercial (350^{o}C), c) 20%PtCo/C Commercial (650^{o}C) and d) 20%PtCo/C Commercial (800^{o}C) electro-catalysts

The 20%PtCo/C commercial catalyst was heat treated at different temperatures. The HRTEM images for the catalyst heat treated at different temperatures are given in Figure 4.7. In Figure 4.7a, the image of the un-sintered 20%PtCo/C commercial catalyst, the particles are nicely dispersed onto the carbon support and the particles are easy to point out. It is observed that with the un-sintered catalyst the particles are quite big compared to the sintered catalyst at different temperatures. The particles are nicely dispersed on the carbon support for the catalysts heat treated at different temperatures and shows a bit of agglomeration on some parts of the image observed in Figure 4.7d, the 20%PtCo/C commercial (800^{o}C). The particle

sizes of the commercial catalyst was found to be 3.30 nm for the 20%PtCo/C commercial (350^{o}C), 3.45 nm for the 20%PtCo/C commercial (650^{o}C), and 3.67 nm for the 20%PtCo/C commercial (800^{o}C). The particles size of the un-sintered 20%PtCo/C commercial was found to be 3.14 nm and it is observed that the particle size slightly increased when the catalyst was heat treated with increasing temperature as illustrated in Table 4.7 and this shows that there is particle size growth with increasing temperature.

Table 4.7: Particle sizes of heat treated 20%PtCo/C Commercial electro-catalysts

Catalysts	**20%PtCo/C Commercial (Un-sintered)**	**20%PtCo/C Commercial (350^{o}C)**	**20%PtCo/C Commercial (650^{o}C)**	**20%PtCo/C Commercial (800^{o}C)**
Particle sizes (nm)	3.14	3.30	3.45	3.67

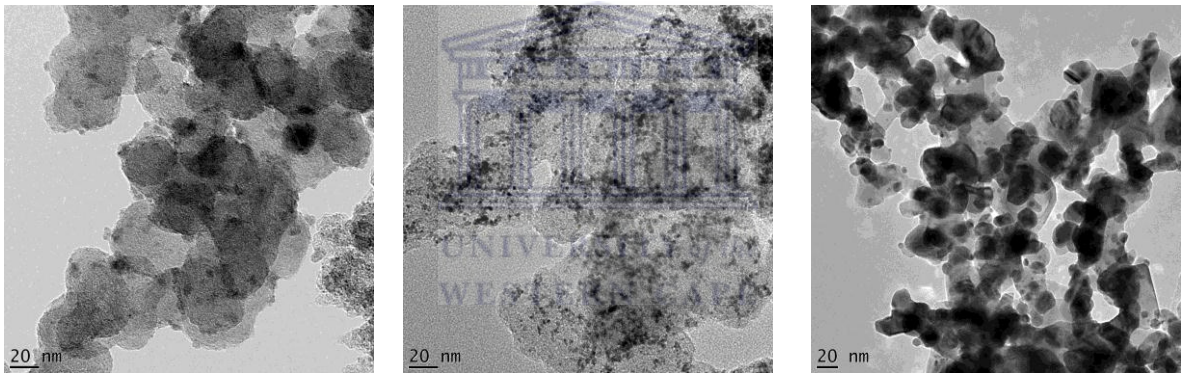

(a) (b) (c)

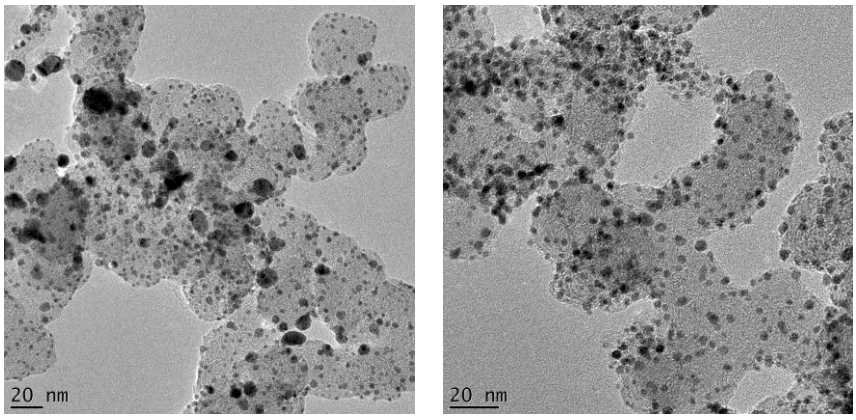

(d) (e)

Figure 4.8: HRTEM images of a) 30%PtCo/C In-house (un-sintered), b) 30%PtCo/C In-house (350^{o}C), c) 30%PtCo/C In-house (650^{o}C), d) 30%PtCo/C In-house (800^{o}C) and e) 20%PtCo/C In-house (800^{o}C) electro-catalysts

Figure 4.8 portrays the HRTEM images of the heat treated 30%PtCo/C in-house catalysts. From Figure 4.8a which represents the image of the un-sintered 30%PtCo/C in-house catalyst, the particles are very much agglomerated but when this catalyst was heat treated at 350 ^{0}C and 800 ^{0}C the particles showed less agglomeration. The particles are also observed to be agglomerated when this catalyst was heat treated at 650 ^{0}C. The particle sizes of the 30%PtCo/C in-house (350 ^{0}C), 30%PtCo/C in-house (650 ^{0}C), 350%PtCo/C in-house (800 ^{0}C) and 20%PtCo/C in-house (800 ^{0}C) were found to be 3.00 nm, 5.02 nm, 4.50 nm and 2.98 nm, respectively (see Table 4.8). The particle size of the 30%PtCo/C un-sintered catalyst was found to be 3.89 nm and when this catalyst was heat treated at 650 ^{0}C and 800 ^{0}C the particle size increased and decreased when heat treated at 350 ^{0}C. The 20%PtCo/C in-house (800 ^{0}C) catalyst particle size decreased compared to that of the 30%PtCo/C in-house (800 ^{0}C) catalyst. The particle size growth is increasing with increasing the temperature for the PtCo/C catalyst.

Table 4.8: Particle sizes of heat treated 30%PtCo/C In-house electro-catalyst

Catalysts	**30%PtCo/C In-house (Un-sintered)**	**30%PtCo/C In-house (350^{o}C)**	**30%PtCo/C In-house (650^{o}C)**	**30%PtCo/C In-house (800^{o}C)**	**20%PtCo/C In-house (800^{o}C)**
Particle size (nm)	3.89	3.00	5.02	4.50	2.98

4.1.1 Summary of particle size and particle distribution of supported catalysts (HRTEM)

From the HRTEM analysis above, it is observed that the catalyst with small particle size was found to be 20%Pt10%Ru/C with a particle size of 2.75 nm. The particles were nicely dispersed on the carbon support with other catalysts but with the PtRu/C and PtCo/C in-house catalysts the particles were agglomerated. The PtCo/C commercial and in-house catalysts were heat treated and it was observed that with the in-house catalyst the particle size decreased for the catalyst heat treated at 350 ^{0}C and was smaller compared to the un-sintered PtCo/C in-house and commercial catalysts .The particle size of the commercial PtCo/C catalyst was observed to increase as the heating temperature increased.

4.2 PARTICLE SIZE AND CRYSTALLINITY STUDY OF SUPPORTED CATALYSTS (XRD)

The XRD technique reveals information on the crystallinity of the catalysts, particle size, degree of alloying and lattice spacing of platinum based catalysts. This section presents the results based on the above mentioned parameters.

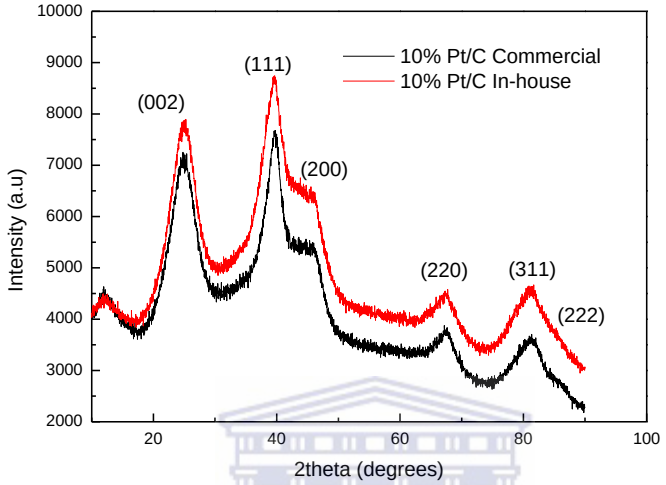

Figure 4.9: X-ray diffraction patterns of 10%Pt/C Commercial and 10%Pt/C In-house electro-catalysts

The XRD results in Figure 4.9 show a peak (002) at 2θ approximately 25^0 corresponding to the carbon support. The peaks at 40^0, 46^0, 68^0, 82^0 and 90^0 are attributed to Pt (111), (200), (220), (311) and (222) crystal facet, respectively. This graph shows a peak at 40^0 (2θ) corresponding to Pt(111) with 2θ values not far from the expected 40 degrees . These peaks indicate that Pt is present in the face centred cubic (fcc) structure. From the extent of the line broadening of Pt(111) peak of the 10%Pt/C commercial and in-house catalysts the particle sizes were estimated to be about 3.50 nm for the 10%Pt/C commercial and 3.06 nm for the 10%Pt/C in-house catalysts, the results agrees with the HRTEM results with a slight difference (see Table 4.9). The peaks are almost similar in broadness and intensity which could mean that the crystallinity of these samples doesn't differ much just like it is observed that the particle size does not differ much.

Table 4.9: XRD analysis of 10%Pt/C electro-catalysts

Catalysts	D (nm)	*a* (nm)	$2\Theta_{max}$ (degrees)	Θ (degrees)
10%Pt/C Commercial	3.50	3.21	39.72	19.86
10%Pt/C In-house	3.06	3.2	39.8	19.79

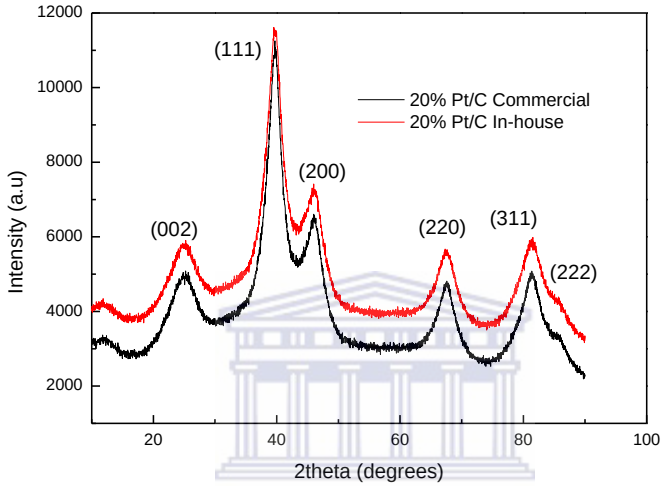

Figure 4.10: X-ray diffraction patterns of 20%Pt/C Commercial and 20%Pt/C In-house electro-catalysts

Figure 4.10 compares the XRD patterns of 20%Pt/C commercial and in-house catalysts. Similar trends to Figure 4.9 were observed for these catalysts where the XRD patterns of these catalysts were found to be without any additional peaks. The XRD patterns of these catalysts show narrow and more intense peaks, suggesting that the particles are more crystalline. The particle size of the 20%Pt/C commercial catalyst was found to be 3.40 nm and that of the 20%Pt/C in-house catalyst was found to be 2.97 nm, respectively (see Table 4.10) and the results agree with the TEM results with a slight difference.

Table 4.10: XRD analysis of 20%Pt/C electro-catalysts

Catalysts	D (nm)	*a* (nm)	$2\Theta_{max}$ (degees)	ϴ (degrees)
20%Pt/C Commercial	3.40	3.20	39.75	19.88
20%Pt/C In-house	2.97	3.21	39.70	19.85

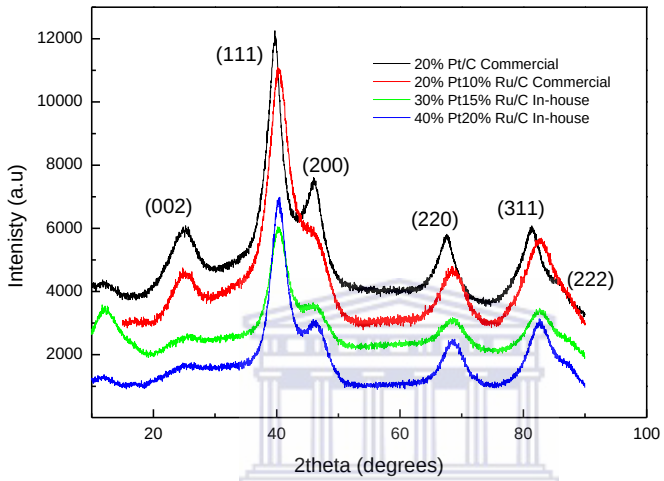

Figure 4.11: X-ray diffraction patterns of 20%Pt/C Commercial, 20%Pt10%Ru/C Commercial, 30%Pt15%Ru/C In-house and 40%Pt20%Ru/C In-house electro-catalysts

The first peak at 25^0 in Figure 4.11 is attributed to the carbon support as observed for previous catalysts. The other peaks are characteristic reflections of Pt corresponding to the fcc crystalline structure of Pt. The lattice parameters obtained for these catalysts in Figure 4.11 are smaller than that of Pt/C catalyst indicating a lattice contraction upon alloying. The Pt(111) peak increases in intensity as the Pt and Ru content increases suggesting high current densities of (111) orientated crystals. A degree of alloying was found for the platinum binary catalysts as indicated by the shift of the reflection peaks to higher 2θ values and to the decrease of the lattice parameter (see Table 4.11) as it is previously mentioned. The particle size D and the lattice parameter were calculated from the Pt(111) peak position. For the 20%Pt10%Ru/C commercial the particle size was found to be 2.72 nm, for 30%Pt15%Ru/C in-house was found to be 2.94 nm and 40%Pt20%Ru/C in-house was found to be 2.98 nm.

Table 4.11: XRD analysis of PtRu/C electro-catalysts

Catalysts	D (nm)	*a* (nm)	$2\theta_{max}$ (degrees)	θ (degrees)
20%Pt/C Commercial	3.40	3.20	39.75	19.88
20%Pt10%Ru/ Commercial	2.72	3.16	40.36	20.18
30%Pt15%Ru/C In-house	2.94	3.16	40.32	20.16
40%Pt20%Ru/C In-house	2.98	3.17	40.23	20.11

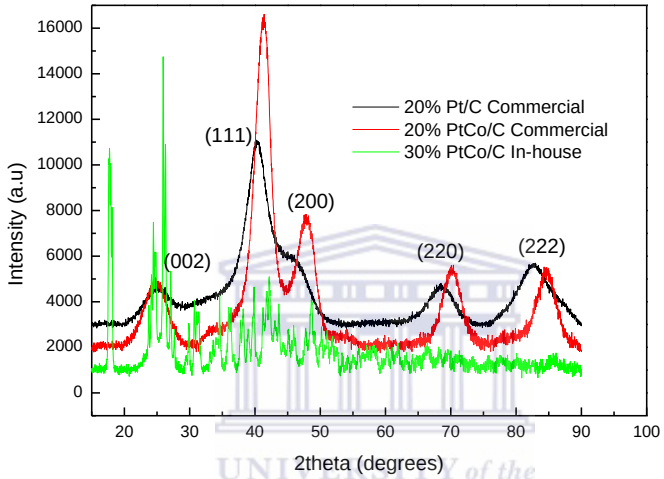

Figure 4.12: X-ray diffraction patterns of 20%Pt/C Commercial, 20%PtCo/C Commercial and 30%PtCo/C In-house electro-catalysts

Figure 4.12 clearly shows the characteristic diffraction peaks of the fcc Pt and this implies that a successful reduction of Pt precussor to metallic form has been achieved with the commercial catalyst. The commercial catalyst show well defined peaks compared to the in-house catalyst. The commercial catalyst reveals the peaks characteristic of the fcc Pt without any additional peaks and that is not the case for the in-house catalyst as this catalyst does not show clear peaks and was repeated but did not seem to show clear peaks, that could be due to experimental error.. It is observed that the peaks of commercial catalyst shift to more positive values and this indicates alloy formation between Pt and Co, and indicates a lattice contraction, which is caused by the incorporation of Co into the Pt fcc structure. The lattice parameter (see Table 4.12) obtained for the 20%PtCo/C commercial catalysts is smaller than that of the Pt/C catalyst, indicative of a lattice contraction upon alloying but that is not the

case for the in-house catalyst since its lattice parameter is the same as that of the Pt/C catalyst. The particle size of the 20%PtCo/C commercial catalyst was found to be 3.11 nm and that of the 30%PtCo/C in-house was found to be 4.81 nm and was calculated from the peak at 40 degrees, the Pt(111) facet.

Table 4.12: XRD analysis of PtCo/C electro-catalysts

Catalysts	**D (nm)**	***a* (nm)**	**$2\theta_{max}$ (degrees)**	**θ (degrees)**
20%Pt/C Commercial	3.40	3.20	39.75	19.88
20%PtCo/C Commercial	3.11	3.09	41.32	20.66
30%PtCo/C In-house	4.81	3.20	39.86	19.93

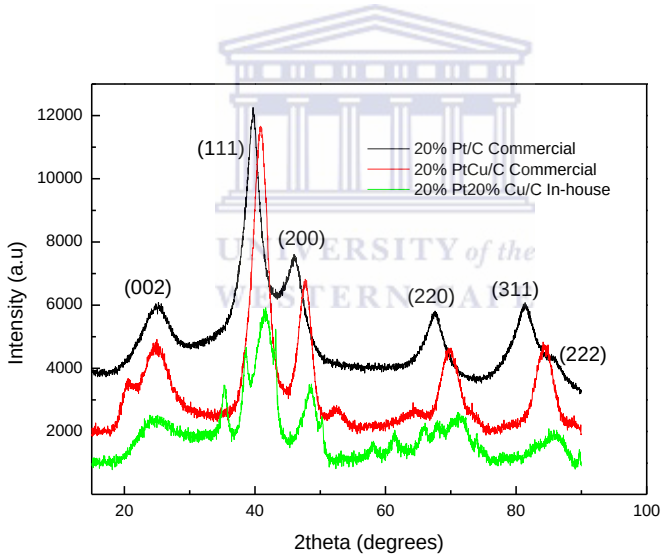

Figure 4.13: X-ray diffraction patterns of 20%Pt/C Commercial, 20%PtCu/C Commercial and 20%Pt20%Cu/C In-house electro-catalysts

With the 20%PtCu/C commercial catalyst given in Figure 4.13, the peaks characteristic of the fcc Pt are observed. The peaks of the commercial catalyst are more intense and narrow compared to the in-house catalyst suggesting that the particles of the commercial catalyst are more crystalline. The Pt fcc peaks are well defined for the commercial catalyst without any additional peaks compared to that of the in-house catalyst with additional peaks. The peaks of

the commercial catalyst shift to more positive values indicating alloy formation and this is in good agreement with the smaller values of the lattice parameter compared to the Pt/C catalyst and this is observed with the in-house catalyst as the lattice parameter also decreases. The particle size of the 20%PtCu/C commercial catalyst and that of the 20%Pt20%Cu/C in-house were found to be 2.85 nm and 4.62 nm, respectively as shown in Table 4.13.

Table 4.13: XRD analysis of PtCu/C electro-catalysts

Catalysts	**D (nm)**	***a* (nm)**	**$2\theta_{max}$ (degrees)**	**θ (degrees)**
20%Pt/C Commercial	3.40	3.20	39.75	19.88
20%PtCu/C Commercial	2.85	3.12	40.90	20.45
20%Pt20%Cu/C In-house	4.62	3.07	41.51	20.76

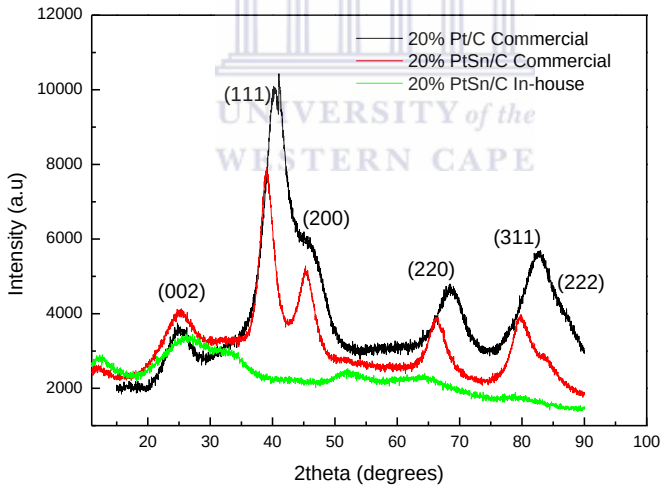

Figure 4.14: X-ray diffraction patterns of 20%Pt/C Commercial, 20%PtSn/C Commercial and 20%PtSn/C In-house electro-catalysts

It is observed (see Figure 4.14) that the 20%PtSn/C commercial catalyst XRD patterns are similar to that of the 20%Pt/C commercial catalyst indicating alloy formation. The peaks characteristic of a Pt fcc are slightly observed with the 20%PtSn/C in-house catalyst but the peaks are not clear and are observed at very small intensities. The particle sizes of the

20%PtSn/C commercial and in-house catalyst were calculated and found to be 3.39 nm and 4.62 nm, respectively (see Table 4.14). It is observed that the in-house catalyst has a bigger particle size than the commercial catalyst.

Table 4.14: XRD analysis of PtSn/C electro-catalysts

Catalysts	D (nm)	*a* (nm)	$2\theta_{max}$ (degrees)	θ (degrees)
20%Pt/C Commercial	3.40	3.20	39.75	19.88
20%PtSn/C Commercial	3.39	3.26	39.01	19.50
20%PtSn/C In-house	4.62	3.82	39.13	19.57

(a) Effect of heat treatment on the morphology of the 20%PtCo/C Commercial and 30%PtCo/C In-house electro-catalysts

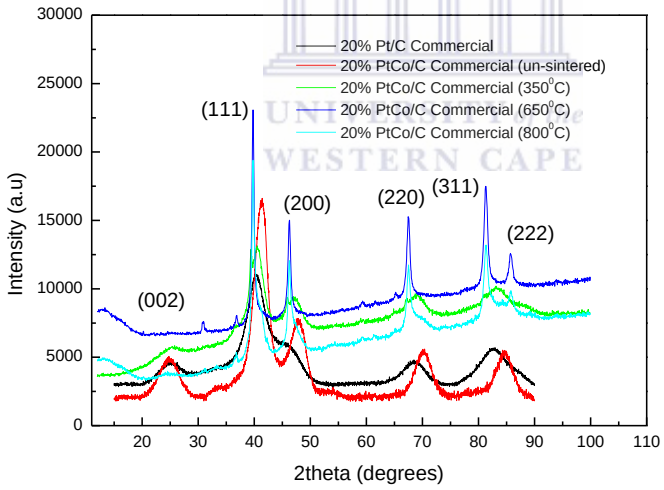

Figure 4.15: X-ray diffraction patterns of 20%Pt/C Commercial, 20%PtCo/C Commercial (un-sintered), 20%PtCo/C Commercial (350^0C), 20%PtCo/C Commercial (650^0C), and 20%PtCo/C Commercial (800^0C) electro-catalysts

Figure 4.15 represents the XRD patterns of the heat treated 20%PtCo/C commercial catalyst. It is clear from the Figure that the catalyst heat treated at 650 ^{0}C and 800 ^{0}C shows more intense and narrow peaks and this suggests that the particles are more crystalline. The particle

sizes of the 20%PtCo/C commercial (350 ^{0}C), 20%PtCo/C commercial (650 ^{0}C), and 20%PtCo/C commercial (800 ^{0}C) were found to be 3.15 nm, 3.28 nm and 3.59 nm, respectively. It is observed that the particle size increased drastically when the catalyst was heat treated at 650 ^{0}C and 800 ^{0}C but did not increase that much when heat treated at 350 ^{0}C.

Table 4.15: XRD analysis of heat treated PtCo/C Commercial electro-catalysts

Catalysts	**D (nm)**	***a* (nm)**	**$2\theta_{max}$ (degrees)**	**θ (degrees)**
20%Pt/C Commercial	3.40	3.20	39.75	19.88
20%PtCo/C Commercial (un-sintered)	3.11	3.09	41.32	20.66
20%PtCo/C Commercial (350^{0}C)	3.15	3.16	40.34	20.17
20%PtCo/C Commercial (650^{0}C)	3.28	3.20	39.76	19.89
20%PtCo/C Commercial (800^{0}C)	3.59	3.20	39.75	19.88

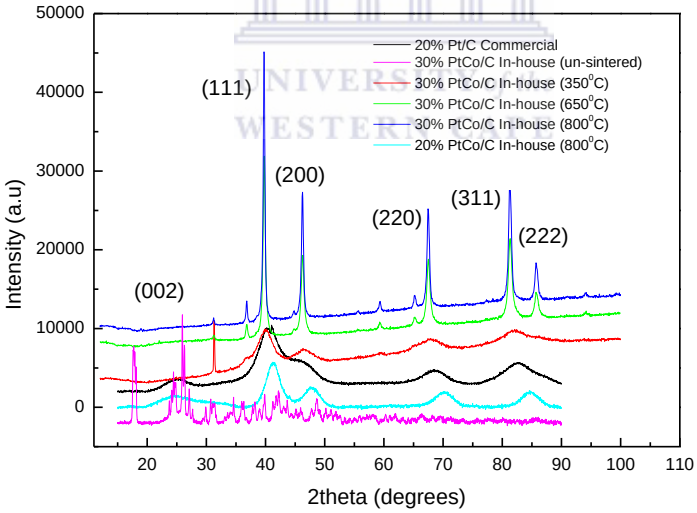

Figure 4.16: X-ray diffraction patterns of 20%Pt/C Commercial, 30%PtCo/C In-house (un-sintered), 30%PtCo/C In-house (350^{0}C), 30%PtCo/C In-house (650^{0}C), 30%PtCo/C In-house (800^{0}C) and 20%PtCo/C In-house (800^{0}C) electro-catalysts

The 20%PtCo/C in-house (800 ^{0}C) and 30%PtCo/C in-house (350 ^{0}C) catalysts show peaks similar to the 20%Pt/C commercial catalyst when heat treated at 350^{0}C (see Figure 4.16). The

lattice parameter (see Table 4.16) decreased for the 20%PtCo/C in-house (800 ^{0}C) and 30%PtCo/C in-house (350 ^{0}C) catalyst indicating alloy formation. It can be seen in Figure 4.16 that the un-sintered catalyst gave several peaks but the 20%PtCo/C in-house (800 ^{0}C) and 30%PtCo/C in-house (350 ^{0}C) catalysts gave peaks characteristic of the Pt fcc but when the 30%PtCo/C in-house catalyst was heat treated at 650 ^{0}C and 800 ^{0}C few small peaks were still observed. The particle size of the un-sintered 30%PtCo/C in-house catalyst was found to be 4.81nm and that of the 20%PtCo/C in-house (800 ^{0}C) and 30%PtCo/C in-house (350 ^{0}C) was found to be 2.92 nm and 2.79 nm, respectively. 30%PtCo/C in-house (650 ^{0}C) and 30%PtCo/C In-house (800 ^{0}C) were found to have particle sizes of 4.96 nm and 4.20 nm, respectively. It is observed that the particle size of the 30%PtCo/C in-house (650 ^{0}C) increased slightly whereas for other heat treated catalysts the particle size decreased and it very much decreased for 30%PtCo/C In-house (350 ^{0}C) and 20%PtCo/C In-house (800 ^{0}C).

Table 4.16: XRD analysis of heat treated PtCo/C In-house electro-catalysts

Catalysts	**D (nm)**	***a* (nm)**	**$2\Theta_{max}$ (degrees)**	**Θ degrees)**
20%Pt/C Commercial	3.40	3.20	39.75	19.88
30%PtCo/C In-house (un-sintered)	4.81	3.20	39.86	19.93
30%PtCo/C In-house (350^{0}C)	2.79	3.18	40.01	20.01
30%PtCo/C In-house (650^{0}C)	4.96	3.20	39.77	19.88
30%PtCo/C In-house (800^{0}C)	4.20	3.20	39.74	19.87
20%PtCo/C In-house (800^{0}C)	2.92	2.78	46.20	23.10

4.2.1 Summary of Particle size and crystallinity study of supported catalysts (XRD)

The XRD study shows that the 20%Pt10%Ru/C commercial catalyst has a smaller particle size compared to other catalysts with a particle size of 2.72 nm which is in good agreement

with the HRTEM results. The 30%PtCo/C in-house catalyst was found to have a bigger particle size compared to other catalysts. This catalyst was observed to have additional peaks compared to the Pt/C fcc peaks together with the 20%Pt20%Cu/C in-house catalysts with similar trends.

4.3 CYCLIC VOLTAMMETRIC STUDY OF THE ACTIVITY AND OXYGEN REDUCTION ON SUPPORTED ELECTRO-CATALYSTS

The Cyclic voltammetry technique was used to electrochemically characterize the electro-catalysts in terms of their electrochemical surface area and their activity towards ORR. The Cyclic voltammograms were screened at -0.2 and 1.2V vs SCE for a normal CV and screened at 1.2 and -0.2V for ORR studies at 20mV/s.

4.3.1 Electrochemical study of the Pt based electro-catalysts

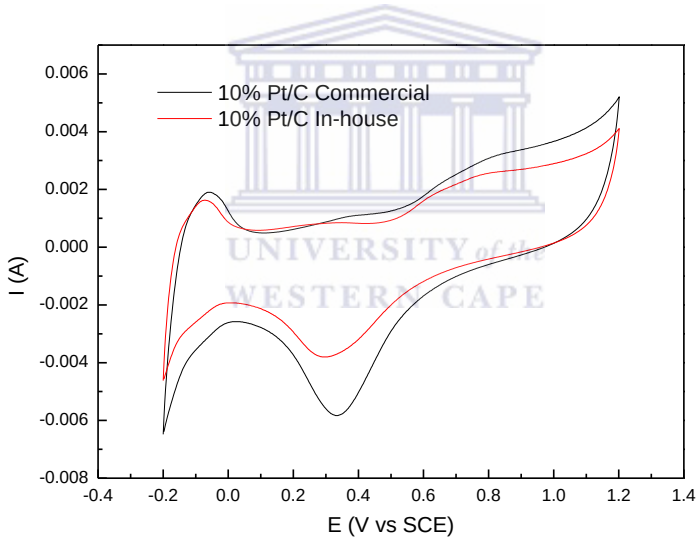

Figure 4.17: Cyclic voltammograms of 10%Pt/C Commercial and 10%Pt/C In-house electro-catalysts in N_2 saturated 0.5M H_2SO_4 at a scan rate of 20mV using a SCE +0.250V reference electrode

The cyclic voltammograms in Figure 4.17 show well defined peaks. Hydrogen desorption, where hydrogen is desorbed from the platinum surface, the double layer region, Pt oxide formation, Platinum reduction and hydrogen adsorption onto Pt surface [118]. The Pt-hydride desorption peak potential appears from -0.2-0.1V for all catalysts, the double layer region appears at the potential of 0.15-0.56V, the Pt-oxide formation appears at 0.6-1.2V, the peak at

0.1 to -0.2 may be attributed to hydrogen adsorption onto the Pt surface [118]. In Figure 4.17 it is observed that 10%Pt/C Commercial has significantly large activity compared to the in-house catalyst and this is also shown by the electrochemical surface area (ECSA) of these catalysts with 10%Pt/C commercial having the ECSA value (see Table 4.17) of 14.7m^2/g compared to 10.7m^2/g for the in-house catalyst and in literature was found to be 14.0m^2/g for the 10%Pt/C commercial catalyst [119].

Table 4.17: Electro-active and electrochemical surface area of 10%Pt/C electro-catalysts

Catalysts	10%Pt/C Commercial	10%Pt/C In-house
Electro-chemical surface area (m^2/g)	14.7	10.7
Electro-active surface area (cm^2)	36.7	26.7

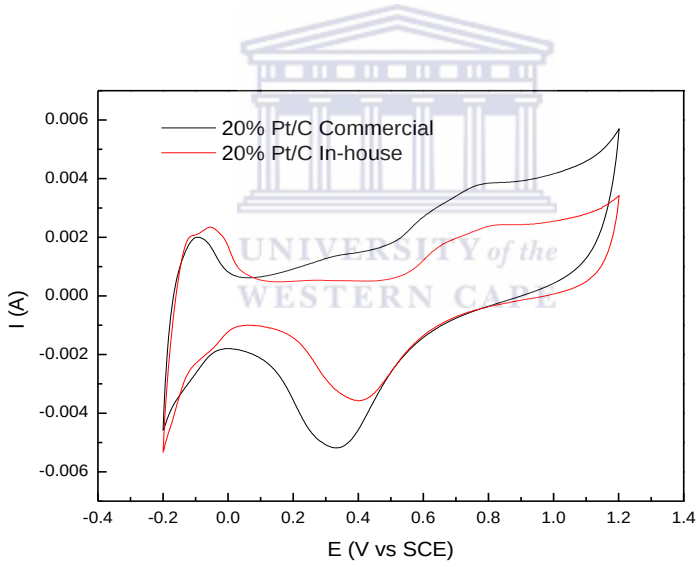

Figure 4.18: Cyclic voltammograms of 20%Pt/C Commercial and 20%Pt/C In-house electro-catalysts in N_2 saturated 0.5M H_2SO_4 at a scan rate of 20mV

Similar trends seen in Figure 4.17 are observed in Figure 4.18, the catalysts exhibit the features of the hydrogen adsorption-desorption region followed by the double layer region and this region is a bit flat or steep compared to the one observed in Figure 4.17. The oxide peak is also observed. The hydrogen adsorption-desorption peaks for the 20%Pt/C commercial catalyst are observed to be smaller than that of the 20%Pt/C in-house catalyst. The ECSA derived from the hydrogen adsorption-desorption peaks was found to be 41.3m^2/g

for the 20%Pt/C in-house catalyst and 34.9 m^2/g for the commercial catalyst (see Table 4.18) and in literature was found to be 56.5 m^2/g for the 20%Pt/C commercial catalyst [119]. Figure 4.18 shows an enhancement in the activity of the 20%Pt/C in-house catalyst and there is a slight shift of the reduction peak towards positive values observed in the in-house catalyst.

Table 4.18: Electro-active and electrochemical surface area of 20%Pt/C electro-catalysts

Catalysts	20%Pt/C Commercial	20%Pt/C In-house
Electrochemical surface area (m^2/g)	34.9	41.3
Electro-active surface area (cm^2)	87.4	103

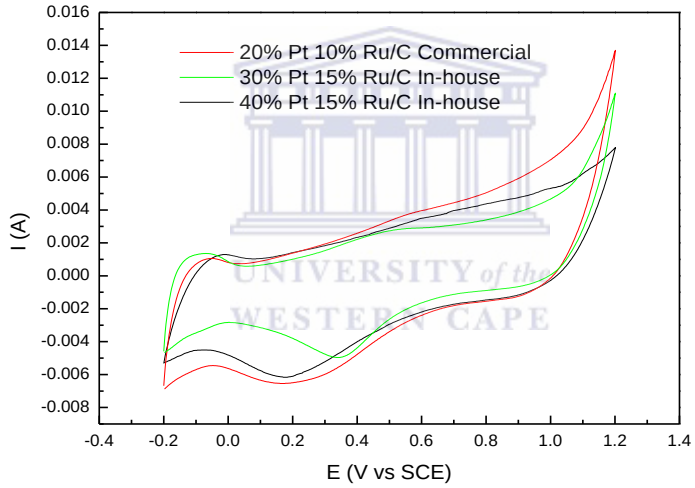

Figure 4.19: Cyclic voltammograms of 20%Pt10%Ru/C Commercial, 30%Pt15%Ru/C and 40%Pt20%Ru/C In-house electro-catalysts in N_2 saturated 0.5M H_2SO_4 at a scan rate of 20mV

The CV curves for all the electro-catalysts in Figure 4.19 exhibit typical cyclic voltammograms with hydrogen adsorption (-0.2-0.1V) and hydrogen desorption (0.1 to -0.2V), no well-defined hydrogen adsorption/desorption peaks are observed for 30%Pt15%Ru/C and 40%Pt20%Ru/C in-house catalysts, suggesting the high dispersion of the catalysts with disordered surface structure was obtained [120]. The Pt-oxide peak was not observed for the 30%Pt15%Ru/C and 40%Pt20%Ru/C in-house catalysts and this absence of the Pt-oxide peak demonstrated that these catalysts are reasonably stable in acidic medium in the applied potential range [69]. The activity enhancement of the catalysts (20%Pt10%Ru/C

commercial, 40%Pt20%Ru/C in-house and 30%Pt15%Ru/C in-house) was found to be with ECSA values of 21.0m^2/g, 4.52m^2/g and 12.6m^2/g, respectively as shown in Table 4.19. The ECSA of 20%PtRu/C catalyst in literature was found to be 91.4 m^2/g which is much higher than the one obtained in this work and this could be attributed to the agglomeration observed in HRTEM for these catalysts [121]. The ECSA increased as the Pt-Ru content increased.

Table 4.19: Electro-active and electrochemical surface area of PtRu/C electro-catalysts

Catalysts	20%Pt10%Ru/C Commercial	30%Pt15%Ru/C In-house	40%Pt20%Ru/C In-house
Electrochemical surface area (m^2/g)	21.0	4.52	12.6
Electro-active surface area (cm^2)	52.5	11.3	31.6

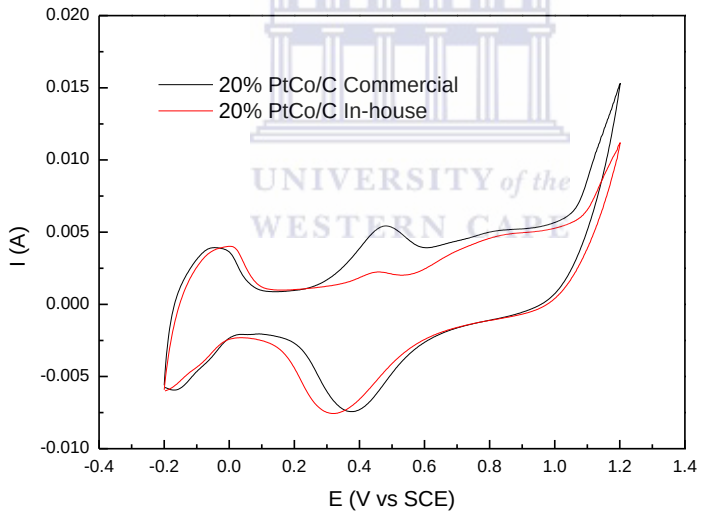

Figure 4.20: Cyclic voltammograms of 20%PtCo/C Commercial and 30%PtCo/C In-house electro-catalysts in N_2 saturated 0.5M H_2SO_4 at a scan rate of 20mV

Figure 4.20 shows the cyclic voltammograms of 20%PtCo/C commercial catalyst and 30%PtCo/C in-house catalyst. The CV's show clear hydrogen adsorption-desorption peaks. The 30%PtCo/C commercial catalyst shows a strong oxidation peak in the potential range between 1.0 and 1.2V and it is also observed for the in-house catalyst but it is not that strong. There is a peak at about 0.75 V for Pt-O. The reduction peak for the 20%PtCo/C commercial catalyst shifts to the positive value. The 30%PtCo/C in-house catalyst is observed to be the

catalyst with the lowest activity compared to the commercial catalyst due to its lower ECSA value compared to the commercial catalyst. This may be attributed to the high particle size and the agglomeration observed in the previous chapter using HRTEM. The ECSA of the 30%PtCo/C in-house catalyst and the 20%PtCo/C commercial catalyst was found to be 12.44m^2/g and 39.2m^2/g, respectively (see Table 4.20).

Table 4.20: Electro-active and electrochemical surface area of PtCo/C electro-catalysts

Catalysts	20%PtCo/C Commercial	30%PtCo/C In-house
Electrochemical surface area (m^2/g)	39.2	12.44
Electro-active surface area (cm^2)	98.1	26.11

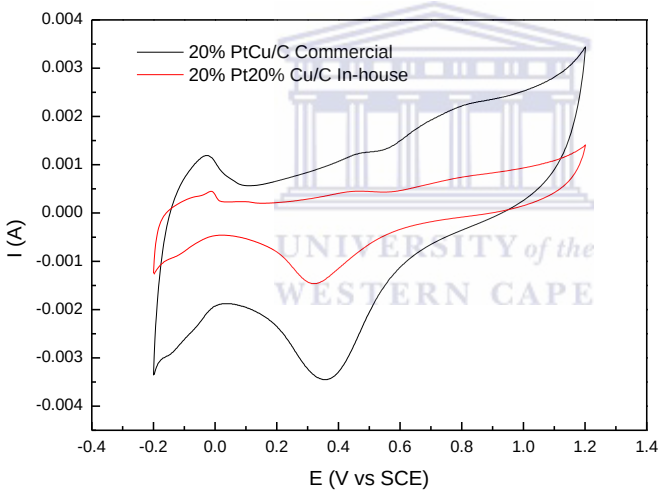

Figure 4.21: Cyclic voltammograms 20%PtCu/C Commercial and 20%Pt20%Cu/C In-house electro-catalysts in N_2 saturated 0.5M H_2SO_4 at a scan rate of 20mV

The characteristic peaks associated with Pt-supported on carbon catalysts are displayed in Figure 4.21. In the anodic scan hydrogen is desorbed (-0.2-0.09V) vs SCE and upon further scanning Pt oxides are formed beyond 0.6V for both these catalysts. During the cathodic scan hydrogen was then adsorbed at potentials between 0.09 to -0.2V vs SCE. The 20%PtCu/C commercial is found to be the catalyst with enhanced activity than the in-house catalyst with electrochemical surface area (ECSA) values of 8.76m^2/g and 3.29m^2/g, respectively (see Table 4.21). The ECSA of the 20%PtCu/C catalyst in literature was found to be 22 m^2/g and

is higher than the one found for this work and this could be attributed to the preparation of the catalysts [122].

Table 4.21: Electro-active and electrochemical surface area of PtCu/C electro-catalysts

Catalyst	20%PtCu/C Commercial	20%Pt20%Cu/C In-house
Electrochemical surface area (m^2/g)	8.76	3.29
Electro-active surface area (cm^2)	21.9	8.23

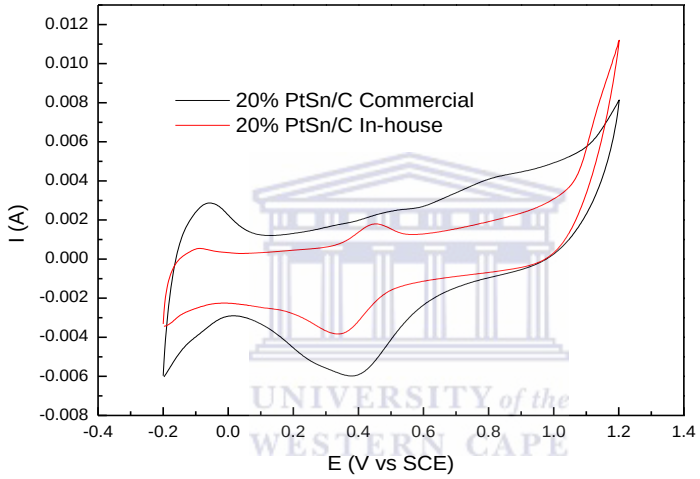

Figure 4.22: Cyclic voltammograms 20%PtSn/C Commercial and 20%PtSn/C In-house electro-catalysts in N_2 saturated 0.5M H_2SO_4 at a scan rate of 20mV

The Cyclic voltammograms in Figure 4.22 show well defined peaks, the Pt-hydride desorption peak -(0.2-0.1V), the double layer region (0.15-0.56V), the Pt-oxide formation (0.6-1.2V) except for 20%PtSn/C in-house there is no Pt-oxide formation. The absence of oxidation peaks in these catalysts demonstrated that they are reasonably stable in acidic medium in the applied potential range. The peak at 0.1 to -0.2 may be attributed to hydrogen adsorption onto the Pt surface [119]. It is observed that the 20%PtSn/C in-house catalyst has a strong oxidation peak between 1.0 and 1.2V but was absent for 20%PtSn/C commercial catalyst. The ECSA of these catalysts was found to be 18.7m^2/g and 3.00m^2/g for the 20%PtSn/C commercial catalyst and 20%PtSn/C in-house catalyst, respectively (see Table

4.22) and the ECSA of the 20%PtSn/C in-house catalyst being low could be attributed to the sample preparation.

Table 4.22: Electro-active and electrochemical surface area of PtSn/C electro-catalysts

Catalysts	20%PtSn/C Commercial	20%PtSn/C In-house
Electrochemical surface area (m^2/g)	18.7	3.00
Electro-active surface area (cm^2)	46.6	7.50

(a) Effect of heat treatment on the electrochemical activity of the 20%PtCo/C Commercial and 30%PtCo/C In-house electro-catalysts

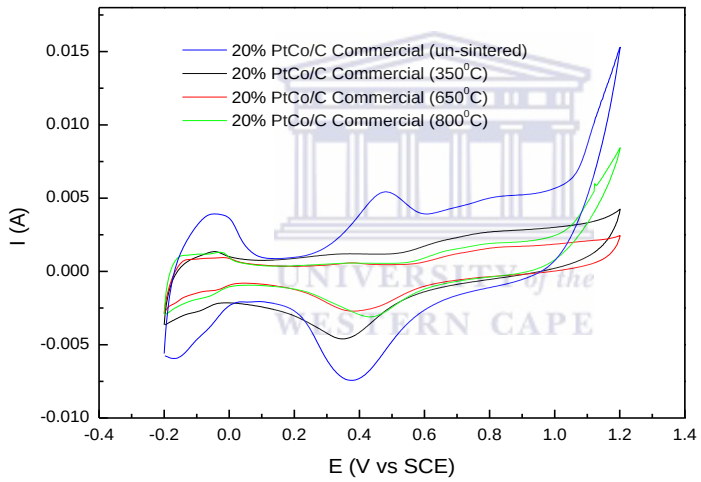

Figure 4.23: Cyclic voltammograms of 20%PtCo/C Commercial (un-sintered), 20%PtCo/C Commercial (350^0C), 20%PtCo/C Commercial (650^0C) and 20%PtCo/C Commercial (800^0C) electro-catalysts in N_2 saturated 0.5M H_2SO_4 at a scan rate of 20mV

Figure 4.23 compares the cyclic voltammograms of 20%PtCo/C commercial catalyst heat treated at 350^0C, 650^0C and 800^0C as well as it shows the electrochemical finger print associated with Pt based electro-catalysts. It is observed that the 20%PtCo/C commercial catalyst heat treated at 350^0C gave better activity compared to when this catalyst was heat treated at other temperatures. The hydrogen adsorption-desorption peaks observed between 0.2-0.1V for the 20%PtCo/C commercial catalyst heat treated at 350^0C are quite bigger than those of the other catalysts. A strong oxidation peak is observed for the 20%PtCo/C

commercial 800^{0}C at potentials between 1.0 and 1.2V. The activity of the heat treated catalyst was found to be in the order of 20%PtCo/C commercial (350^{0}C), 20%PtCo/C commercial (800^{0}C) and 20%PtCo/C commercial (650^{0}C) with the ECSA values of 15.0m^2/g, 11.2m^2/g and 7.96m^2/g, respectively (see Table 4.23). It is observed that the ECSA decreased when the catalyst was heat treated, the 20%PtCo/C commercial un-sintered having an ECSA of 39.2m^2/g. The heat treatment did not improve the ECSA of this catalyst as it was seen with HRTEM results. The catalyst's activity decreased as the temperature increased.

Table 4.23: Electro-active and electrochemical surface area of heat treated PtCo/C commercial electro-catalysts

Catalysts	20%PtCo/C Commercial (Un-sintered)	20%PtCo/C Commercial (350^{0}C)	20%PtCo/C Commercial (650^{0}C)	20%PtCo/C Commercial (800^{0}C)
Electrochemical Surface area (m^2/g)	39.2	15.0	7.96	11.2
Electro-active surface area (cm^2)	98.1	37.6	19.9	28.1

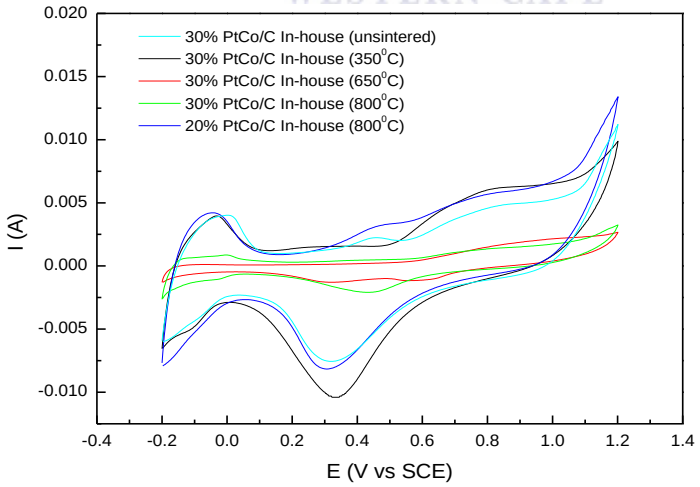

Figure 4.24: Cyclic voltammograms of 30%PtCo/C In-house (un-sintered), 30%PtCo/C In-house (350^{0}C), 30%PtCo/C In-house (650^{0}C), 30%PtCo/C In-house (800^{0}C) and 20%PtCo/C In-house (800^{0}C) electro-catalysts in N_2 saturated 0.5M H_2SO_4 at a scan rate of 20mV

The cyclic voltammograms of 30%PtCo/C in-house catalyst heat treated at 350^0C, 650^0C and 800^0C and 20%PtCo/C in-house catalyst heat treated at 800^0C are displayed in Figure 4.24. The hydrogen adsorption is observed at 0.1 to -0.2V. The Pt-hydride desorption peak potential is from -0.2-0.1V for all the catalysts, the double layer region is observed at the potential of 0.15-0.56V, the Pt-oxide formation appears at 0.6-1.2V. The hydrogen adsorption-desorption peaks and other electrochemical peaks are suppressed in the case of the 30%PtCo/C in-house (650^0C) and 30%PtCo/C in-house (800^0C). The ECSA (see Table 4.24) of the catalysts was found to be 28.9m^2/g for 30%PtCo/C in-house (350^0C), 2.00m^2/g for 30%PtCo/C in-house (650^0C), 10.3m^2/g 30%PtCo/C in-house (800^0C) and 10.94m^2/g for 20%PtCo/C in-house (800^0C). It was found that the 30%PtCo/C in-house (350^0C) gave better ECSA compared to other catalysts heat treated at other temperatures followed by the 20%PtCo/C in-house heat treated at 800^0C. The 30%PtCo/C in-house un-sintered catalyst was found to have an ECSA of 12.44m^2/g. The ECSA decreased dramatically for the 30%PtCo/C in-house (650^0C) and decreased a bit less for the 30%PtCo/C in-house (800^0C). With the 30%PtCo/C in-house (350^0C) the ECSA improved and enhanced indicating that the heat treatment had an effect on the ECSA of this catalyst at this particular temperature. This observation where heat treatment increases the ECSA of a catalyst can also be found in the literature. The catalyst when heat treated at 650 ^{0}C the activity dropped and this could be attributed to the higher particle size observed with HRTEM.

Table 4.24: Electro-active and electrochemical surface area of heat treated PtCo/C in-house electro-catalysts

Catalysts	**30%PtCo/C In-house (Un-sintered)**	**30%PtCo/C In-house (350^0C)**	**30%PtCo/C In-house (650^0C)**	**30%PtCo/C In-house (800^0C)**	**20%PtCo/C In-house (800^0C)**
Electro-active surface area (m^2/g)	12.44	28.9	2.00	10.3	10.94
Electrochemical surface area (cm^2)	26.11	72.3	5.00	25.6	34.9

4.3.2 ORR study of platinum based electro-catalysts

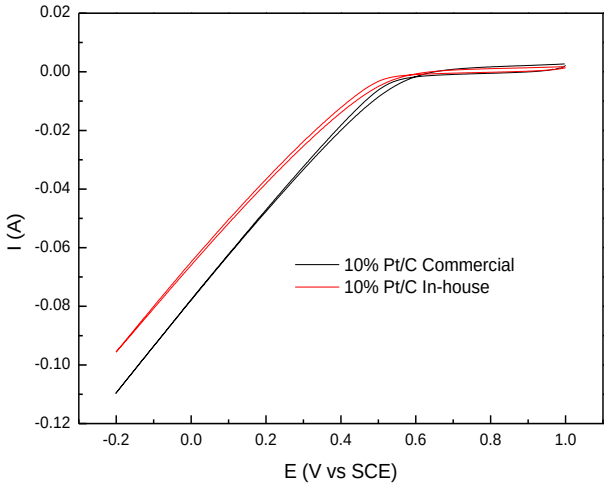

Figure 4.25: Cyclic voltammograms for ORR of 10%Pt/C Commercial and 10%Pt/C In-house electro-catalysts in O_2 saturated 0.5M H_2SO_4 at a scan rate of 20mV

From Figure 4.25 the cyclic voltammograms of the catalysts are displayed in order to the catalyst that will give better ORR activity. The 10%Pt/C commercial catalyst gives a better ORR activity. It can be noted that the 10%Pt/C commercial has a current enhancement than 10%Pt/C in-house catalyst with a current densities of 3.36 A/cm^2 and 2.44 A/cm^2, respectively tabulated in Table 4.25. The mass activities (MA) of the 10%Pt/C commercial and 10%Pt/C in-house were found to be 13.4A/g and 9.74A/g, respectively and the specific activities (SA) were found to be 0.054A/cm^2 and 0.039A/cm^2, respectively as shown in Table 4.25.

Table 4.25: Current density, mass activity and specific activity of 10%Pt/C electro-catalysts

Catalysts	10%Pt/C Commercial	10%Pt/C In-house
Current density (A/cm^2)	3.36	2.44
Mass activity (A/g) Pt	13.4	9.74
Specific activity (A/cm^2) Pt	0.054	0.039

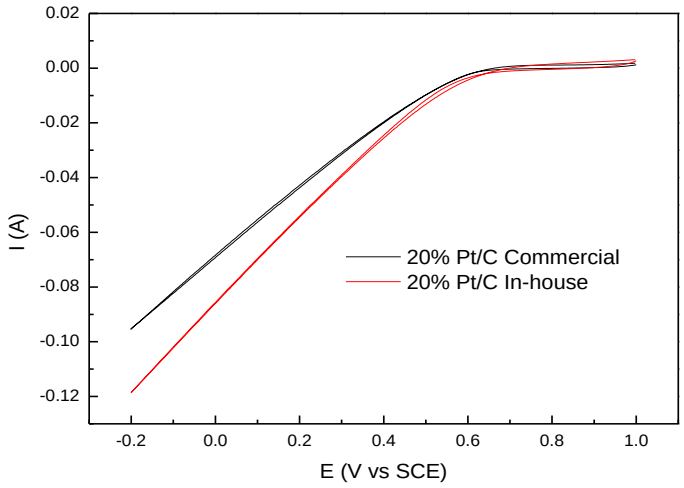

Figure 4.26: Cyclic voltammograms for ORR of 20%Pt/C Commercial and In-house electro-catalysts in O_2 saturated 0.5M H_2SO_4 at a scan rate of 20mV

Figure 4.26 shows the ORR activity of the 20%Pt/C commercial and in-house catalysts. The 20%Pt/C in-house catalyst has enhanced ORR activity than 20%Pt/C commercial catalyst which was found at lower current densities than the 20%Pt/C in-house catalyst. This is confirmed by the HRTEM and XRD results given that the 20%Pt/C in-house has small particle size. The 20%Pt/C commercial catalyst gave the current density of 3.15 A/cm^2 and the 20%Pt/C in-house catalyst gave the current density of 3.96 A/cm^2. The MA of 20%Pt/C commercial and 20%Pt/C in-house catalyst were found to be 12.6A/g and 15.8A/g, respectively and the SA were found to be 0.060 A/cm^2 and 0.063A/cm^2, respectively (see Table 4.26).

Table 4.26: Current density, mass activity and specific activity of 20%Pt/C electro-catalysts

Catalysts	**20%Pt/C Commercial**	**20%Pt/C In-house**
Current density (A/cm^2)	3.15	3.96
Mass activity (A/g)	12.6	15.8
Specific activity (A/cm^2)	0.060	0.063

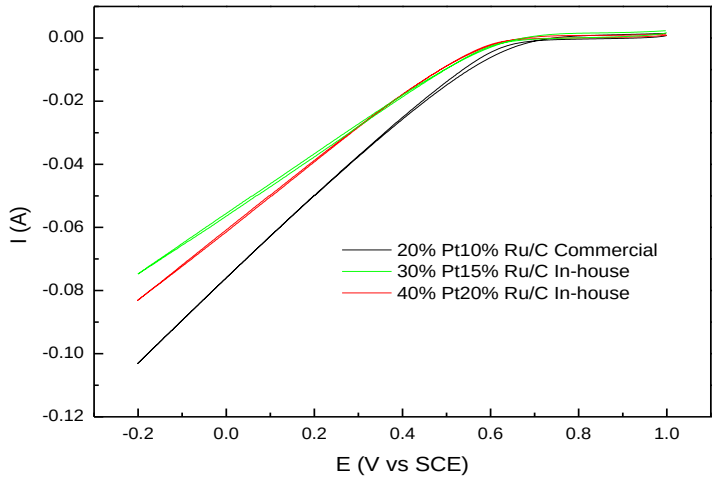

Figure 4.27: Cyclic voltammograms for ORR of 20%Pt10%Ru/C Commercial, 30%Pt15%Ru/C In-house and 40%Pt20%Ru/C In-house electro-catalysts in O_2 saturated 0.5M H_2SO_4 at a scan rate of 20mV

Figure 4.27 indicates that the 20%Pt10%Ru/C commercial with a current density of 3.78A/cm^2 is better than the other two catalysts. This means that it is a better cathode catalyst compared to the other two catalysts.. The current densities of the 30%Pt15%Ru/C in-house and the 40%Pt20%Ru/C in-house are almost the same, as depicted by the CV curves which lie almost on one another, the current densities were found to be 2.78A/cm^2 and 2.88A/cm^2, respectively. The MA of the 20%Pt10%Ru/C commercial, 30%Pt15%Ru/C in-house and 40%Pt20%Ru/C in-house were found to be 15.1A/g, 11.1A/g and 11.5A/g, respectively and the SA were found to be 0.050A/cm^2, 0.045A/cm^{2}and 0.046A/cm^2, respectively (see Table 4.27).

Table 4.27: Current density, mass activity and specific activity of PtRu/C electro-catalysts

Catalysts	**20%Pt10%Ru/C Commercial**	**30%Pt15%Ru/C In-house**	**40%Pt20%Ru/C In-house**
Current density (A/cm^2)	3.78	2.78	2.88
Mass activity (A/g)	15.1	11.1	11.5
Specific activity (A/cm^2)	0.050	0.045	0.046

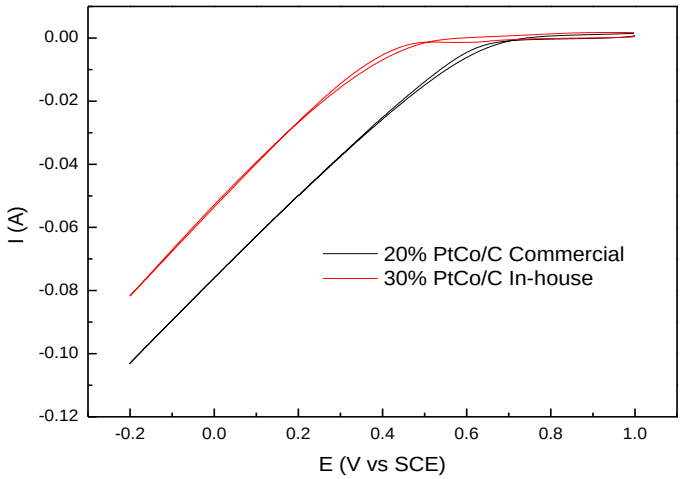

Figure 4.28: Cyclic voltammograms for ORR of 20%PtCo/C Commercial and 30%PtCo/C In-house electro-catalysts in O_2 saturated 0.5M H_2SO_4 at a scan rate of 20mV

It can be seen in Figure 4.28 that the 20%PtCo/C commercial catalyst gives better performances of ORR than the 30%PtCo/C in-house catalyst. The inactivity towards ORR of the 30%PtCo/C in-house catalyst may be due to the big particle size observed with HRTEM and XRD and due to the fact that the particle of this catalyst were very much agglomerated. The in-house catalyst gave very low current density than the commercial catalyst with current density values of 1.49A/cm^2 and 3.79A/cm^2, respectively. The MA of the 20%PtCo/C commercial and 30%PtCo/C in-house catalyst were found to be 15.1A/g and 5.96A/g, respectively and the SA were found to be 0.061A/cm^2 and 0.024A/cm^2, respectively (see Table 4.28).

Table 4.28: Current density, mass activity and specific activity of PtCo/C electro-catalysts

Catalysts	**20%PtCo/C Commercial**	**30%PtCo/C In-house**
Current density (A/cm^2)	3.79	1.49
Mass activity (A/g)	15.1	5.96
Specific activity (A/cm^2)	0.061	0.024

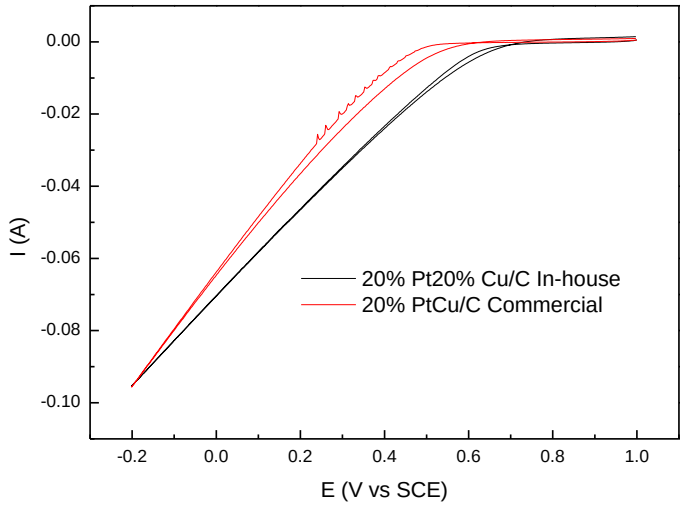

Figure 4.29: Cyclic voltammograms for ORR of 20%PtCu/C Commercial and 20%Pt20%Cu/C In-house electro-catalysts in O_2 saturated 0.5M H_2SO_4 at a scan rate of 20mV

At the mixed control zone at potentials of 0.3V the current density of the 20%PtCu/C commercial catalyst is lower than that of the 20%Pt20%Cu/C in-house meaning that the 20%Pt20%Cu/C in-house is a better cathode catalyst than the commercial catalyst as shown in Figure 4.29. The current density of these catalysts was found to be 2.41A/cm^2 for the commercial catalyst and 3.44A/cm^2 for the in-house catalyst (see Table 4.29). It is also observed (Figure 4.29) that the catalysts have similar diffusion control zone currents. The MA of the 20%PtCu/C commercial and 20%Pt20%Cu/C in-house catalyst were found to be 9.66A/g and 13.7A/g, respectively and the SA were found to be 0.039A/cm^2 and 0.055A/cm^2, respectively.

Table 4.29: Current density, mass activity and specific activity of PtCu/C electro-catalysts

Catalysts	20%PtCu/C Commercial	20%Pt20%Cu/C In-house
Current density (A/cm^2)	2.41	3.44
Mass activity (A/g)	9.66	13.7
Specific activity (A/cm^2)	0.039	0.055

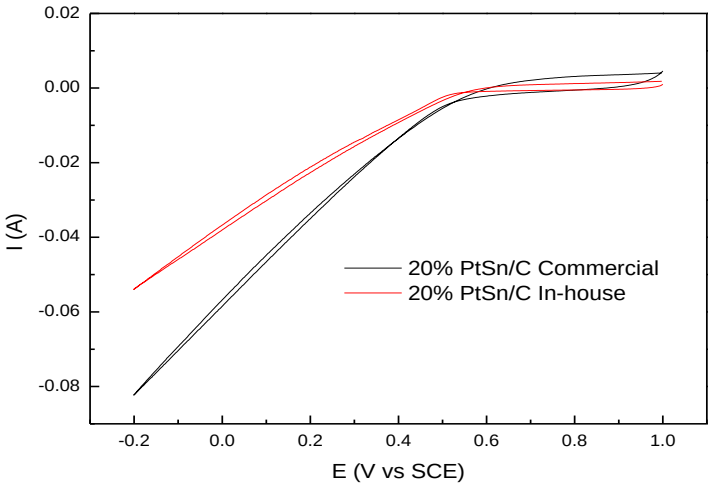

Figure 4.30: Cyclic voltammograms for ORR of 20%PtSn/C Commercial and 20%PtSn/C In-house electro-catalysts in O_2 saturated 0.5M H_2SO_4 at a scan rate of 20mV

Figure 4.30 shows the cyclic voltammograms for ORR of 20%PtSn/C commercial and in-house electro-catalysts. The commercial catalyst has a better ORR activity than 20%PtSn/C in-house catalyst. Moreover, the 20%PtSn/C commercial with a current density of 2.32A/cm^2 is higher than that of 20%PtSn/C in-house catalyst. The in-house catalyst was found to have a current density of 1.53A/cm^2. The MA of the 20%PtSn/C commercial and 20%PtSn/C in-house catalyst were found to be 9.26A/g and 6.10A/g, respectively and the SA were found to be 0.037A/cm^2 and 0.024A/cm^2, respectively (see Table 4.30).

Table 4.30: Current density, mass activity and specific activity of PtSn/C electro-catalysts

Catalysts	20%PtSn/C Commercial	20%PtSn/C In-house
Current density (A/cm^2)	2.32	1.53
Mass activity (A/g)	9.26	6.10
Specific activity (A/cm^2)	0.037	0.024

(a) Effect of heat treatment on the ORR activity of the 20%PtCo/C Commercial and 30%PtCo/C In-house electro-catalysts

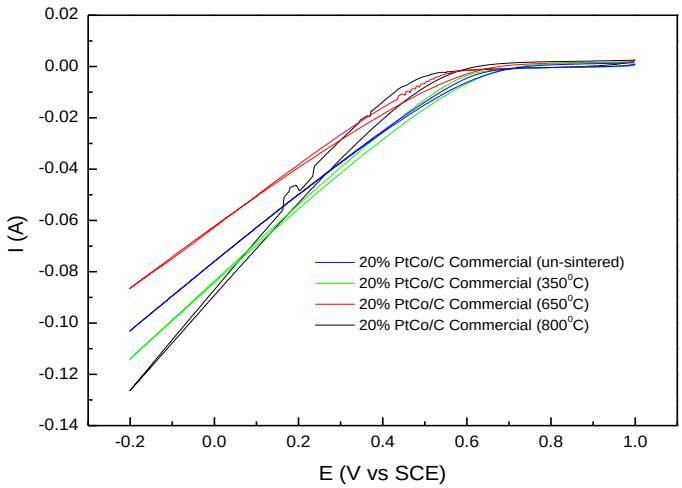

Figure 4.31: Cyclic voltammograms for ORR of 20%PtCo/C Commercial (un-sintered), 20%PtCo/C Commercial (350^{0}C), 20%PtCo/C Commercial (650^{0}C) and 20%PtCo/C Commercial (800^{0}C) electro-catalysts in O_2 saturated 0.5M H_2SO_4 at a scan rate of 20mV

Figure 4.31 shows the cyclic voltammograms for PtCo/C commercial catalyst heat treated at different temperatures. At the mixed control region that is at a potential of 0.3V the 20%PtCo/C commercial (350^{0}C) has a better ORR activity compared to when the catalyst was heat treated at 650^{0}C and 800^{0}C followed by the 20%PtCo/C commercial 800^{0}C. The current densities of this catalyst heat treated at different temperatures was found to be 4.13A/cm^2 for the 20%PtCo/C commercial (350^{0}C), 2.65A/cm^2 for the 20%PtCo/C commercial (650^{0}C) and 2.97A/cm^2 for the 20%PtCo/C commercial (800^{0}C) as shown in Table 4.31. It is observed that the ORR activity decreased slightly for the 20%PtCo/C commercial (650^{0}C) and the 20%PtCo/C commercial (800^{0}C) but increased for the 20%PtCo/C commercial (350^{0}C). The current density of the un-sintered 20%PtCo/C commercial was found to be 3.79A/cm^2. Heat treating the catalyst at 350^{0}C enhanced the ORR activity of this catalyst. The MA of the 20%PtCo/C commercial (350^{0}C), 20%PtCo/C commercial (650^{0}C) and 20%PtCo/C commercial (800^{0}C) were found to be 16.5A/g, 10.6A/g and 11.9A/g, respectively and the SA were found to be 0.066A/cm^2, 0.042A/cm^{2}and

0.048A/cm^2, respectively and these results are in good agreement with HRTEM and XRD as the activity decreases with decreasing temperature.

Table 4.31: Current density, mass activity and specific activity of heat treated PtCo/C Commercial electro-catalysts

Catalysts	20%PtCo/C Commercial (Un-sintered)	20%PtCo/C Commercial (350^{0}C)	20%PtCo/C Commercial (650^{0}C)	20%PtCo/C Commercial (800^{0}C)
Current density (A/cm^2)	3.79	4.13	2.65	2.97
Mass activity (A/g)	15.1	16.5	10.6	11.9
Specific activity (A/cm^2)	0.061	0.066	0.042	0.048

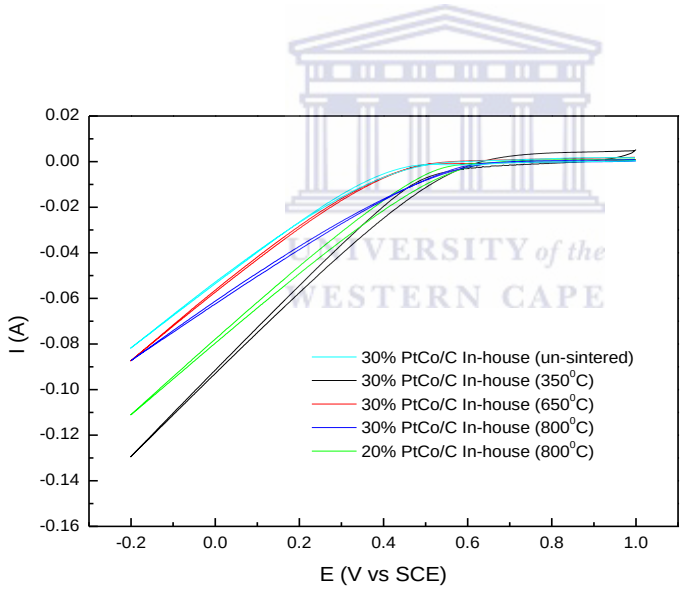

Figure 4.32: Cyclic voltammograms for ORR of 30%PtCo/C In-house (un-sintered), 30%PtCo/C In-house (350^{0}C), 30%PtCo/C In-house (650^{0}C), 30%PtCo/C In-house (800^{0}C), and 20%PtCo/C In-house (800^{0}C) electro-catalysts in O_2 saturated 0.5M H_2SO_4 at a scan rate of 20mV

The cyclic voltammograms of 30%PtCo/C in-house catalyst heat treated at different temperatures are depicted in Figure 4.32. It can be noted that the 30%PtCo/C in-house (350^{0}C) gives better ORR activity than when heat treated at other temperatures followed by the 20%PtCo/C in-house (800^{0}C) and then the 30%PtCo/C in-house when heat treated at

800^0C. From the literature the PtCo/C catalyst was heat treated at different temperatures and it was found that the heat treatment of the catalyst at 800^0C leads to enhanced ORR activity [120]. This was not the case in this work and this may be due to the fact that in the literature the heat-treatment was done for 1hour and in this work it was done for 3hour. The ORR activity of the 30%PtCo/C (350^0C) in-house catalyst increased compared to the PtCo/C un-sintered in-house and commercial catalysts after heat treatment. The current densities of the catalyst at these different temperatures are as follows, 4.07A/cm^2 for 30%PtCo/C in-house (350^0C), 1.60A/cm^2 for 30%PtCo/C in-house (650^0C), 3.18A/cm^2 30%PtCo/C in-house (800^0C) and 2.59A/cm^2 for the 20%PtCo/C in-house (800^0C) (see Table 4.32). The heat treatment of this catalyst enhanced the ORR activity as it is observed that with all the temperatures the current density increased compared to when it was un-sintered (1.49 A/cm^2). This enhancement is more clear with the 30%PtCo/C in-house (350^0C) compared to when this catalyst was heat treated at other heat treatment temperatures used in this study. The MA of the 30%PtCo/C in-house (350^0C), 30%PtCo/C in-house (650^0C), 30%PtCo/C in-house (800^0C), and 20%PtCo/C in-house (800^0C) were found to be 16.3A/g, 6.40A/g, 12.7A/g and 10.4A/g, respectively and the SA were found to be 0.065A/cm^2, 0.026A/cm^2, 0.051A/cm^2 and 0.041A/cm^2, respectively.

Table 4.32: Current density, mass activity and specific activity of heat treated PtCo/C In-house electro-catalysts

Catalysts	**30%PtCo/C In-house (Un-sintered)**	**30%PtCo/C In-house (350^0C)**	**30%PtCo/C In-house (650^0C)**	**30%PtCo/C In-house (800^0C)**	**20%PtCo/C In-house (800^0C)**
Current density (A/cm^2)	1.49	4.07	1.60	2.59	3.18
Mass activity (A/g)	5.96	16.3	6.40	10.4	12.7
Specific activity (A/cm^2)	0.024	0.065	0.026	0.041	0.051

4.3.3 Summary of cyclic voltammetric study of the activity and oxygen reduction reaction on supported electro-catalysts

The study above shows that the catalyst with higher ECSA was found to be 20%Pt/C in-house catalyst and the catalyst with the lowest ECSA was found to be 20%PtSn/C in-house catalyst. It is also observed that the heat treatment of the 20%PtCo/C commercial decreased the ECSA but increased for the 30%PtCo/C in-house heat treated at 350^0C. From the ORR study results above it is observed that 20%Pt/C in-house catalyst has higher ORR activity and 30%PtCo/C in-house has lower activity but after heat treatment of this catalyst the activity increased when heat treated at 350^0C and 800^0C and was even better than the un-sintered PtCo/C commercial catalyst.

4.4 ROTATING DISK ELECTRODE STUDY OF THE ACTIVITY OF OXYGEN REDUCTION ON SUPPORTED ELECTRO-CATALYSTS

In this study electro-catalysts are characterized in terms of their activity towards ORR using the rotating disk electrode. Hydrodynamic voltammograms were studied at rotation speed varied from 500 to 2500rpm for ORR and recorded between 1.0 and 0.0V versus SCE, at a scan rate of 5mV/s.

(1) 10%Pt/C Commercial and In-house electro-catalysts

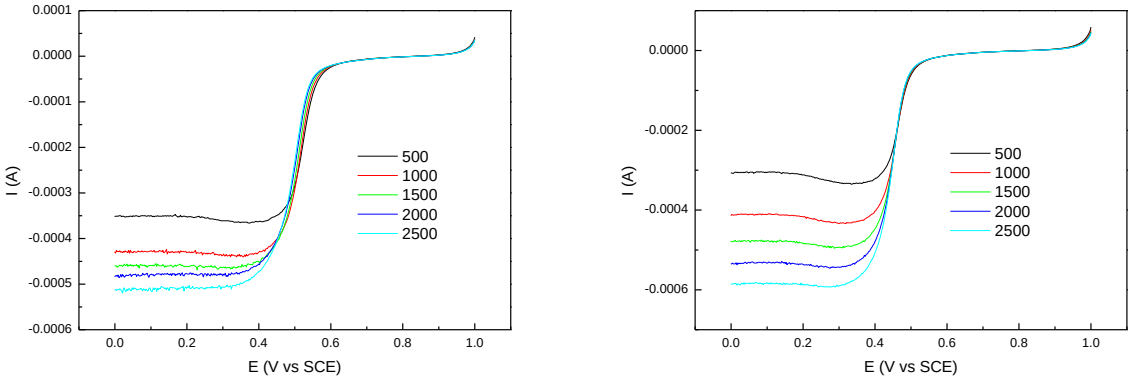

(a) (b)

Figure 4.33: Oxygen reduction polarization curves for 500, 1000, 1500, 2000, 2500 rpm speed rates of a) 10%Pt/C Commercial and b) 10%Pt/C In-house electro-catalysts in O_2 saturated 0.5M H_2SO_4 at a scan rate of 20mV

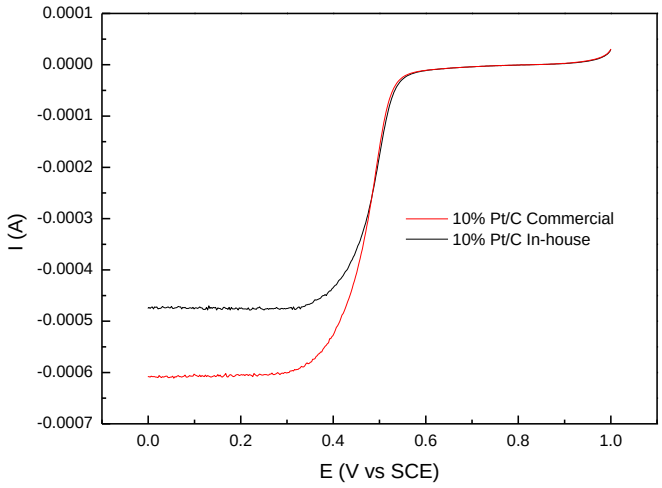

Figure 4.34: Polarization curves for the ORR on 10%Pt/C Commercial and 10%Pt/C In-house electro-catalysts in O_2 saturated 0.5M H_2SO_4 at a sweep rate of 5mV/s, rotating velocity of 1500rpm, at room temperature

Figure 4.34 shows the polarization curves (see 1500rpm from Figure 4.33) for the oxygen reduction reaction of the 10%Pt/C commercial and in-house catalysts. The in-house catalysts are better cathode catalyst for ORR when compared to the commercial catalysts. It was found that the curve obtained for 10%Pt/C in-house was similar to that of 10%Pt/C commercial. At the mixed control zone that is at potentials of 0.5V, it can be seen that there is a possibility that the activities of the catalysts are the same or very close to one another. The half wave potentials of both these catalysts were found to be about 0.5V. This indicated that the 10%Pt/C in-house has an activity toward ORR similar to that of 10%Pt/C commercial. It was also observed that diffusion limited current density of 10%Pt/C commercial catalyst since it was bigger than that of 10%Pt/C in-house and this agrees with the HRTEM results. The diffusion current densities were 0.06 A/cm^2 and 0.047A/cm^2, respectively. The ORR activity current densities of these catalysts was calculated and it was found that the 10%Pt/C commercial catalyst exhibited a current density (see Table 4.33) of 0.042A/cm^2 and the 10%Pt/C in-house catalyst exhibited a current density of 0.037A/cm^2. It is clear that the catalysts exhibit an ORR activity close to one another with a very small difference. The MA of the 10%Pt/C Commercial and 10%Pt/C in-house catalyst were found to be 0.168A/g and 0.148A/g, respectively and the SA were found to be 0.067A/cm^2 and 0.059A/cm^2, respectively.

Table 4.33: Current density, mass activity and activity of 10%Pt/C electro-catalysts at i=0.45V

Catalysts	10%Pt/C Commercial	10%Pt/C In-house
Current density (A/cm^2)	0.042	0.037
Mass activity (A/g)	0.168	0.148
Specific activity (A/cm^2)	0.067	0.059

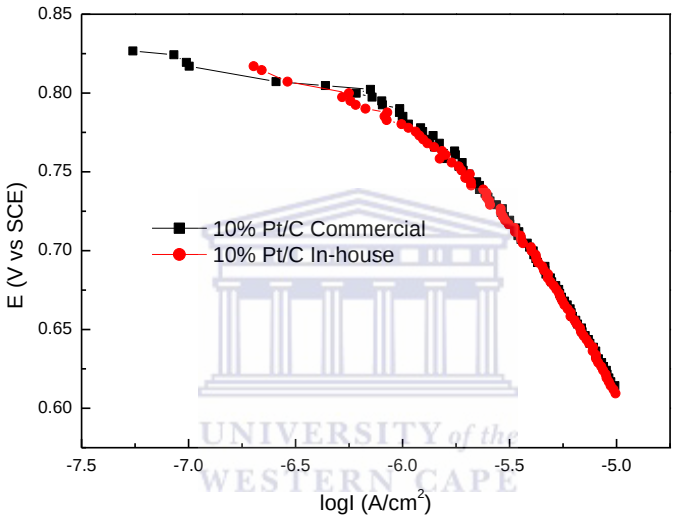

Figure 4.35: Mass transfer polarization curves for the ORR on 10%Pt/C Commercial and 10%Pt/C In-house electro-catalysts in O_2 saturated 0.5M H_2SO_4 at a sweep rate of 5mV/s, rotating velocity of 1500rpm, at room temperature

The plot shown in Figure 4.35 is the mass Tafel polarization curve of the 10%Pt/C commercial and in-house catalyst at 1500rpm rotating speed. The plot gives a clear analysis of the ORR activity of the catalysts. From the plot it can be deduced that the activity of the catalysts is similar since the curves are laying on one another. These plots gave Tafel slopes of two regions; region one giving 65mV/dec and region two giving 189mV/dec for the 10%Pt/C commercial catalyst. Similarly, 63mV/dec and 180mV/dec for the 10%Pt/C in-house catalyst was recorded for region one and region two, respectively (see Table 4.34). This indicates that both these catalysts have similar ORR activity as the slopes are close to one another.

Table 4.34: Tafel slopes of the 10%Pt/C electro-catalysts

Catalysts	10%Pt/C Commercial	10%Pt/C In-house
Region1 (mV/dec)	65	63
Region2 (mV/dec)	189	180

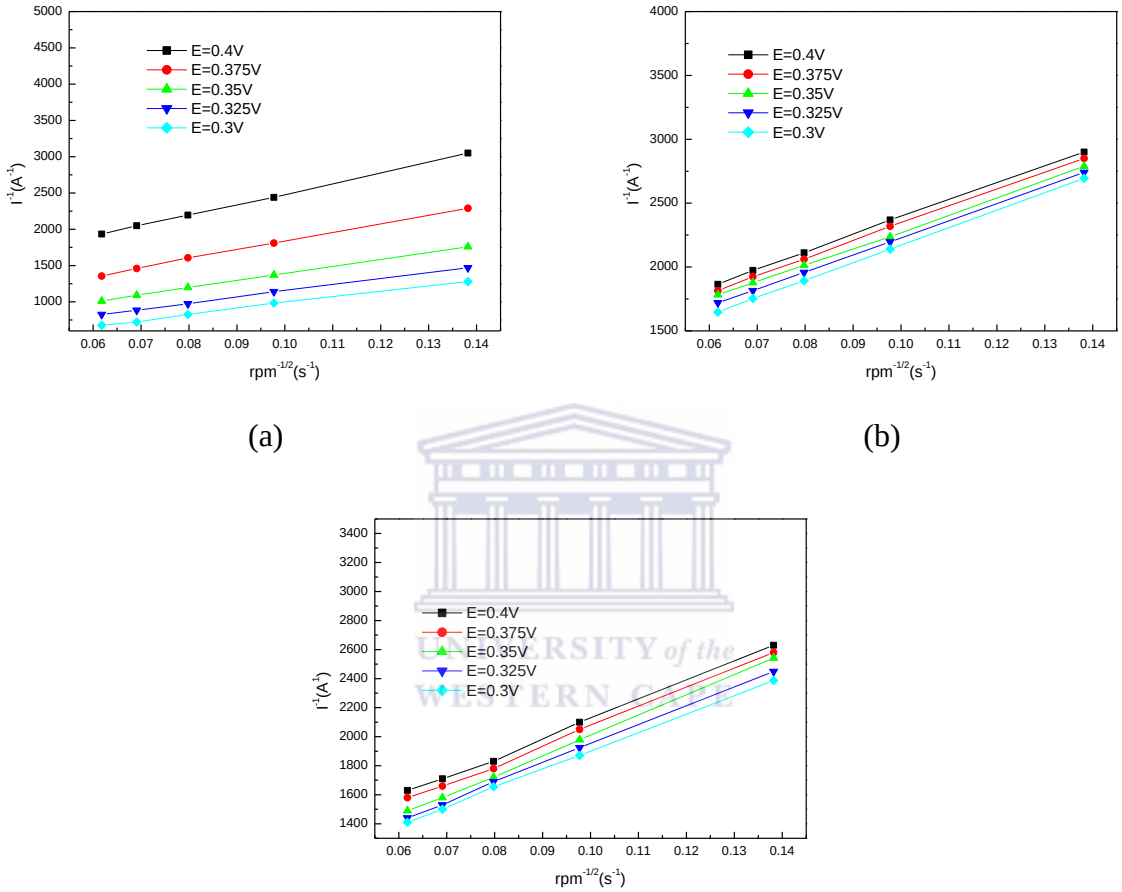

Figure 4.36: Koutecky-Levich plots of a) Pt Bare, b) 10%Pt/C Commercial and c) 10%Pt/C In-house electro-catalysts at different potentials (0.4V, 0.375V, 0.35V, 0.325V and 0.3V)

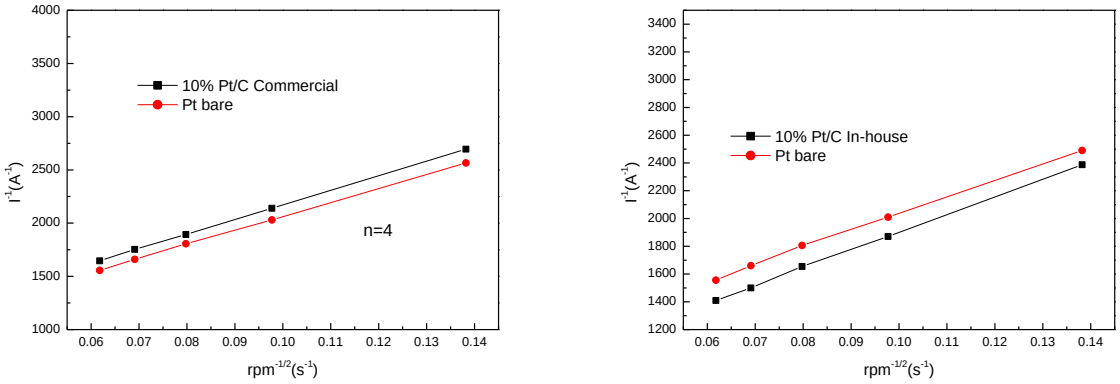

(a) (b)

Figure 4.37: Koutecky-Levich plots of a) 10%Pt/C Commercial and b) 10%Pt/C In-house electro-catalysts at a potential of 0.375V

The oxygen reduction reaction that is desired is the four-electron transfer that is the electro-reduction of oxygen to water. Figure 4.37 displays the Koutecky-Levich plot abbreviated as a K-L plot. In Figure 4.36 we are given K-L plots at different potentials that are prepared from data for Figure 4.33. The K-L plots at E=0.375V were taken for each catalyst and compared to a Pt bare electrode so as to see whether the K-L plot for the catalyst will give a straight line similar to the one of the Pt Bare electrode, the four-electron transfer line. This was done to investigate the electron transfer of these electro-catalysts. In Figure 4.37 we observe that the lines for both catalysts are similar to the one of the Pt bare electrode indicating that this is a four-electron transfer reaction for both catalysts.

(2) 20%Pt/C Commercial and In-house electro-catalysts

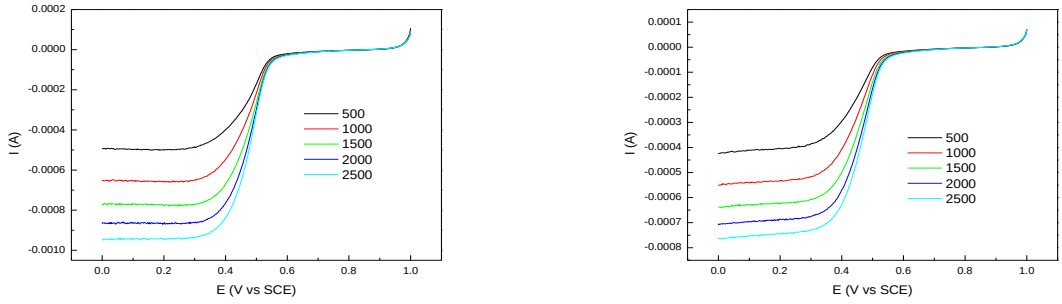

(a) (b)

Figure 4.38: Oxygen reduction polarization curves for 500, 1000, 1500, 2000, 2500 rpm speed rates of a) 20%Pt/C Commercial and b) 20%Pt/C In-house electro-catalysts in O_2 saturated 0.5M $H2SO_4$ at a scan rate of 20mV

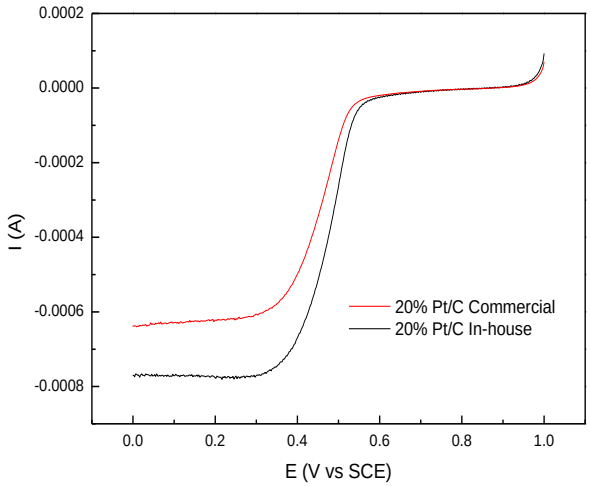

Figure 4.39: Polarization curves for the ORR on 20%Pt/C Commercial and 20%Pt/C In-house electro-catalysts in O_2 saturated 0.5M H_2SO_4 at a sweep rate of 5mV/s, rotating velocity of 1500rpm, at room temperature

The 20%Pt/C commercial and the 20%Pt/C in-house catalysts (1500rpm curves from Figure 4.38) were compared for the ORR activity (see Figure 4.39). The enhancement of ORR is observed for 20%Pt/C in-house, especially at potentials more positive than the half wave potential, the so-called mixed control region. The half wave potential of 20%Pt/C in-house was found to be 0.5V and that of 20%Pt/C commercial to be 0.4V, which means that the 20%Pt/C in-house is more active than 20%Pt/C commercial. It is also observed that the 20%Pt/C in-house has higher diffusion current density, at the diffusion control zone. The current density of 20%Pt/C in-house catalyst was found to be 0.053A/cm^2 and 20%Pt/C commercial catalyst was found to be 0.036A/cm^2 (see Table 4.35). This shows that the 20%Pt/C in-house catalyst is more active for ORR than the commercial catalyst. The MA of the 20%Pt/C commercial and 20%Pt/C in-house catalyst were found to be 0.144A/g and 0.213A/g, respectively and the SA were found to be 0.066A/cm^2 and 0.085A/cm^2, respectively.

Table 4.35: Current density, mass activity and specific activity of 20%Pt/C electro-catalysts at i=0.45V

Catalysts	20%Pt/C Commercial	20%Pt/C In-house
Current density (A/cm^2)	0.036	0.053
Mass activity (A/g)	0.144	0.213
Specific activity (A/cm^2)	0.066	0.085

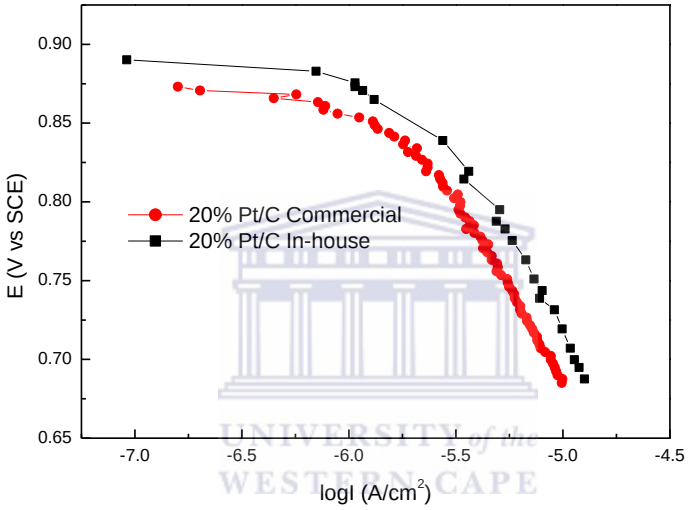

Figure 4.40: Mass transfer polarization curves for the ORR on 20%Pt/C Commercial and 10%Pt/C In-house electro-catalysts in O_2 saturated 0.5M H_2SO_4 at a sweep rate of 5mV/s, rotating velocity of 1500rpm, at room temperature

The Tafel plots for the 20%Pt/C commercial and in-house catalyst are given in Figure 4.40. The 20%Pt/C in-house catalyst is observed at higher potentials than the 20%Pt/C commercial catalyst which is observed at lower potentials. From the plot it is clear that the 20%Pt/C in-house catalyst is more active that the commercial catalyst. It is stated in the literature that for an electrochemical reaction to obtain a high current at low overpotential, the reaction should exhibit a low Tafel slope. The slopes were determined for these electro-catalysts and it was found that the 20%Pt/C in-house catalyst exhibited the low Tafel slopes with slopes of 57mV/dec and 102mV/dec for region one and two, respectively. In literature the Tafel slope for the 20%Pt/C catalyst was found to be 60 mV/dec and 120 mV/dec [123]. On the other

hand the commercial catalyst exhibited slopes of 68mV/dec and 191mV/dec for region one and two, respectively (see Table 4.36).

Table 4.36: Tafel slopes of the 20%Pt/C electro-catalysts

Catalysts	20%Pt/C Commercial	20%Pt/C In-house
Region1 (mV/dec)	68	57
Region2 (mV/dec)	191	102

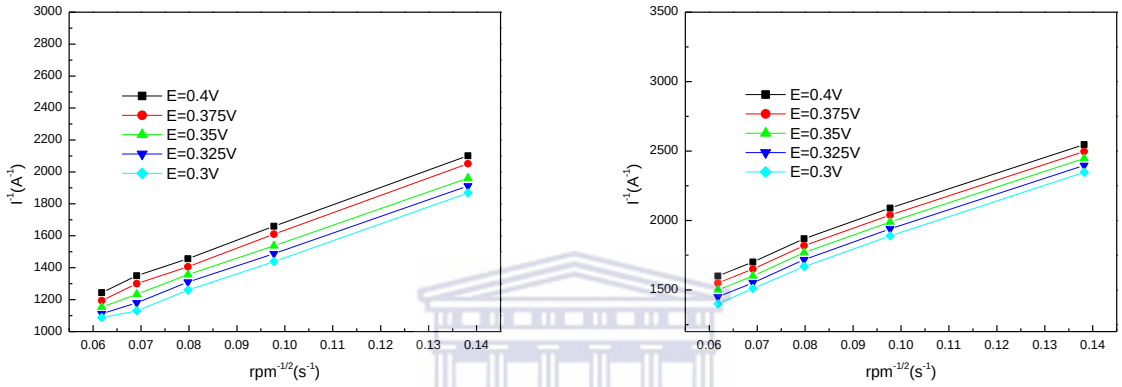

(a) (b)

Figure 4.41: Koutecky-Levich plots of a) 20%Pt/C Commercial and b) 20%Pt/C In-house electro-catalysts at different potentials (0.4V, 0.375V, 0.35V, 0.325V and 0.3V)

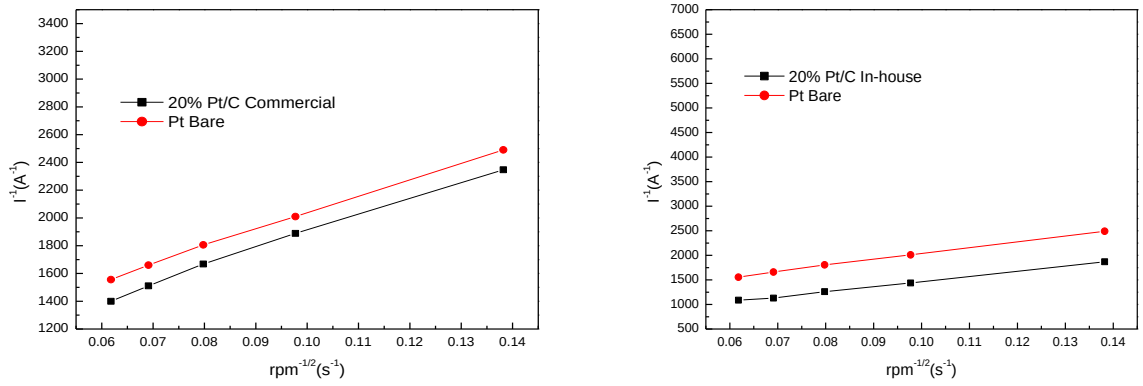

(a) (b)

Figure 4.42: Koutecky-Levich plots of a) 20%Pt/C Commercial and b) 20%Pt/C In-house electro-catalysts at a potential of 0.375V

Figure 4.42 displays the K-L plots (at 0.375V from Figure 4.41) of 20%Pt/C commercial and in-house catalysts. The plots of the catalysts are compared to a K-L plot of a Pt bare electrode. The comparison is done to check whether the plots of the catalysts will be similar to the plots of the Pt bare electrode in order to investigate the possibility of the electro-reduction of oxygen to water. From the plots it is observed that the K-L plots for both catalysts are similar to that of the Pt bare electrode which means that this reaction follows the four-electron transfer for both catalysts.

(3) 20%Pt10%Ru/C Commercial, 30%Pt15%Ru/C and 40%Pt20%Ru/C In-house electro-catalysts

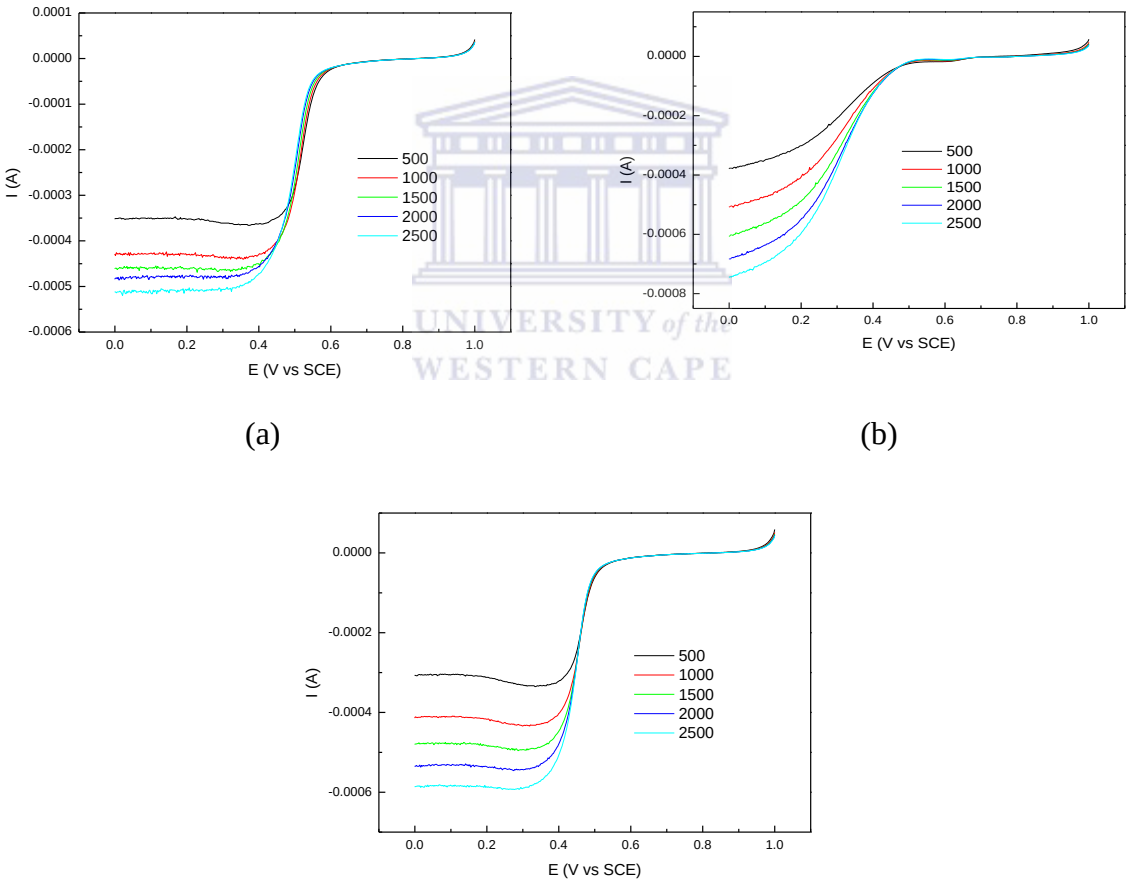

Figure 4.43: Oxygen reduction polarization curves for 500, 1000, 1500, 2000, 2500 rpm speed rates of a) 20%Pt10%Ru/C Commercial, b) 30%Pt15%Ru/C In-house and c) 40%Pt20%Ru/C In-house electro-catalysts in O_2 saturated 0.5M H_2SO_4 at a scan rate of 20mV

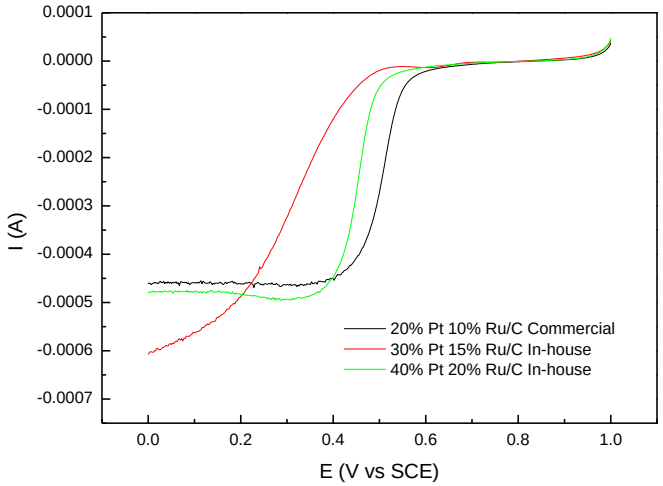

Figure 4.44: Polarization curves for the ORR on 20%Pt10%Ru/C Commercial, 30%Pt15%Ru/C and 40%Pt20%Ru/C In-house electro-catalysts in O_2 saturated 0.5M H_2SO_4 at a sweep rate of 5mV/s, rotating velocity of 1500rpm, at room temperature

From Figure 4.44 it is observed that the 20%Pt10%Ru/C commercial catalyst is more active than the 30%Pt15%Ru/C in-house and the 40%Pt20%Ru/C in-house (1500rpm curves from Figure 4.43). The half wave potential of the 20%Pt10%Ru/C commercial is the most positive (0.5V), indicating that it is the most active among the catalysts it is comparison with , followed by the 40%Pt20%Ru/C in-house catalyst at 0.41V and 30%Pt15%Ru/C in-house catalyst at 0.35V. The diffusion limiting current of 40%Pt20%Ru/C in-house and 20%Pt10%Ru/C commercial catalyst are almost similar. The 30%Pt15%Ru/C in-house catalyst is the lowest compared to the other Ru catalysts. The activity enhancement of the catalysts was found to be in the following order 20%Pt10%Ru/C commercial with a current density of 0.041A/cm^2, 40%Pt20%Ru/C in-house with a current density of 0.030A/cm^2 and lastly 30%Pt15%Ru/C in-house with a current density of 0.006A/cm^2 (Table 4.37). The MA of the 20%Pt10%Ru/C Commercial, 30%Pt15%Ru/C In-house and 40%Pt20%Ru/C In-house catalysts were found to be 0.165A/g, 0.024A/g and 0.119A/g and the SA were found to be 0.058A/cm^2, 0.010A/cm^2 and 0.048A/cm^2, respectively. The mass activity of the 30%Pt15%Ru/C in-house catalyst is observed to be low and this could be due to the preparation method.

Table 4.37: Current density, mass activity and specific activity of PtRu/C electro-catalysts at i=0.45V

Catalysts	20%Pt10%Ru/C Commercial	30%Pt15%Ru/C In-house	40%Pt20%Ru/C In-house
Current density (A/cm^2)	0.041	0.006	0.030
Mass activity (A/g)	0.165	0.024	0.119
Specific (A/cm^2)	0.058	0.010	0.048

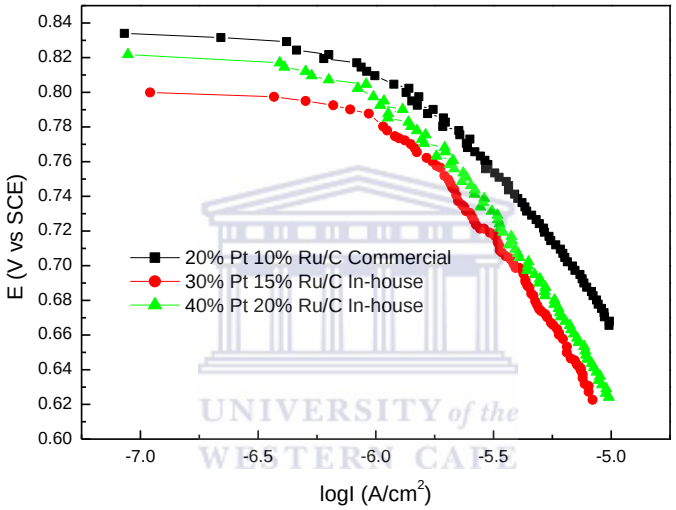

Figure 4.45: Mass transfer polarization curves for the ORR on 20%Pt10%Ru/C Commercial, 30%Pt15%Ru/C In-house and 40%Pt20%Ru/C In-house electro-catalysts in O_2 saturated 0.5M H_2SO_4 at a sweep rate of 5mV/s, rotating velocity of 1500rpm, at room temperature

A comparison of the Tafel plots (Figure 4.45) gives a clear indication of the ORR activity of the catalysts. From the plots the 20%Pt10%Ru/C commercial catalyst is observed at higher potentials than the in-house catalysts. This indicates that the 20%Pt10%Ru/C commercial catalyst is the most active of all the catalysts. The Tafel slopes were determined and found to be 63mV/dec and 179mV/dec, 66mV/dec and 189mV/dec and lastly 72mV/dec and 196mV/dec for the 20%Pt10%Ru/C commercial catalyst, 40%Pt20%Ru/C in-house catalyst and 30%Pt15%Ru/C in-house catalyst, respectively (see Table 4.38). The catalyst with low Tafel slopes is the most active towards ORR and in this case that catalyst was found to be 20%Pt10%Ru/C commercial catalyst.

Table 4.38: Tafel slopes of the PtRu/C electro-catalysts

Catalysts	20%Pt10%Ru/C Commercial	30%Pt15%Ru/C In-house	40%Pt20%Ru/C In-house
Region1 (mV/dec)	63	66	72
Region2 (mV/dec)	179	189	196

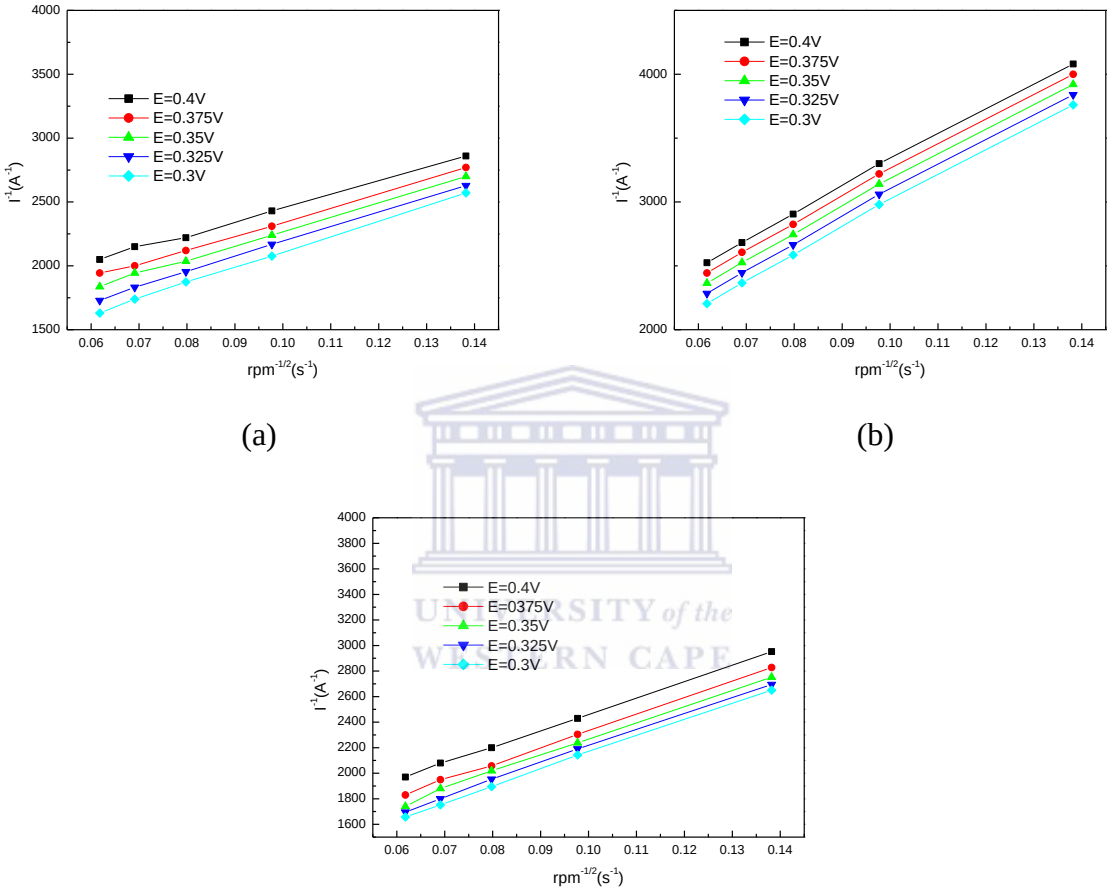

(a) (b)

(c)

Figure 4.46: Koutecky-Levich plots of a) 20%Pt10%Ru/C Commercial, b) 30%Pt15%Ru/C and c) 40%Pt20%Ru/C In-house electro-catalysts at different potentials (0.4V, 0.375V, 0.35V, 0.325V and 0.3V)

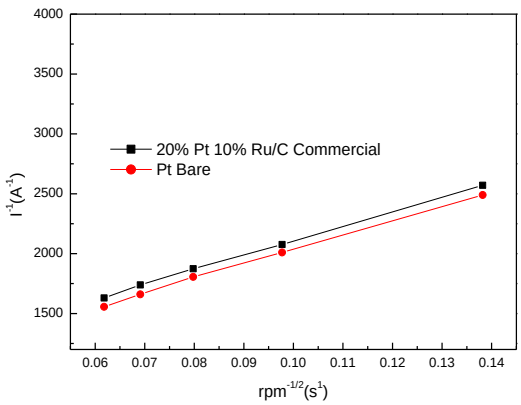

(a)

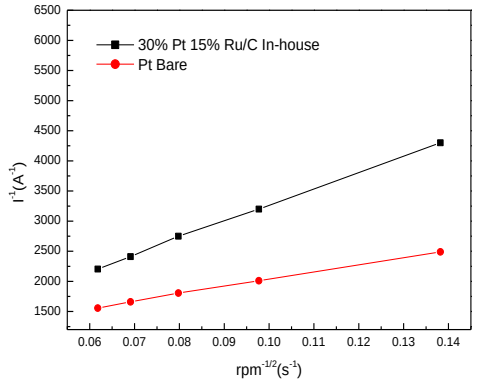

(b)

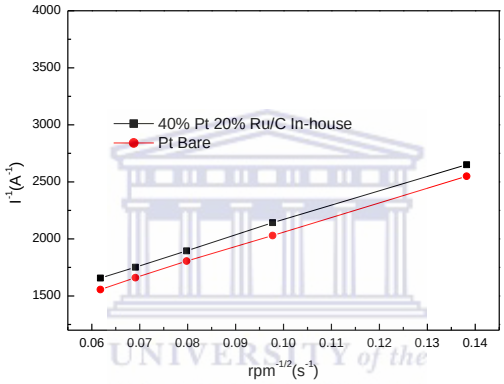

(c)

Figure 4.47: Koutecky-Levich plots of a) 20%Pt10%Ru/C Commercial, b) 30%Pt15%Ru/C and c) 40%Pt20%Ru/C In-house electro-catalysts at a potential of 0.375V

In Figure 4.47 K-L plots (at 0.375V from Figure 4.46) for the PtRu/C electro-catalysts are given. It can be seen that the K-L plot of the 20%Pt10%Ru/C commercial and that of the 40%Pt20%Ru/C in-house catalyst are similar to the K-L plot of the Pt bare electrode. This implies that the reaction occurring at these catalysts follows the four-electron transfer. This is not the case for the 30%Pt15%Ru/C in-house catalyst, the K-L plot of this catalyst is not similar to that of the Pt bare electrode. In this Figure a sharp straight line similar to the one observed in the literature for a two-electron transfer is observed. This means that this catalyst is not a good cathode catalyst as it follows the electro-reduction of oxygen to hydrogen peroxide which is low in efficiency and very much corrosive. This may be attributed to the agglomeration of the particles in this catalyst.

(4) 20%PtCo/C Commercial and 30%PtCo/C In-house electro-catalysts

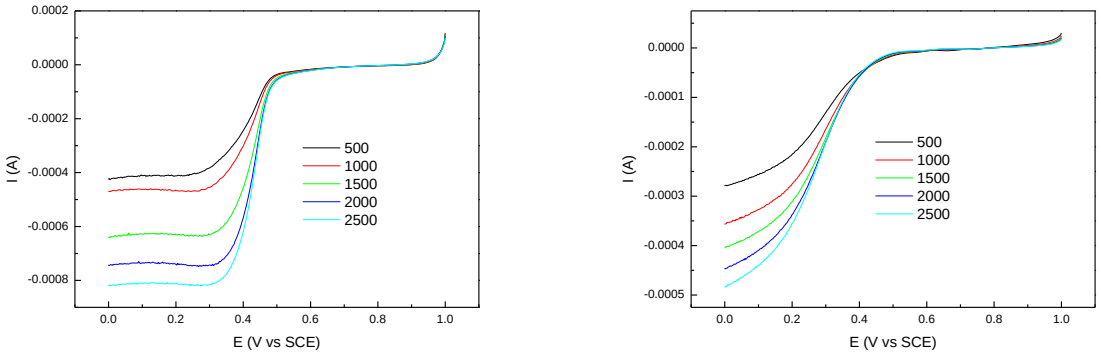

(a) (b)

Figure 4.48: Oxygen reduction polarization curves for 500, 1000, 1500, 2000, 2500 rpm speed rates of a) 20%PtCo/C Commercial and b)30%PtCo/C In-house electro-catalysts in O_2 saturated 0.5M H_2SO_4 at a scan rate of 20mV

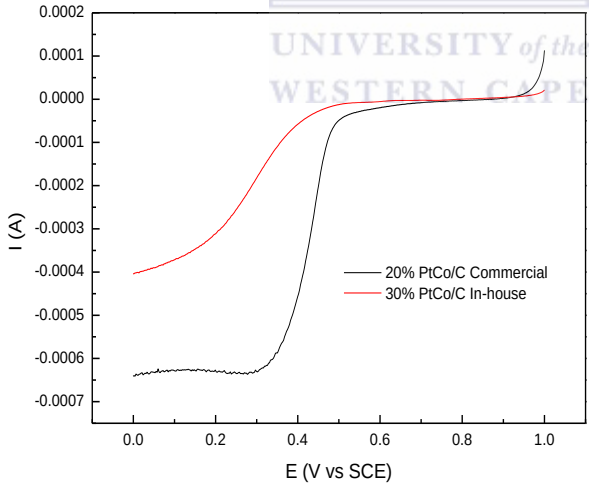

Figure 4.49: Polarization curves for the ORR on 20%PtCo/C Commercial and 30%PtCo/C In-house electro-catalysts in O_2 saturated 0.5M H_2SO_4 at a sweep rate of 5mV/s, rotating velocity of 1500rpm, at room temperature

It is observed (see Figure 4.49) that 20%PtCo/C commercial catalyst has the highest activity compared to the in-house catalyst (1500rpm curves from Figure 4.48). The commercial

catalyst is observed at more positive potentials with a half wave potential of 0.5V and that of the In-house catalyst was found to be 0.3V. The diffusion limiting current density of the 30%PtCo/C in-house catalysts is the lowest and that of 20%PtCo/C commercial is the highest. The current densities of the 20%PtCo/C commercial and 30%PtCo/C in-house catalysts are as follows, 0.023A/cm^2 and 0.003A/cm^2, respectively (see Table 4.39). The 30%PtCo/C in-house catalyst is observed to have a very much lower ORR activity compared to the commercial catalyst. The MA of the 20%PtCo/C commercial and 30%PtCo/C in-house electro-catalysts were found to be 0.090A/g and 0.012A/g, respectively and the SA were found to be 0.036A/cm^2 and 0.005A/cm^2, respectively. The mass activity and the specific activity of the 20%PtCo/C catalyst in literature was found to be MA 0.017 A/g and SA 0.0698 A/cm^2 [124]. The MA of the in-house catalyst is almost the same with the one obtained in literature but the SA is low and this could be attributed to an experimental error.

Table 4.39: Current density, mass activity and specific activity of PtCo/C electro-catalysts at i=0.45V

Catalysts	20%PtCo/C Commercial	30%PtCo/C In-house
Current density (A/cm^2)	0.023	0.003
Mass activity (A/g)	0.090	0.012
Specific activity (A/cm^2)	0.036	0.005

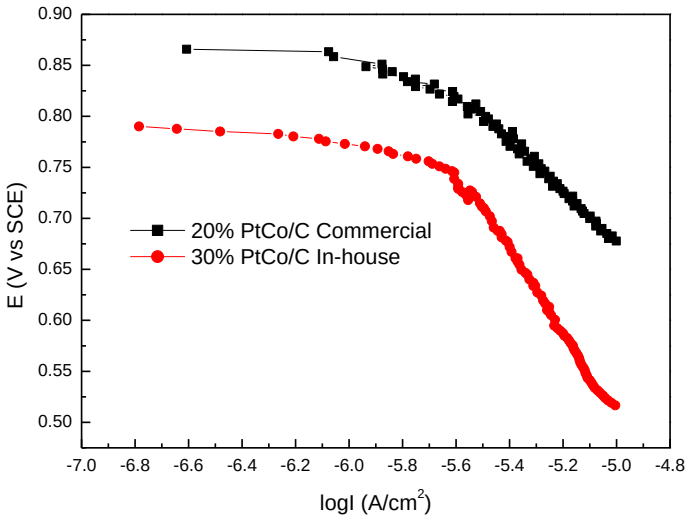

Figure 4.50: Mass transfer polarization curves for the ORR on 20%PtCo/C

Commercial and 30%PtCo/C In-house electro-catalysts in O_2 saturated 0.5M H_2SO_4 at a sweep rate of 5mV/s, rotating velocity of 1500rpm, at room temperature

The Tafel plot (see Figure 4.50) is in good agreement with Figure 4.49. This plot presents a comparison of the ORR activity of these catalysts. It was found that the 30%PtCo/C in-house is very much low in activity compared to the commercial catalyst. Note that the in-house catalyst's Tafel plot at the lower current region is observed at very low potentials than the commercial catalyst. This was further confirmed by the Tafel slopes since the in-house exhibited higher Tafel slopes compared to the commercial catalysts. The in-house catalyst Tafel slopes were found to be 73mV/dec and 223mV/dec while the commercial catalyst Tafel slopes were 58mV/dec and 163mV/dec (see Table 4.40). This very low activity of the in-house catalyst could be attributed to the fact that this catalyst exhibited a large particle size and the particles were agglomerated as seen by HRTEM Figure 4.4. The higher Pt catalyst content of the in-house did not have any effect on the activity of the catalyst as seen by HRTEM in section 4.1.

Table 4.40: Tafel slopes of the PtCo/C electro-catalysts

Catalysts	20%PtCo/C Commercial	30%PtCo/C In-house
Region1 (mV/dec)	58	73
Region2 (mV/dec)	163	223

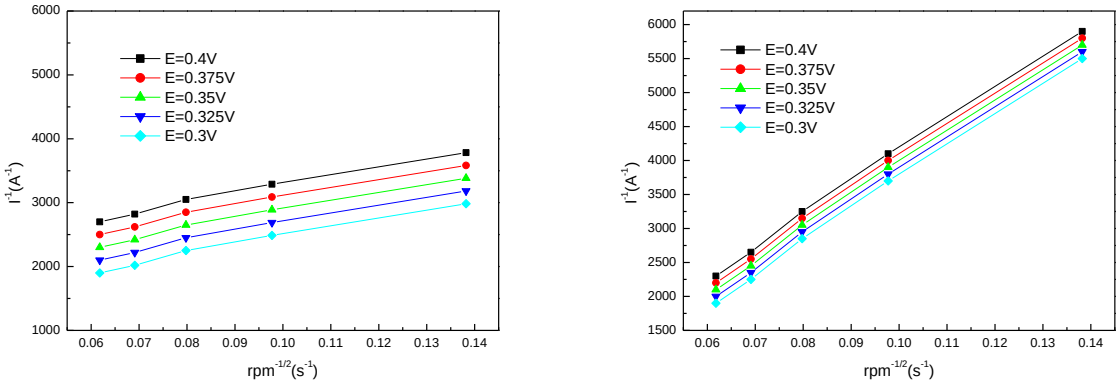

(a) (b)

Figure 4.51: Koutecky-Levich plots of a) 20%PtCo/C Commercial and b) 30%PtCo/C In-house electro-catalysts at different potentials (0.4V, 0.375V, 0.35V, 0.325V and 0.3V)

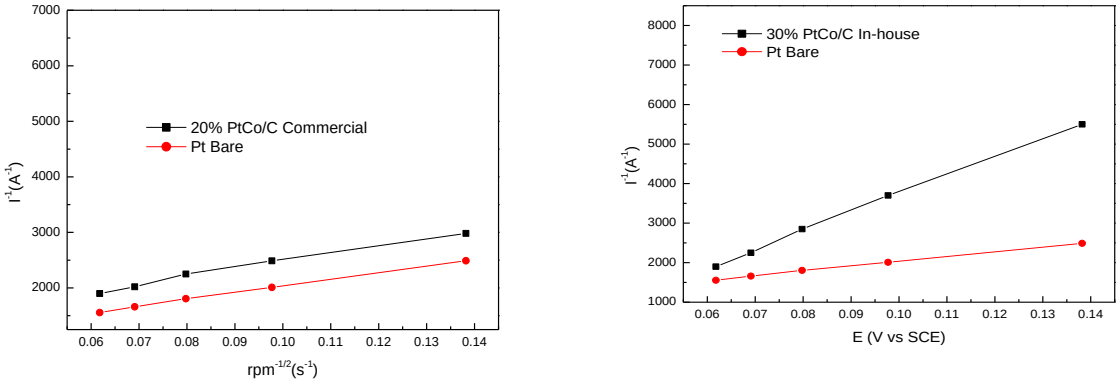

(a) (b)

Figure 4.52: Koutecky-Levich plots of a) 20%PtCo/C Commercial and b) 30%PtCo/C In-house electro-catalysts at a potential of 0.375V

Figure 4.51 presents the K-L plots of 20%PtCo/C commercial and 30%PtCo/C in-house catalysts prepared from data in Figure 4.48. In Figure 4.52a the K-L plot of the commercial catalyst is similar to that of the Pt bare electrode indicative of a four-electron transfer but for the in-house catalyst the K-L plot is not similar to that of the Pt bare electrode. The K-L plot of the 30%PtCo/C in-house catalyst indicates that the catalyst is inactive towards ORR. This catalyst is not a good cathode catalyst.

(5) 20%PtCu/C Commercial and 20%Pt20%Cu/C In-house electro-catalysts

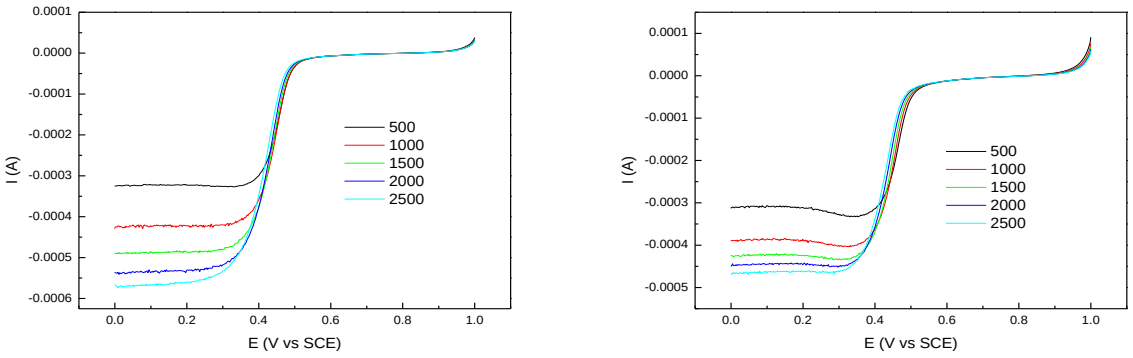

(a) (b)

Figure 4.53: Oxygen reduction polarization curves for 500, 1000, 1500, 2000, 2500 rpm speed rates of a) 20%PtCu/C Commercial and b) 20%Pt20%Cu/C In-house electro-catalysts in O_2 saturated 0.5M H_2SO_4 at a scan rate of 20mV

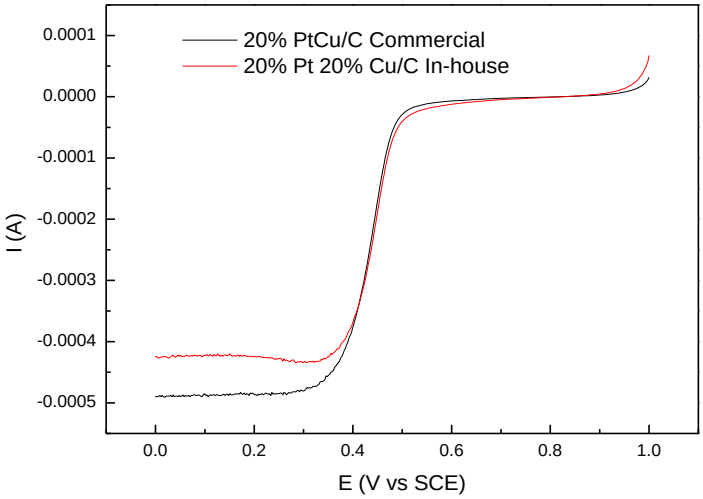

Figure 4.54: Polarization curves for the ORR on 20%PtCu/C Commercial and 20%Pt20%Cu/C In-house electro-catalysts in O_2 saturated 0.5M H_2SO_4 at a sweep rate of 5mV/s, rotating velocity of 1500rpm, at room temperature

In Figure 4.54 the activity of the 20%PtCu/C Commercial and 20%Pt20%Cu/C In-house catalysts (1500rpm curves from Figure 4.53) is observed to be the same since the curves at the mixed control region for both catalysts is the same that is they have the same half wave potential, 0.4V. The diffusion limiting current density of the catalysts differ in that the diffusion limiting current density of 20%PtCu/C commercial is slightly higher than that of 20%Pt20%Cu/C in-house. The current densities of these catalysts were found to be 0.019A/cm^2 and 0.021 A/cm^2 for both 20%PtCu/C commercial and 20%Pt20%PtCu/C in-house catalyst, respectively (see Table 4.41). The current densities of these catalysts differ but the difference is not big and the in-house catalyst seems to have more current density than the commercial catalyst. The MA of the 20%PtCu/C commercial and 20%Pt20%Cu/C in-house catalysts were found to be 0.076A/g and 0.083A/g, respectively and the SA were found to be 0.030A/cm^2 and 0.033A/cm^2, respectively.

Table 4.41: Current density, mass activity and specific activity of PtCu/C electro-catalysts at i=0.45V

Catalysts	**20%PtCu/C Commercial**	**20%Pt20%Cu/C In-house**
Current density (A/cm^2)	0.019	0.021
Mass activity (A/g)	0.076	0.083
Specific activity (A/cm^2)	0.030	0.033

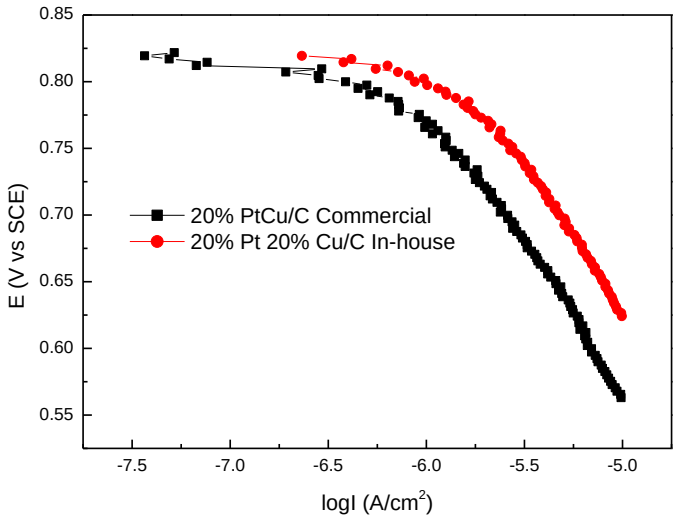

Figure 4.55: Mass transfer polarization curves for the ORR on 20%PtCu/C Commercial and 20%Pt20%Cu/C In-house electro-catalysts in O_2 saturated 0.5M H_2SO_4 at a sweep rate of 5mV/s, rotating velocity of 1500rpm, at room temperature

The comparison of the ORR activity of the catalyst's polarization curves in Figure 4.54 is not very clear, the curves are on top of one another and the current of the in-house catalyst is slightly higher than that of the commercial catalyst. From the Tafel plot shown the 20%Pt20%Cu/C in-house catalyst is identified as the most active catalyst when compared to the commercial catalyst. The in-house catalyst exhibited high currents in the high current region than the commercial catalyst. This is further emphasized by the Tafel slopes where 20%PtCo/C commercial gives a slope of 76mV/dec and 194mV/dec while the 20%Pt20%Cu/C in-house catalyst gives a slope of 72mV/dec and 176mV/dec (see Table 4.42). This is in good agreement with the current density found in Figure 4.53 since the difference was slightly higher in the activity of the in-house catalyst and with the Tafel slopes also the catalyst's slopes don't differ much.

Table 4.42: Tafel slopes of the PtCu/C electro-catalysts

Catalysts	20%PtCu/C Commercial	20%Pt20%Cu/C In-house
Region1 (mV/dec)	76	72
Region2 (mV/dec)	194	176

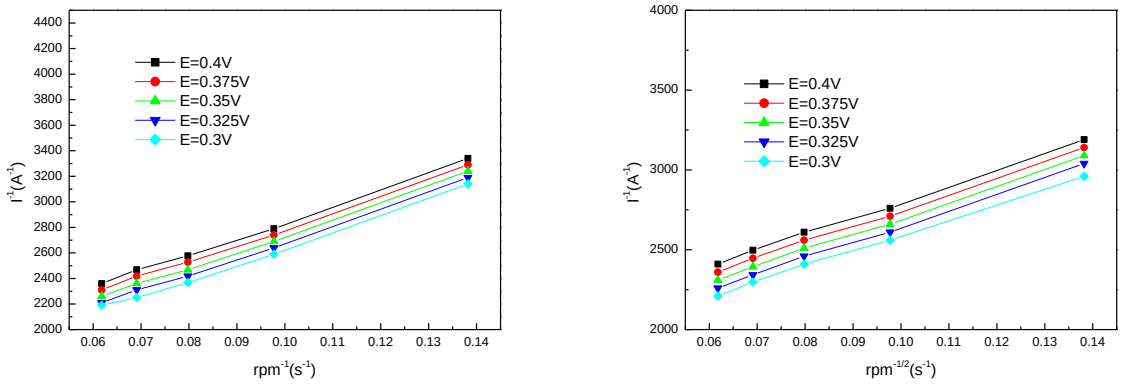

(a) (b)

Figure 4.56: Koutecky-Levich plots of a) 20%PtCu/C Commercial and b) 20%Pt20%Cu/C In-house electro-catalysts at different potentials (0.4V, 0.375V, 0.35V, 0.325V and 0.3V)

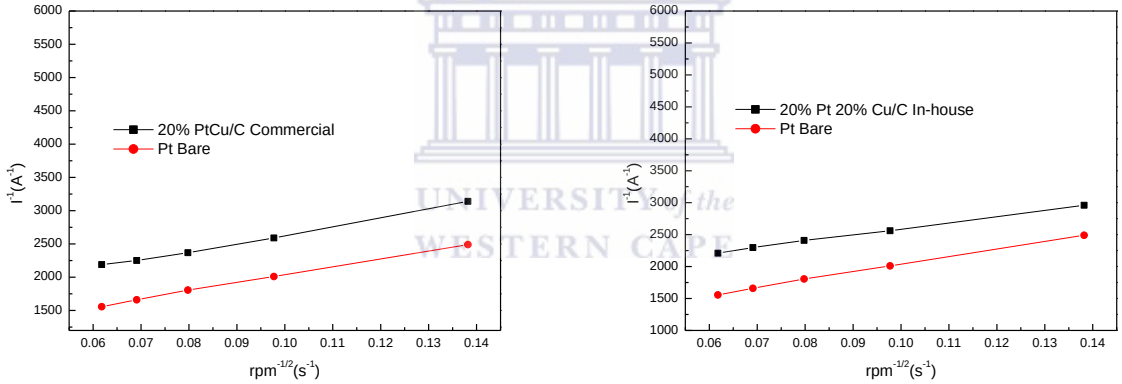

(a) (b)

Figure 4.57: Koutecky-Levich plots of a) 20%PtCu/C Commercial and b) 20%Pt20%Cu/C In-house electro-catalysts at a potential of 0.375V

Both catalysts follow the same trend of the four-electron transfer and this is observed by the similarity of the K-L plots (at 0.375V from Figure 4.56) of these catalysts with that of the Pt bare electrode. Both catalysts give a straight line, meaning that these electro-catalysts are good cathode catalysts.

(6) 20%PtSn/C Commercial and 20%PtSn/C In-house electro-catalysts

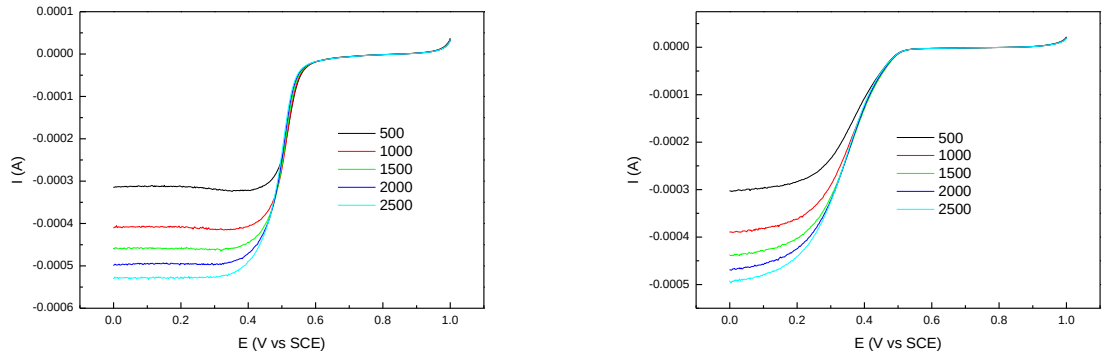

(a) (b)

Figure 4.58: Oxygen reduction polarization curves for 500, 1000, 1500, 2000, 2500 rpm speed rates of a) 20%PtSn/C Commercial and b)20%PtSn/C In-house electro-catalysts in O_2 saturated 0.5M H_2SO_4 at a scan rate of 20mV

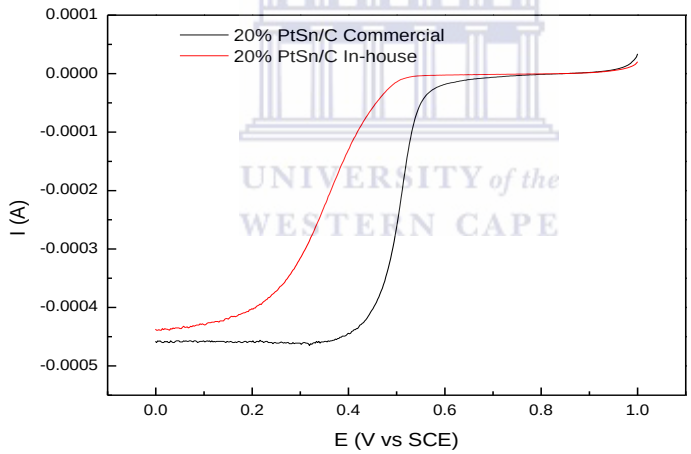

Figure 4.59: Polarization curves for the ORR on 20%PtSn/C Commercial and 20%PtSn/C In-house electro-catalysts in O_2 saturated 0.5M H_2SO_4 at a sweep rate of 5mV/s, rotating velocity of 1500rpm, at room temperature

Polarization curves (1500rpm curves from Figure 4.58) showing the ORR activity of the PtSn/C catalysts are given in Figure 4.59. Figure 4.59 clearly shows that the 20%PtSn/C commercial catalyst has enhanced activity than the 20%PtSn/C in-house catalyst. The diffusion limiting current densities of these catalysts are almost the same. The half wave potential of these catalysts proves that the 20%PtSn/C commercial (0.5V) has more activity than 20%PtSn/C in-house (0.3V) with current densities of 0.041A/cm^2 and 0.006 A/cm^2, respectively (Table 4.43). The in-house catalyst is very much inactive towards ORR. The MA

of the 20%PtSn/C commercial and 20%PtSn/C in-house catalysts were found to be 0.163A/g and 0.025A/g, respectively and the SA were found to be 0.065A/cm^2 and 0.010A/cm^2, respectively.

Table 4.43: Current density, mass activity and specific activity of PtSn/C electro-catalysts at i=0.45V

Catalyst	20%PtSn/C Commercial	20%PtSn/C In-house
Current density (A/cm^2)	0.041	0.006
Mass activity (A/g)	0.163	0.025
Specific activity (A/cm^2)	0.065	0.010

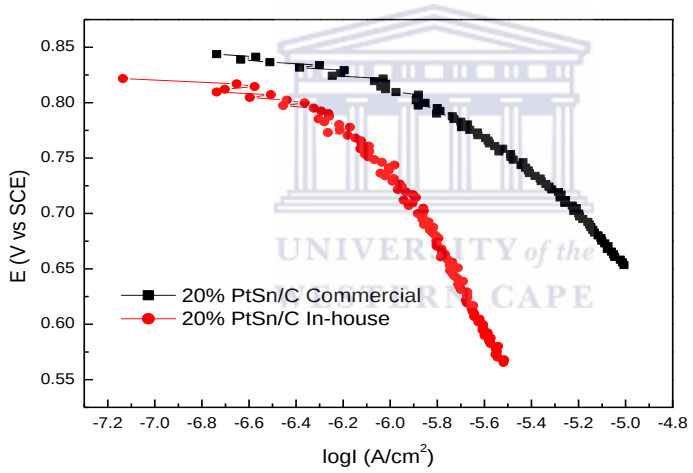

Figure 4.60: Mass transfer polarization curves for the ORR on 20%PtSn/C Commercial and 20%PtSn/C In-house electro-catalysts in O_2 saturated 0.5M H_2SO_4 at a sweep rate of 5mV/s, rotating velocity of 1500rpm, at room temperature

The curves obtained as illustrated in Figure 4.60 are in good agreement with Figure 4.59. From the curves it can be seen that the 20%PtSn/C in-house catalyst is very much inactive compared to the commercial catalyst which is observed at higher potentials in the low current region than the in-house catalyst. The Tafel slopes obtained were 67mV/dec and 188mV/dec for the commercial catalyst, while the slopes for the in-house catalyst were 79mV/dec and 243mV/dec (see Table 4.44). The higher the Tafel slope the faster the overpotential increase with the current density. This was observed for the in-house catalyst since it exhibits a high Tafel slope than the commercial catalyst.

Table 4.44: Tafel slopes of the PtSn/C electro-catalysts

Catalysts	20%PtSn/C Commercial	20%PtSn/C In-house
Region1 (mV/dec)	67	79
Region2 (mV/dec)	243	243

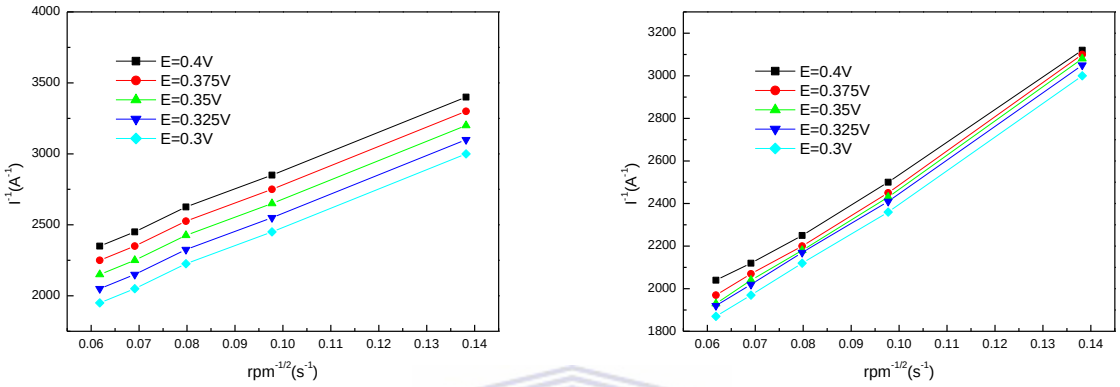

(a) (b)

Figure 4.61: Koutecky-Levich plots of a) 20%PtSn/C Commercial and b) 20%PtSn/C In-house electro-catalysts at different potentials (0.4V, 0.375V, 0.35V, 0.325V and 0.3V)

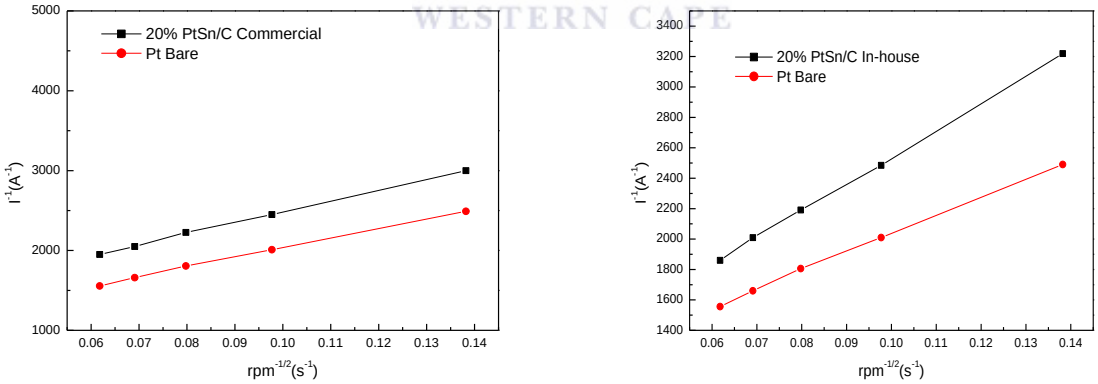

Figure 4.62: Koutecky-Levich plots of a) 20%PtSn/C Commercial and b) 20%PtSn/C In-house electro-catalysts at a potential of 0.375V

Figure 4.62 shows that the oxygen reduction reaction (ORR) of the 20%PtSn/C in-house catalyst (at 0.375V from Figure 4.61) follows the electro-reduction of oxygen to hydrogen peroxide which means that this catalyst is not good for ORR, therefore it cannot be used as a cathode catalyst. The 20%PtSn/C commercial catalyst shows a four-electron transfer, therefore it means that this catalyst is a better cathode catalyst than the in-house catalyst.

(7) Effect of heat treatment on the ORR activity of the 20%PtCo/C Commercial and 30%PtCo/C In-house electro-catalysts

(a) 20%PtCo/C Commercial electro-catalyst

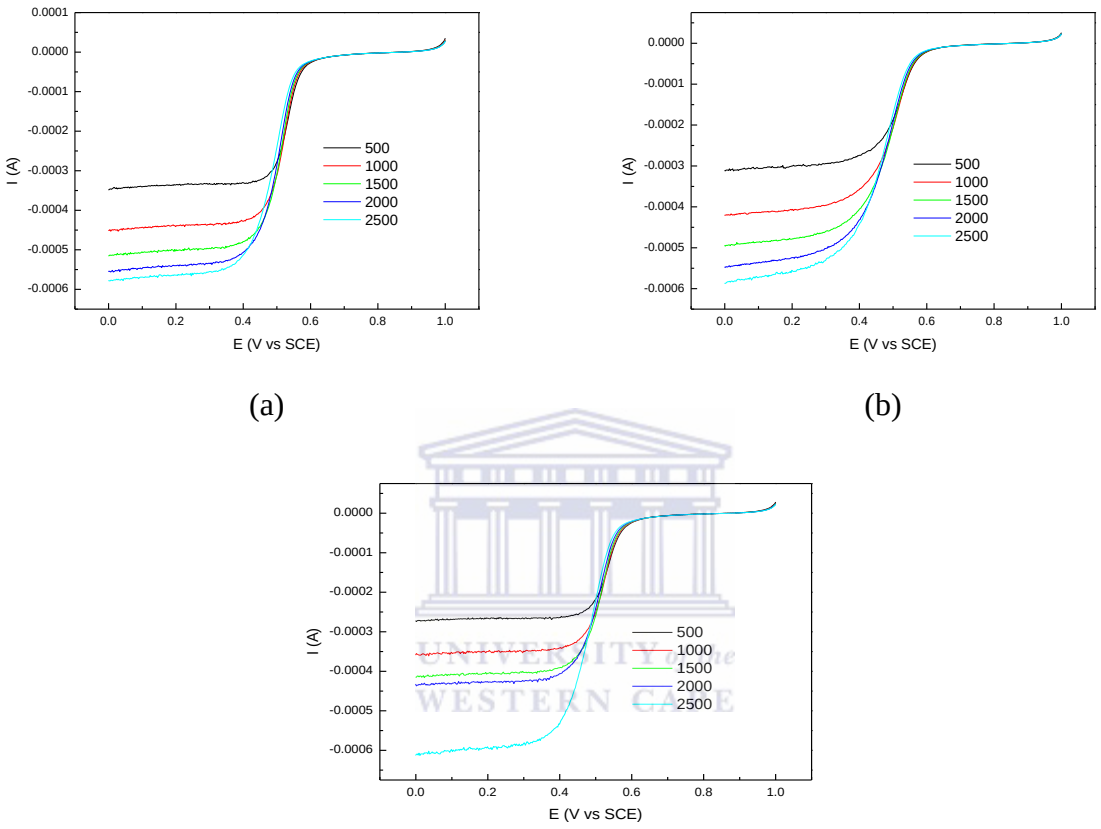

Figure 4.63: Oxygen reduction polarization curves for 500, 1000, 1500, 2000, 2500 rpm speed rates of a) 20%PtCo/C Commercial (350^0C), b) 20%PtCo/C Commercial (650^0C) and c) 20%PtCo/C Commercial (800^0C) electro-catalysts in O_2 saturated 0.5M H_2SO_4 at a scan rate of 20mV

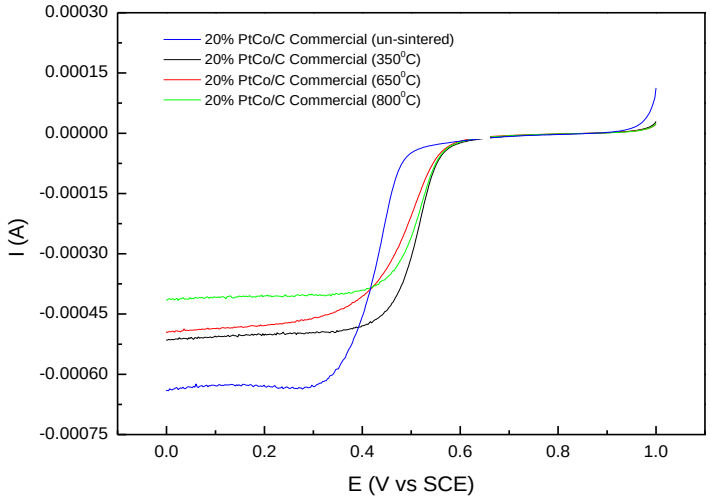

Figure 4.64: Polarization curves for the ORR of 20%PtCo/C Commercial (un-sintered), 20%PtCo/C Commercial (350^0C), 20%PtCo/C Commercial (650^0C), and 20%PtCo/C Commercial (800^0C) electro-catalysts in O_2 saturated 0.5M H_2SO_4 at a sweep rate of 5mV/s, rotating velocity of 1500rpm, at room temperature

The 20%PtCo/C commercial catalyst was heat treated at different temperatures to see whether the heat treatment will enhance the ORR activity. From Figure 4.64 (1500rpm curves from Figure 4.63) it is observed that this catalyst heated at 350^0C gives slightly better ORR activity compared to when this catalyst is heated at other temperatures. This catalyst heat treated at 350^0C is observed at a half wave potential not too different from those of the other catalyst that it is compared with. The current density was found to be 0.045A/cm^2 for the 20%PtCo/C commercial (350^0C), 0.034 A/cm^2 for the 20%PtCo/C commercial (650^0C) and 0.036A/cm^{2}for the 20%PtCo/C commercial (800^0C) as shown in Table 4.45. This shows that there isn't much difference in the activity of this catalyst after being heat treated at different temperatures. The current density of the un-sintered catalyst was found to be 0.023 A/cm^2. It can be noted that the current density of the catalyst after the heat treatment shows that the heat treatment indeed enhanced the activity of this catalyst. The MA of the 20%PtCo/C commercial (350^0C), 20%PtCo/C commercial (650^0C), and 20%PtCo/C commercial (800^0C) were found to be 0.178A/g, 0.135A/g and 0.144A/g, respectively and the SA were found to be 0.071A/cm^2, 0.054A/cm^2 and 0.057A/cm^2, respectively.

Table 4.45: Current density, mass activity and specific activity of heat treated PtCo/C commercial electro-catalysts at i=0.45V

Catalyst	20%PtCo/C Commercial (Un-sintered)	20%PtCo/C Commercial (350^0C)	20%PtCo/C Commercial (650^0C)	20%PtCo/C Commercial (800^0C)
Current density (A/cm^2)	0.023	0.045	0.034	0.036
Mass activity (A/g)	0.090	0.178	0.135	0.144
Specific activity (A/cm^2)	0.036	0.071	0.054	0.057

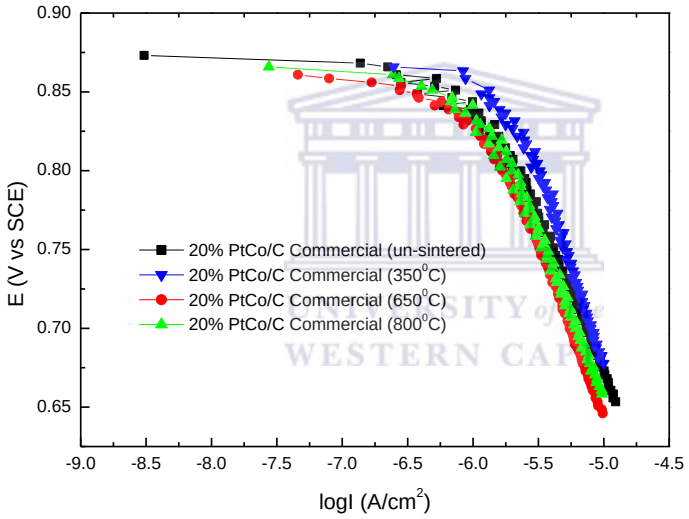

Figure 4.65: Mass transfer polarization curves for the ORR on 20%PtCo/C Commercial (un-sintered), 20%PtCo/C Commercial (350^0C), 20%PtCo/C Commercial (650^0C) and 20%PtCo/C Commercial (800^0C) electro-catalysts in O_2 saturated 0.5M H_2SO_4 at a sweep rate of 5mV/s, rotating velocity of 1500rpm, at room temperature

Figure 4.65 shows that the activity of the catalyst heat treated at different temperatures does not differ much from un-sintered catalyst. This Figure is in good agreement with Figure 4.64 since it is observed that the curves are on top of one another indicating that the activity of the catalyst heat treated at different temperatures does not differ much or the activity of the catalyst at different temperatures are very much close to one another. The Tafel slopes for the 20%PtCo/C commercial catalyst heat treated at 350^0C, 650^0C and 800^0C were found to be

61mV/dec and 174mV/dec, 79mV/dec and 242mV/dec and lastly 72mV/dec and 207mV/dec, respectively (see Table 4.46).

Table 4.46: Tafel slopes of the heat treated PtCo/C commercial electro-catalysts

Catalyst	20%PtCo/C Commercial (Un-sintered)	20%PtCo/C Commercial (350^0C)	20%PtCo/C Commercial (650^0C)	20%PtCo/C Commercial (800^0C)
Region1 (mV/dec)	58	61	79	72
Region2 (mV/dec)	163	174	242	207

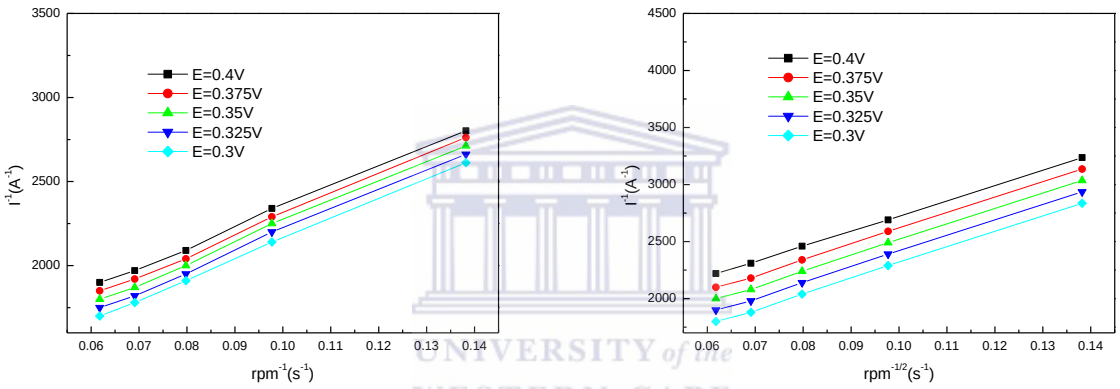

(a) (b)

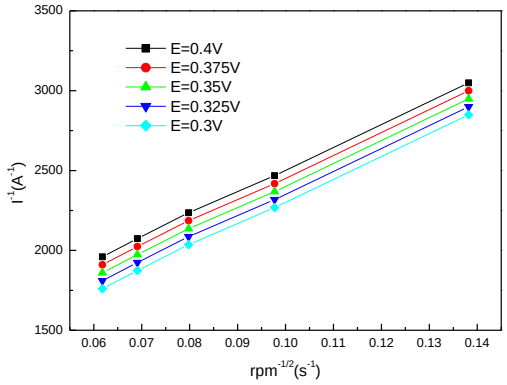

(c)

Figure 4.66: Koutecky-Levich plots of a) 20%PtCo/C Commercial (350^0C), b) 20%PtCo/C Commercial (650^0C), and c) 20%PtCo/C Commercial (800^0C) electro-catalysts at different potentials (0.4V, 0.375V, 0.35V, 0.325V and 0.3V**)**

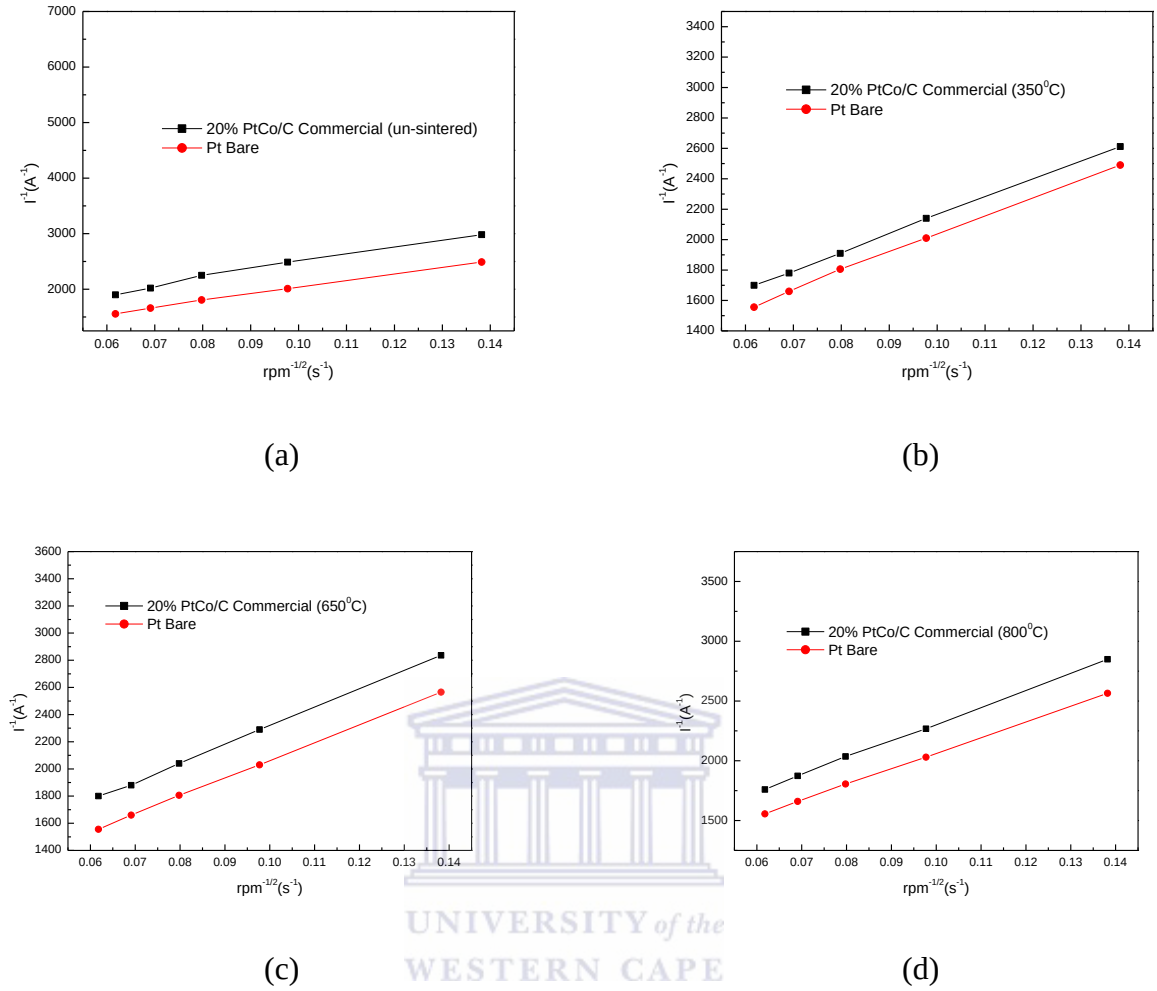

Figure 4.67: Koutecky-Levich plots of a) 20%PtCo/C Commercial (un-sintered), b) 20%PtCo/C Commercial (350^{0}C), c) 20%PtCo/C Commercial (650^{0}C) and d) 20%PtCo/C Commercial (800^{0}C) electro-catalysts at a potential of 0.375V

Figure 4.67 shows that for all the temperatures that the catalyst was heat treated at (data from Figure 6.6 at 0.375V), it did not change the electron transfer or the activity of the catalyst. The catalyst still follows the four-electron transfer reaction as it did in Figure 4.67a.

(b) 30%PtCo/C In-house electro-catalyst

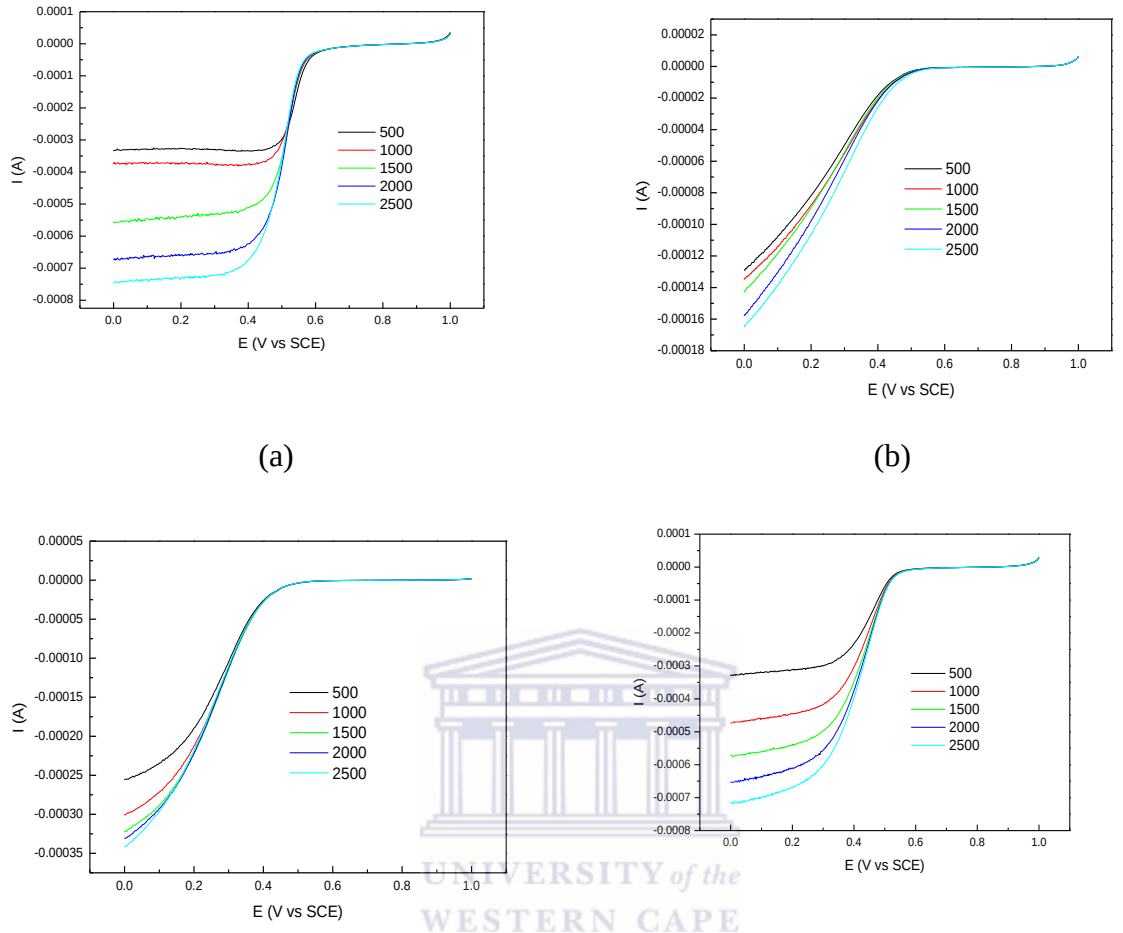

Figure 4.68: Oxygen reduction polarization curves for 500, 1000, 1500, 2000, 2500 rpm speed rates of a) 30%PtCo/C In-house (350^0C), b) 30%PtCo/C In-house (650^0C), c) 30%PtCo/C In-house (800^0C) and d) 20%PtCo/C In-house (800^0C) electro-catalysts in O_2 saturated 0.5M H_2SO_4 at a scan rate of 20mV

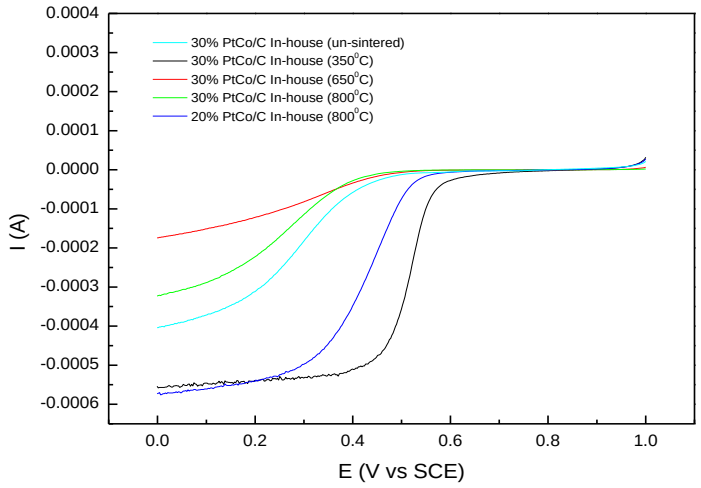

Figure 4.69: Polarization curves for the ORR on 30%PtCo/C In-house (un-sintered), 30%PtCo/C In-house (350^{0}C), 30%PtCo/C In-house (650^{0}C), 30%PtCo/C In-house (800^{0}C) and 20%PtCo/C In-house (800^{0}C) electro-catalysts of in O_2 saturated 0.5M H_2SO_4 at a sweep rate of 5mV/s, rotating velocity of 1500rpm, at room temperature

From Figure 4.69 it is shown that the catalyst heat treated at 350^{0}C gives better ORR activity compared to the catalysts heat treated at 650^{0}C and 800^{0}C (1500rpm curves from Figure 4.68). The catalyst heat treated at 350^{0}C is observed at a half wave potential more positive than the other catalysts heat treated at 650^{0}C and 800^{0}C. The catalyst is followed by the 20%PtCo/C in-house catalyst heat treated at 800^{0}C. The current densities of these catalysts are as follows, 0.048A/cm^2 for the 30%PtCo/C in-house (350^{0}C), 0.001 A/cm^2 for 30%PtCo/C in-house (650^{0}C), 0.002A/cm^2 for the 30%PtCo/C in-house (800^{0}C) and 0.022A/cm^2 for 20%PtCo/C in-house catalyst (800^{0}C) as shown in Table 4.47. The current density of the un-sintered 30%PtCo/C in-house catalyst was found to be 0.003A/cm^2. Comparing it to the current density after the heat treatment it is observed that the current density increased dramatically when the catalyst was heat treated at 350^{0}C. It decreased when heat treated at 650^{0}C and 800^{0}C and the decrease in the last two heat treatment temperatures is almost the same. The MA of the 30%PtCo/C in-house (350^{0}C), 30%PtCo/C in-house (650^{0}C), 30%PtCo/C in-house (800^{0}C) and 20%PtCo/C in-house (800^{0}C) were found to be 0.191A/g, 0.005A/g, 0.008A/g and 0.089A/g and the SA were found to be 0.076A/cm^2, 0.002A/cm^2, 0.003A/cm^2 and 0.036A/cm^2, respectively.

Table 4.47: Current density, mass activity and specific activity of heat treated PtCo/C in-house electro-catalysts at i=0.45V

Catalysts	30%PtCo/C In-house (Un-sintered)	30%PtCo/C In-house (350^0C)	30%PtCo/C In-house (650^0C)	30%PtCo/C In-house (800^0C)	20%PtCo/C In-house (800^0C)
Current density (A/cm^2)	0.003	0.048	0.001	0.002	0.022
Mass activity (A/g)	0.012	0.191	0.005	0.008	0.089
Specific activity (A/cm^2)	0.005	0.076	0.002	0.003	0.036

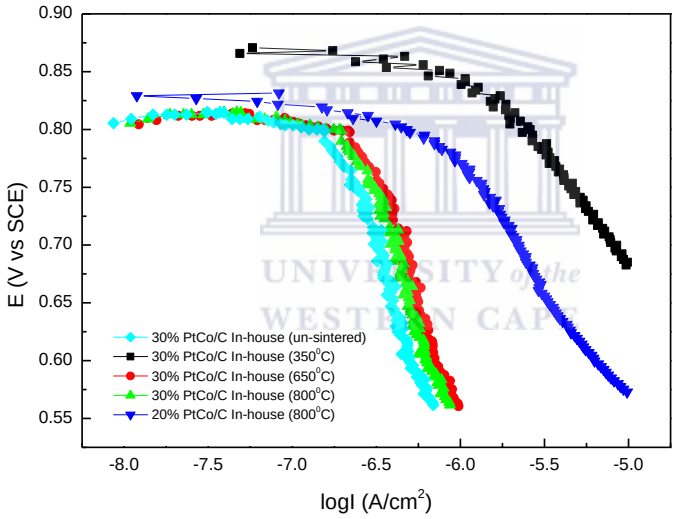

Figure 4.70: Mass transfer polarization curves for the ORR on 30%PtCo/C In-house (un-sintered), 30%PtCo/C In-house (350^0C), 30%PtCo/C In-house (650^0C), 30%PtCo/C In-house (800^0C)and 20%PtCo/C In-house (800^0C) electro-catalysts in O_2 saturated 0.5M H_2SO_4 at a sweep rate of 5mV/s, rotating velocity of 1500rpm, at room temperature

The Tafel plots (see Figure 4.70) shows that the catalyst heat treated at 350^0C gives better ORR activity. This is observed at much higher potentials at the lower current region when it is compared to the other heat treatment temperatures. The 20%PtCo/C in-house (800^0C) catalyst follows the 30%PtCo/C in-house (350^0C) catalyst in activity. The 30%PtCo/C

catalysts heat treated at 650^0Cand 800^0C are observed to have similar curves since the curves are on top of one another. This agrees well with Figure 4.68 since it was observed that the current densities of this catalyst heat treated at such temperatures are close. The Tafel slopes were found to be 51mV/dec and 167mV/dec for 30%PtCo/C in-house (350^0C) catalyst , 89mV/dec and 257mV/dec for 30%PtCo/C in-house (650^0C) catalyst, 76mV/dec and 227mV/dec for 30%PtCo/C in-house (800^0C) catalyst and 66mV/dec and 187mV/dec for 20%PtCo/C in-house (800^0C) catalyst (see Table 4.48).

Table 4.48: Tafel slopes of the heat treated PtCo/C in-house electro-catalysts

Catalysts	**20%PtCo/C In-house (Un-sintered)**	**20%PtCo/C In-house (350^0C)**	**20%PtCo/C In-house (650^0C)**	**20%PtCo/C In-house (800^0C)**	**20%PtCo/C In-house (800^0C)**
Region1 (mV/dec)	73	51	89	76	66
Region2 (mV/dec)	223	167	257	227	187

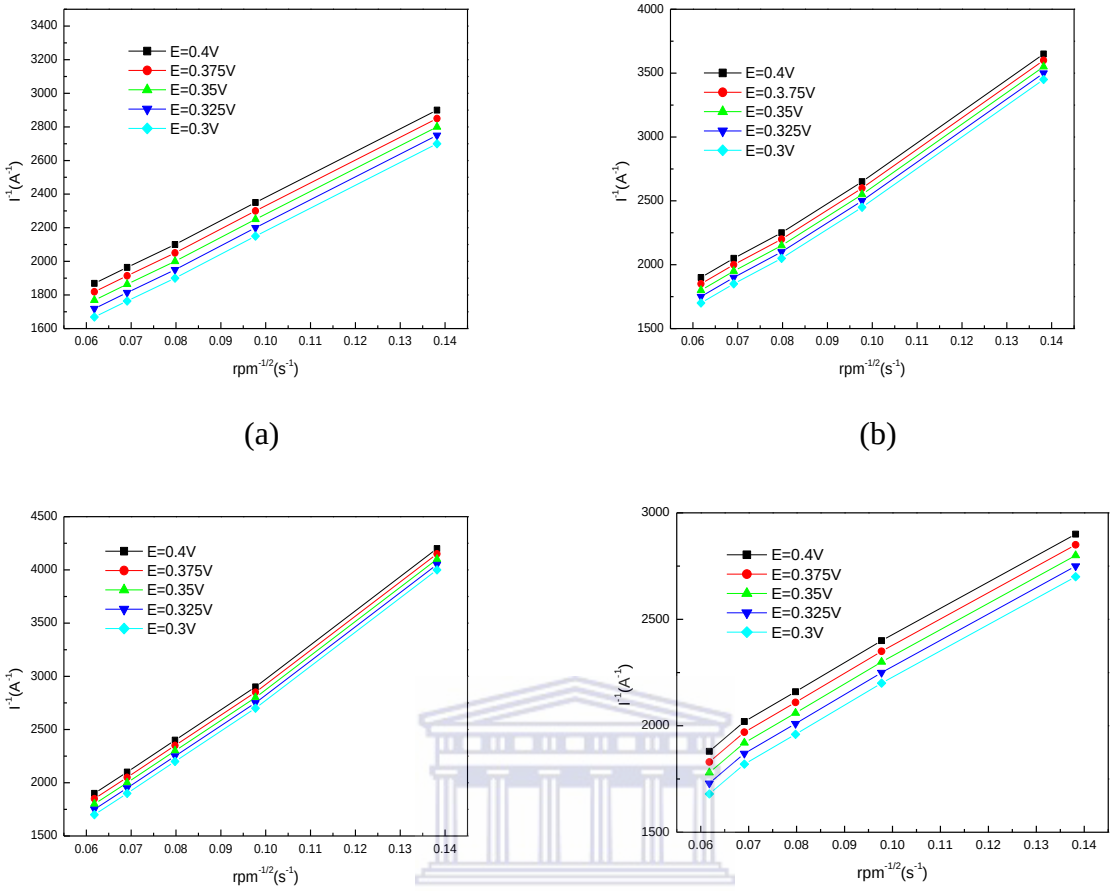

Figure 4.71: Koutecky-Levich plots of a) 30%PtCo/C In-house (350^0C), b) 30%PtCo/C In-house (650^0C), c) 30%PtCo/C In-house (800^0C) and d) 20%PtCo/C In-house (800^0C) electro-catalysts at different potentials (0.4V, 0.375V, 0.35V, 0.325V and 0.3V)

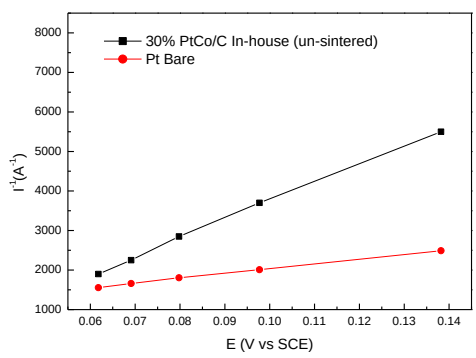

(a)

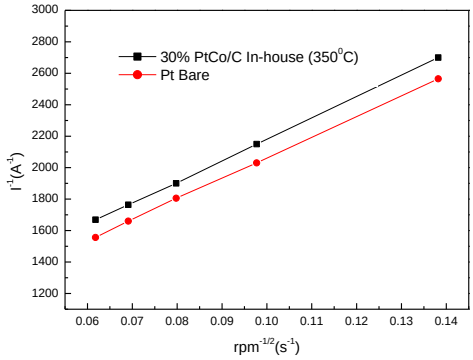

(b)

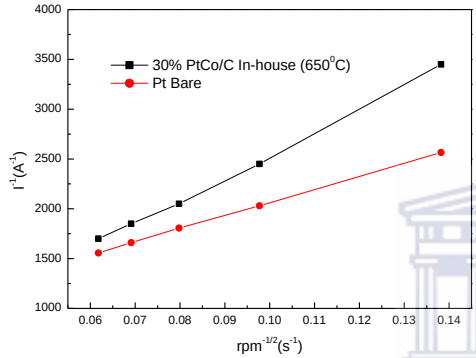

(c)

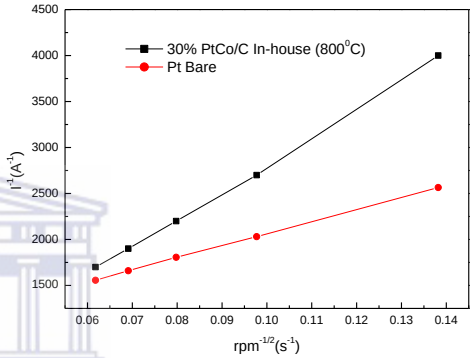

(d)

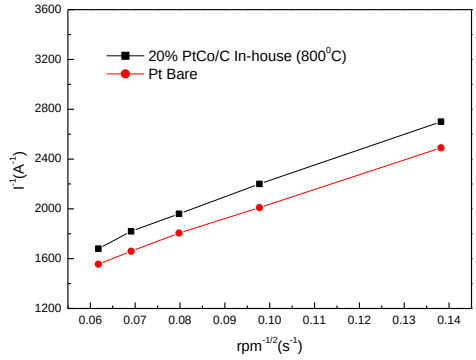

(e)

Figure 4.72: Koutecky-Levich plots of a) 30%PtCo/C In-house (un-sintered), b) 30%PtCo/C In-house (350^{0}C), c) 30%PtCo/C In-house (650^{0}C), d) 30%PtCo/C In-house (800^{0}C), and e) 20%PtCo/C In-house (800^{0}C) electro-catalysts at a potential of 0.375V

The un-sintered catalyst in Figure 4.72a showed that the 30%PtCo/C in-house catalyst exhibit a two-electron transfer reaction (data from Figure 4.71 at 0.375V). It is stated in the literature

that heat treatment enhances ORR activity [72] and this was the case for heat treating the catalyst at 350^0C but when the temperature was raised the oxygen reduction reaction remained a two-electron transfer and was expected to be a four electron transfer for the catalyst to be a good catalyst for ORR. Also the 20%PtCo/C in-house (800^0C) exhibited a four-electron transfer reaction same as the 30%PtCo/C in-house (350^0C).

4.4.1 Summary of rotating disk electrode study of the activity of oxygen reduction reaction on supported electro-catalysts

The results above show that the 20%Pt/C in-house catalyst has enhanced ORR activity. The 30%PtCo/C in-house catalyst has the lowest activity and the activity increased when this catalyst was heat treated at 350^0C. The 20%Pt/C in-house catalyst is observed to have smaller Tafel slopes compared to other electro-catalysts which means that this catalysts' ORR activity enhanced compared to other catalysts.

4.5 STUDY OF DIRECT METHANOL FUEL CELL ELECTRO-CATALYSTS

This section presents the study of direct methanol fuel cell electro-catalysts. This study will be looking at the cathode catalyst that are methanol tolerant, that won't be affected by the methanol crossover. Both the commercial catalysts and the in-house catalysts will be studied. In addition these catalysts will be studied as anode catalysts for the direct methanol fuel cell, that is looking at the methanol oxidation activity of these catalysts. The study of cathode catalysts was done in a rotating disk electrode at a scan rate of 5mV/s and the study of anode catalysts was done in a cyclic voltammetry at a scan rate of 20mV/s. Both these studies were done in 05M Sulphuric acid and 0.5M Methanol.

4.5.1 Study of cathode electro-catalysts

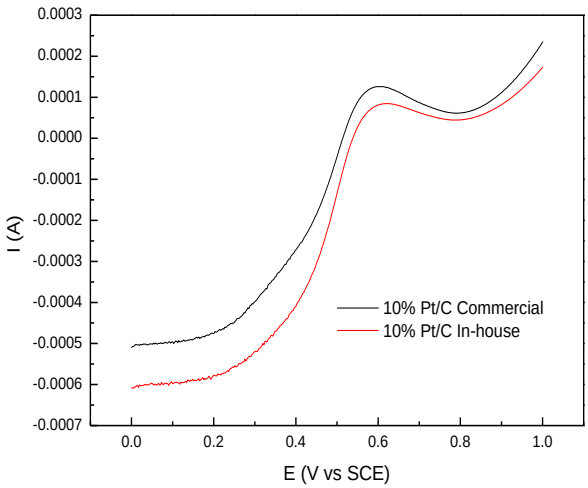

Figure 4.73: Polarization curves for the MOR on 10%Pt/C Commercial and 10%Pt/C In-house electro-catalysts in O_2 saturated 0.5M H_2SO_4 + 0.5M Methanol at a sweep rate of 5mV/s, rotating velocity of 1500rpm, and room temperature

In Figure 4.73 it is observed that the methanol oxidation peaks of the 10%Pt/C commercial and 10%Pt/C in-house are almost the same. This means that both catalysts are active in the presence of methanol, however the 10%Pt/C in-house is slightly methanol tolerant than 10%Pt/C commercial. This then shows that 10%Pt/C in-house is therefore a better cathode catalyst in the presence of methanol with methanol oxidation current densities of 0.009A/cm^2 and 0.013A/cm^2, respectively. The MA of the 10%Pt/C commercial and 10%Pt/C in-house catalysts were found to be 0.052A/g and 0.036A/g, respectively and the SA were found to be 0.021A/cm^2 and 0.014A/cm^2, respectively (see Table 4.49).

Table 4.49: Current density, mass activity and specific activity of 10%Pt/C electro-catalysts as cathode electro-catalysts for a DMFC

Catalysts	10%Pt/C Commercial	10%Pt/C In-house
Current density (A/cm^2)	0.013	0.009
Mass activity (A/g)	0.052	0.036
Specific activity (A/cm^2)	0.021	0.014

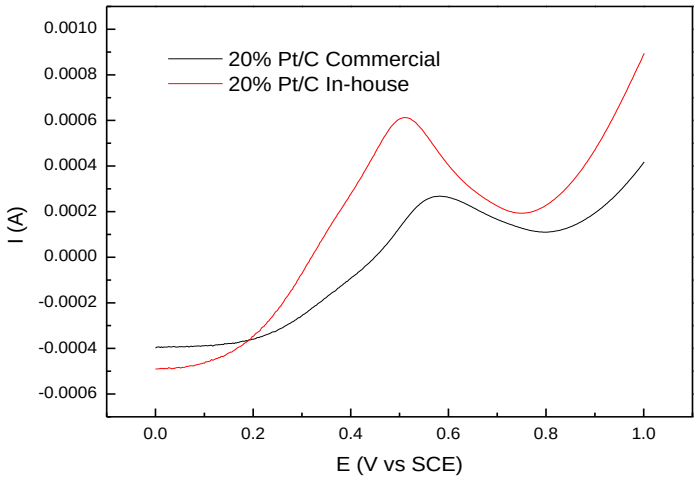

Figure 4.74: Polarization curves for the MOR on 20%Pt/C Commercial and 20%Pt/C In-house electro-catalysts in O_2 saturated 0.5M H_2SO_4 + 0.5M Methanol at a sweep rate of 5mV/s, rotating velocity of 1500rpm, and room temperature

From Figure 4.74 it is observed that the 20%Pt/C in-house catalyst has a high methanol oxidation peak than 20%Pt/C commercial, this proves that the 20%Pt/C in-house catalyst is more active in the presence of methanol and is therefore not methanol tolerant. The 20%Pt/C commercial catalyst is a better cathode catalyst than 20%Pt/C in-house in the presence of methanol because it has a lower methanol oxidation reduction (MOR) peak than the 20%Pt/C in-house catalyst with current densities of 0.024A/cm^2 and 0.060A/cm^2, respectively (see Table 4.50). The MA of the 20%Pt/C commercial and 20%Pt/C in-house catalysts were found to be 0.096A/g and 0.240A/g, respectively and the SA were found to be 0.038A/cm^2 and 0.096A/cm^2, respectively.

Table 4.50: Current density, mass activity and specific activity of 20%Pt/C electro-catalysts catalysts as cathode electro-catalysts for a DMFC

Catalysts	20%Pt/C Commercial	20%Pt/C In-house
Current density (A/cm^2)	0.024	0.060
Mass activity (A/g)	0.096	0.240
Specific activity (A/cm^2)	0.038	0.096

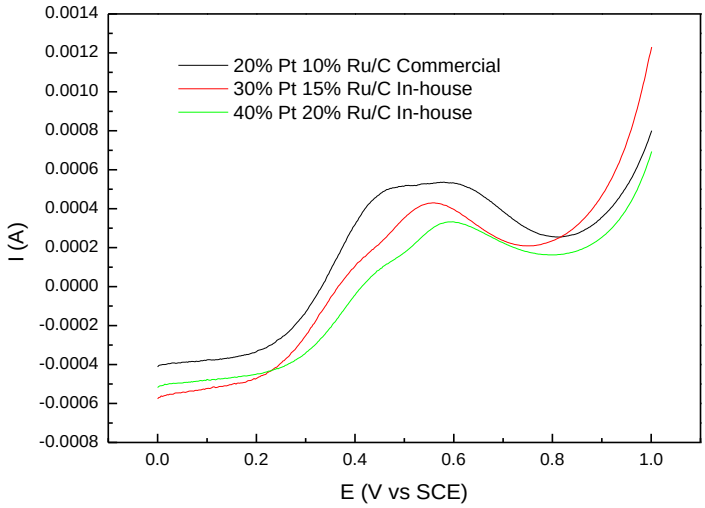

Figure 4.75: Polarization curves for the MOR on 20%Pt10%Ru/C Commercial, 30%Pt15%Ru/C In-house and 40%Pt20%Ru/C In-house electro-catalysts in O_2 saturated 0.5M H_2SO_4 + 0.5M Methanol at a sweep rate of 5mV/s, rotating velocity of 1500rpm, and room temperature

Figure 4.75 shows that 40%Pt20%Ru/C in-house catalyst has a better methanol tolerance. The 20%Pt10%Ru/C commercial catalyst has the highest methanol oxidation peak current than the other catalysts which shows that this catalyst is more active in the presence of methanol, therefore it is not methanol tolerant and not a good cathode catalyst for a direct methanol fuel cell. The methanol tolerant catalysts were found to be 40%Pt20%Ru/C in-house followed by 30%Pt15%Ru/C in-house and then the least methanol tolerant catalyst was found to be 20%Pt10%Ru/C commercial catalyst, the current densities of these catalysts were found to be 0.030A/cm^2, 0.042A/cm^2 and 0.054A/cm^2, respectively (see Table 4.51). The MA of the 20%Pt10%Ru/C commercial, 30%Pt15%Ru/C in-house and 40%Pt20%Ru/C in-house catalysts were found to be 0.216A/g, 0.168A/g and 0.120A/g, respectively and the SA were found to be 0.086A/cm^2, 0.067A/cm^2 and 0.048A/cm^2, respectively.

Table 4.51: Current density, mass activity and specific activity of PtRu/C electro-catalysts as cathode electro-catalysts for a DMFC

Catalysts	**20%Pt10%Ru/C Commercial**	**30%Pt15%Ru/C In-house**	**40%Pt20%Ru/C In-house**
Current density (A/cm^2)	0.054	0.042	0.030
Mass activity (A/g)	0.216	0.168	0.120
Specific activity (A/cm^2)	0.086	0.067	0.048

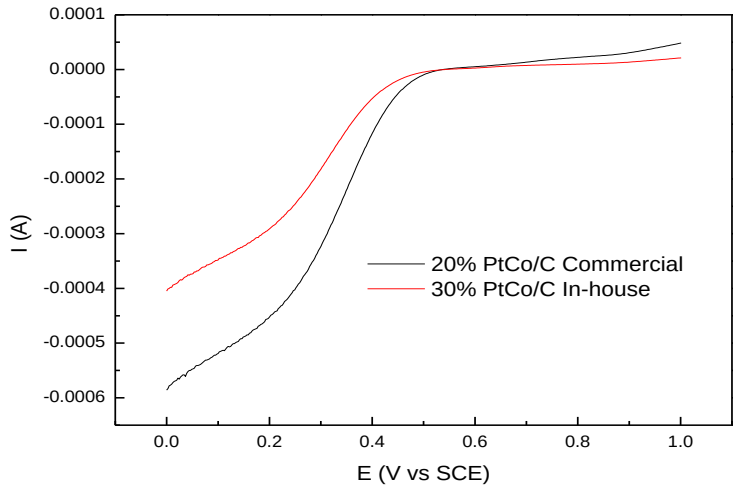

Figure 4.76: Polarization curves for the MOR on 20%PtCo/C Commercial and 30%PtCo/C In-house electro-electro-catalysts electro-catalysts in O_2 saturated 0.5M H_2SO_4 + 0.5M Methanol at a sweep rate of 5mV/s, rotating velocity of 1500rpm, and room temperature

Figure 4.76 reveals the methanol tolerance of PtCo/C catalysts. It is observed that both catalysts that is 20%PtCo/C in-house and 20%PtCo/C commercial are methanol tolerant. The 20%PtCo/C commercial and 30%PtCo/C in-house electro-catalysts have similar polarization curves and no methanol oxidation peaks are observed. The 20%PtCo/C commercial and 30%PtCo/C in-house are therefore inactive in the presence of methanol and are therefore methanol tolerant. The activities of both catalysts are not affected by methanol and are thus good catalysts for ORR. No methanol oxidation peaks were observed (see Table4.52).

Table 4.52: Current density, mass activity and specific activity of PtCo/C electro-catalysts as cathode electro-catalysts for a DMFC

Catalysts	20%PtCo/C Commercial	30%PtCo/C In-house
Current density (A/cm^2)	No MOR peak	No MOR peak
Mass activity (A/g)	No MOR peak	No MOR peak
Specific activity (A/cm^2)	No MOR peak	No MOR peak

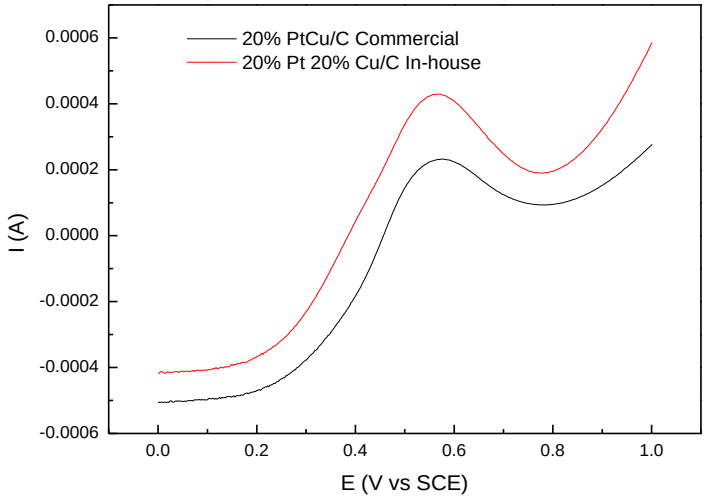

Figure 4.77: Polarization curves for the MOR on 20%PtCu/C Commercial and 20%Pt20%Cu/C In-house electro-catalysts in O_2 saturated 0.5M H_2SO_4 + 0.5M Methanol at a sweep rate of 5mV/s, rotating velocity of 1500rpm, and room temperature

From Figure 4.77 it can be seen that the 20%PtCu/C commercial catalyst is more methanol tolerant than 20%Pt20%Cu/C in-house catalyst. The latter has enhanced methanol oxidation peak than 20%PtCu/C commercial and this shows that the in-house catalyst is more active in the presence of methanol, consequently it is not good for a DMFC cathode catalyst. The current densities of the 20%PtCu/C commercial and the 20%Pt20%Cu/C in-house catalyst were found to be 0.022A/cm^2 and 0.042A/cm^2, respectively (see Table 4.53). The MA of the 20%PtCu/C commercial and 20%Pt20%Cu/C in-house catalysts were found to be 0.088A/g and 0.168A/g, respectively and the SA were found to be 0.037A/cm^2 and 0.069A/cm^2, respectively.

Table 4.53: Current density, mass activity and specific activity of PtCu/C electro-catalysts as cathode electro-catalysts for a DMFC

Catalysts	20%PtCu/C Commercial	20%Pt20%Cu/C In-house
Current density (A/cm^2)	0.022	0.042
Mass activity (A/g)	0.088	0.168
Specific activity (A/cm^2)	0.037	0.069

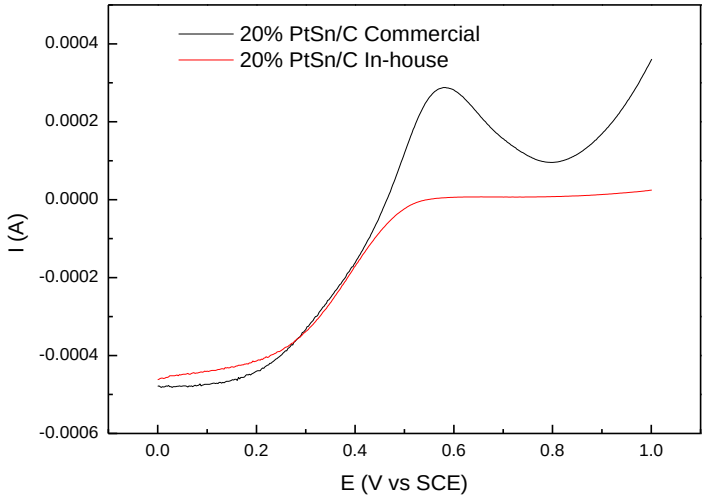

Figure 4.78: Polarization curves for the MOR on 20%PtSn/C Commercial and 20%PtSn/C In-house electro-catalysts in O_2 saturated 0.5M H_2SO_4 + 0.5M Methanol at a sweep rate of 5mV/s, rotating velocity of 1500rpm, and room temperature

Figure 4.78 shows that the 20%PtSn/C commercial has enhanced methanol oxidation peak than 20%PtSn/C in-house which means that it is active in the presence of methanol and is not methanol tolerant. In this case 20%PtSn/C in-house is a good catalyst for ORR because it shows no methanol oxidation peak. It implies that it is inactive in the presence of methanol therefore it is methanol tolerant towards methanol and the ORR activity of this catalyst will not be affected by methanol. The 20%PtSn/C commercial catalyst was found to have a current density of 0.029A/cm^2 and for the in-house catalyst no methanol oxidation peak was observed. The MA of the 20%PtSn/C commercial catalyst was found to be 0.115A/g and the SA was found to be 0.046A/cm^2 (see Table 4.54).

Table 4.54: Current density, mass activity and specific activity of PtSn/C electro-catalysts as cathode electro-catalysts for a DMFC

Catalysts	20%PtSn/C Commercial	20%PtSn/C In-house
Current density (A/cm^2)	0.029	No MOR peak
Mass activity (A/g)	0.115	No MOR peak
Specific activity (A/cm^2)	0.046	No MOR peak

(a) Effect of heat treatment on the ORR activity of the 20%PtCo/C Commercial and 30%PtCo/C In-house electro-catalysts in the presence of methanol

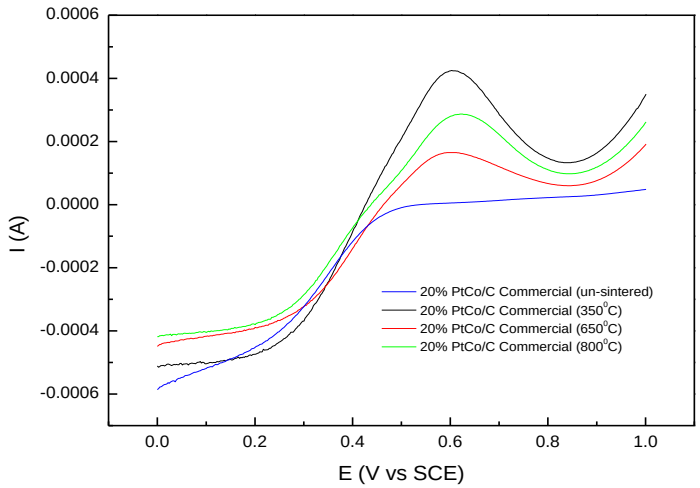

Figure 4.79: Polarization curves for the MOR on 20%PtCo/C Commercial (un-sintered), 20%PtCo/C Commercial (350^0C), 20%PtCo/C Commercial (650^0C), and 20%PtCo/C Commercial (800^0C) electro-catalysts in O_2 saturated 0.5M H_2SO_4 + 0.5M Methanol at a sweep rate of 5mV/s, rotating velocity of 1500rpm, and room temperature

The 20%PtCo/C commercial catalyst depicted in Figure 4.79 was heat treated at different temperatures. For all the temperatures that this catalyst was heat treated it is not methanol tolerant as evidenced by the methanol oxidation peaks observed for this catalyst at different heat treatment temperatures. The current densities for the methanol oxidation peaks observed were found to be 0.042A/cm^2 for 20%PtCo/C commercial (350^0C), 0.017A/cm^2 for 20%PtCo/C commercial (650^0C) and 0.029A/cm^2 for 20%PtCo/C commercial (800^0C). This shows that the 20%PtCo/C commercial (650^0C) is a better methanol tolerant catalyst since it has a low methanol oxidation current density. The 30%PtCo/C commercial (350^0C) has a high methanol oxidation peak and current density, therefore it is not a good cathode catalyst. The MA of the 20%PtCo/C commercial (350^0C), 20%PtCo/C commercial (650^0C), and 20%PtCo/C commercial (800^0C) catalysts were found to be 0.170A/g, 0.067A/g and 0.115A/g, respectively and the SA were found to be 0.068A/cm^2, 0.027A/cm^2 and 0.046A/cm^2, respectively (see Table 4.55).

Table 4.55: Current density, mass activity and specific activity of heat treated PtCo/C commercial electro-catalysts as cathode electro-catalysts for a DMFC

Catalysts	20%PtCo/C Commercial (Un-sintered)	20%PtCo/C Commercial (350^0C)	20%PtCo/C Commercial (650^0C)	20%PtCo/C Commercial (800^0C)
Current density (A/cm^2)	No MOR peak	0.042	0.017	0.029
Mass activity (A/g)	No MOR peak	0.170	0.067	0.115
Specific activity (A/cm^2)	No MOR peak	0.068	0.027	0.046

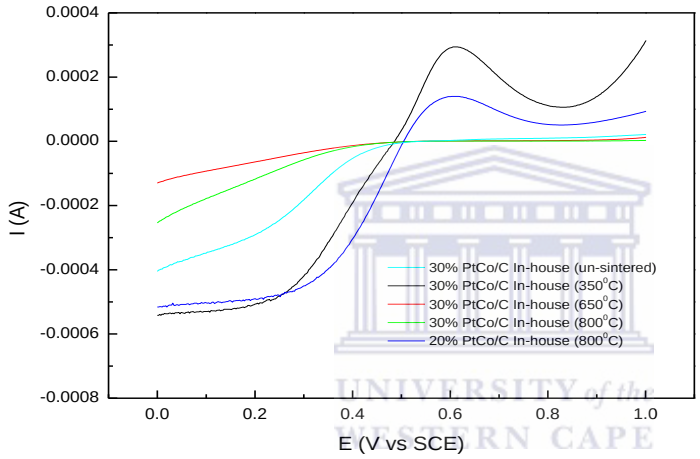

Figure 4.80: Polarization curves for the MOR on 30%PtCo/C In-house (un-sintered), 30%PtCo/C In-house (350^0C), 30%PtCo/C In-house (650^0C), 30%PtCo/C In-house (800^0C) and 20%PtCo/C In-house (800^0C) electro-catalysts in 0.5M H_2SO_4 + 0.5M Methanol at a sweep rate of 5mV/s, rotating velocity of 1500rpm, and room temperature

From Figure 4.80 the 30%PtCo/C in-house (350^0C) catalyst has high methanol oxidation peak followed by the methanol oxidation peak of 20%PtCo/C in-house (800^0C) catalyst. No methanol oxidation peak is observed for the 30%PtCo/C in-house (650^0C) and 30%PtCo/C in-house (800^0C) and this implies that these catalysts heat treated at these temperatures are not affected by methanol in terms of their activity. The current density observed for the 30%PtCo/C in-house (350^0C) catalyst and the 20%PtCo/C in-house (800^0C) catalyst were found to be 0.029A/cm^2 and 0.014A/cm^2, respectively (see Table 4.56). The MA of the 20%PtCo/C in-house (350^0C) and 20%PtCo/C commercial (800^0C) catalysts were found to be 0.116A/g and 0.057A/g, respectively and the SA were found to be0.046A/$cm^2$and 0.023A/cm^2, respectively.

Table 4.56: Current density, mass activity and specific activity of heat treated PtCo/C in-house electro-catalysts as cathode electro-catalysts for a DMFC

Catalysts	30%PtCo/C In-house (Un-sintered)	30%PtCo/C In-house (350^0C)	30%PtCo/C In-house (650^0C)	30%PtCo/C In-house (800^0C)	20%PtCo/C In-house (800^0C)
Current density (A/cm^2)	No MOR peak	0.029	No MOR peak	No MOR peak	0.014
Mass activity (A/g)	No MOR peak	0.116	No MOR peak	No MOR peak	0.057
Specific activity (A/cm^2)	No MOR peak	0.046	No MOR peak	No MOR peak	0.023

4.5.2 Study of anode electro-electro-catalysts

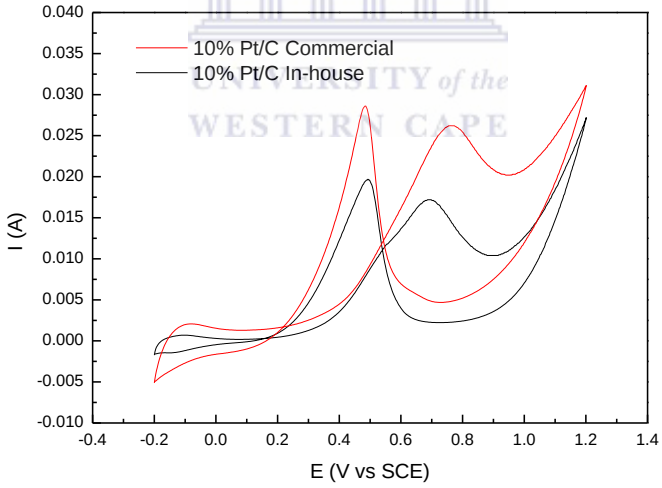

Figure 4.81: Cyclic voltammograms for MOR of 10%Pt/C Commercial and 10%Pt/C In-house electro-catalysts in N_2 saturated 0.5M H_2SO_4 at a scan rate of 20mV

In Figure 4.81 the 10%Pt/C commercial catalyst has a higher methanol oxidation peak compared to the 10%Pt/C in-house. The methanol oxidation peak for 10%Pt/C commercial is higher than that of 10%Pt/C in-house. The methanol oxidation current density of the 10%Pt/C commercial and 10%Pt/C in-house were found to be $2.59A/cm^2$ and $1.69A/cm^2$, respectively. This means that the 10%Pt/C commercial catalyst is a good anode catalyst. The MA of the

10%Pt/C commercial and 10%Pt/C in-house electro-catalysts were found to be 10.4A/g and 6.75A/g, respectively and the SA were found to be 0.042A/cm^2 and 0.027A/cm^2, respectively as shown in Table 4.57.

Table 4.57: Current density, mass activity and specific activity 10%Pt/C electro-catalysts as anode electro-catalysts for a DMFC

Catalysts	10%Pt/C Commercial	10%Pt/C In-house
Current density (A/cm^2)	2.59	1.69
Mass activity (A/g)	10.4	6.75
Specific activity (A/cm^2)	0.042	0.027

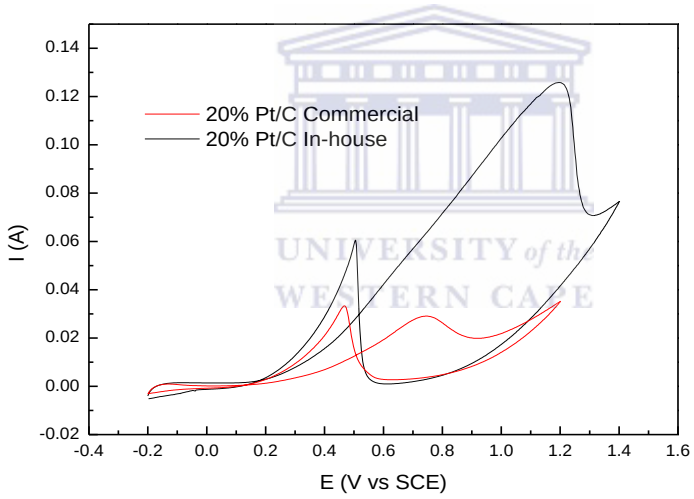

Figure 4.82: Cyclic voltammograms for MOR of 20%Pt/C Commercial and 20%Pt/C In-house electro-catalysts in N_2 saturated 0.5M H_2SO_4 at a scan rate of 20mV

Looking at Figure 4.82, the methanol oxidation peak of 20%Pt/C in-house is higher than that of 20%Pt/C commercial therefore it means that the commercial catalyst is a good anode catalyst for a DMFC. The current densities of the commercial and in-house catalyst were found to be 2.87A/cm^2 and 12.6A/cm^2, respectively (see Table 4.58). The MA of the 20%Pt/C commercial and 20%Pt/C in-house catalysts were found to be 11.5A/g and 50.6A/g, respectively and the SA were found to be 0.202A/cm^2 and 0.046A/cm^2, respectively.

Table 4.58: Current density, mass activity and specific activity 20%Pt/C electro-catalysts as anode electro-catalysts for a DMFC

Catalysts	20%Pt/C Commercial	20%Pt/C In-house
Current density (A/cm^2)	2.87	12.6
Mass activity (A/g)	11.5	50.6
Specific activity (A/cm^2)	0.202	0.046

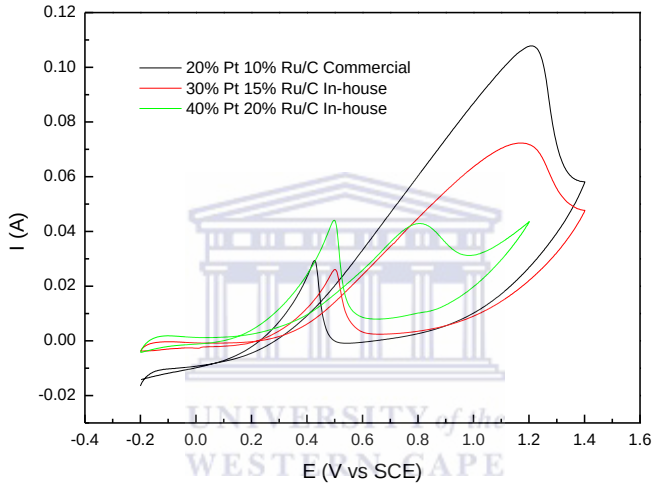

Figure 4.83: Cyclic voltammograms for MOR of 20%Pt10%Ru/C Commercial, 30%Pt15%u/C In-house and 40%Pt20%Ru/C In-house electro-catalysts in N_2 saturated 0.5M H_2SO_4 at a scan rate of 20mV

Figure 4.83 shows that the 20%Pt10%Ru/C commercial catalyst is the most active catalyst in the presence of methanol. The 40%Pt20%Ru/C in-house catalyst gave a lower performance in the presence of methanol. The current densities of these catalysts were found to be 10.6A/cm^2 for 20%Pt10%Ru/C commercial, 7.23A/cm^2 for 30%Pt15%Ru/C in-house and 4.27A/cm^2 for 40%Pt20%Ru/C in-house catalyst as shown in Table 4.59. The MA of the 20%Pt10%Ru/C commercial, 30%Pt15%u/C in-house and 40%Pt20%Ru/C in-house catalysts were found to be 42.4A/g, 28.9A/g and 17.1A/g, respectively and the SA were found to be 0.169A/cm^2, 0.116A/cm^2 and 0.068A/cm^2, respectively.

Table 4.59: Current density, mass activity and specific activity PtRu/C electro-catalysts as anode electro-catalysts for a DMFC

Catalysts	20%Pt10%Ru/C Commercial	30%Pt15%Ru/C In-house	40%Pt20%Ru/C In-house
Current density (A/cm^2)	10.6	7.23	4.27
Mass activity (A/g)	42.4	28.9	17.1
Specific activity (A/cm^2)	0.169	0.116	0.068

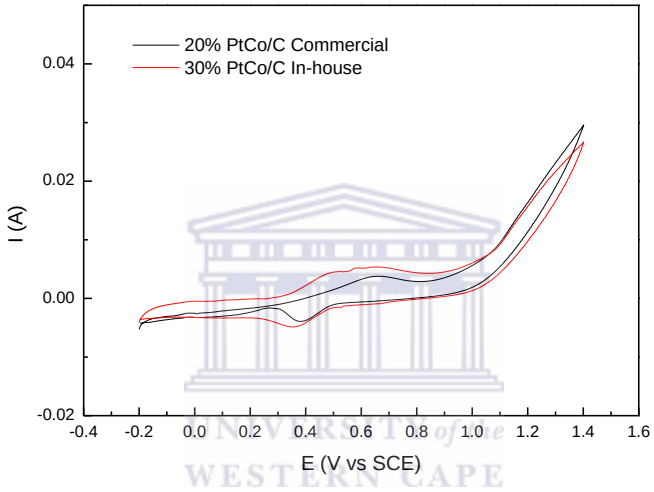

Figure 4.84: Cyclic voltammograms for MOR of 20%PtCo/C Commercial and 30%PtCo/C In-house electro-catalyst in N_2 saturated 0.5M H_2SO_4 at a scan rate of 20mV

The 30%PtCo/C in-house and the 20%PtCo/C commercial catalyst gave the lowest performance in the presence of methanol for (Methanol oxidation reaction) MOR as it can be seen from Figure 4.84 that small methanol oxidation peaks are observed from the CV. The catalysts showed to be inactive in the presence of methanol and as such the catalysts were found not to be good electro-catalysts for MOR. The 30%PtCo/C in-house and the 20%PtCo/C commercial electro-catalysts current densities were found to be 0.66$A/cm^2$and 0.53A/cm^2, respectively (see Table 4.60). The MA of the 20%PtCo/C commercial and 30%PtCo/C in-house electro-catalysts were found to be 0.31A/g and 0.12A/g, respectively and the SA were found to be 0.023 A/cm^2 and 0.008A/cm^2, respectively.

Table 4.60: Current density, mass activity and specific activity PtCo/C catalysts as anode electro-catalysts for a DMFC

Catalysts	20%PtCo/C Commercial	30%PtCo/C In-house
Current density (A/cm^2)	0.66	0.53
Mass activity (A/g)	0.31	0.12
Specific activity (A/cm^2)	0.023	0.008

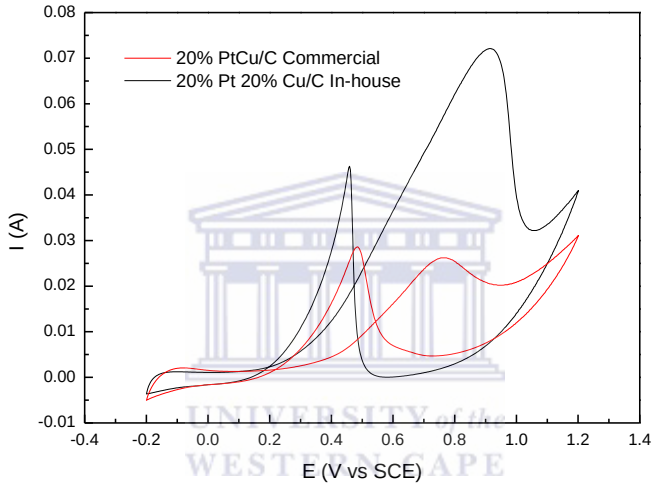

Figure 4.85: Cyclic voltammograms for MOR 20%PtCu/C Commercial and 20%Pt20%Cu/C In-house electro-catalyst in N_2 saturated 0.5M H_2SO_4 at a scan rate of 20mV

In figure 4.85 it can be observed that the 20%PtCu/C commercial gave a lower performance towards MOR in the presence of methanol. Higher methanol oxidation peak was observed for 20%Pt20%Cu/C in-house catalyst and this shows that the catalyst is active towards methanol, therefore it is the best anode catalyst for MOR. The current density of 20%PtCu/C commercial was found to be $2.59A/cm^2$ and that of 20%Pt20%Cu/C in-house was found to be $7.23A/cm^2$. The MA of the 20%PtCu/C commercial and 20%Pt20%Cu/C in-house catalysts were found to be 10.4A/g and 28.9A/g, respectively and the SA were found to be $0.042A/cm^2$ and $0.116A/cm^2$, respectively (see Table 4.61).

Table 4.61: Current density, mass activity and specific activity PtCu/C electro-catalysts as anode electro-catalysts for a DMFC

Catalysts	20%PtCu/C Commercial	20%Pt20%Cu/C In-house
Current density (A/cm^2)	2.59	7.23
Mass activity (A/g)	10.4	28.9
Specific activity (A/cm^2)	0.042	0.116

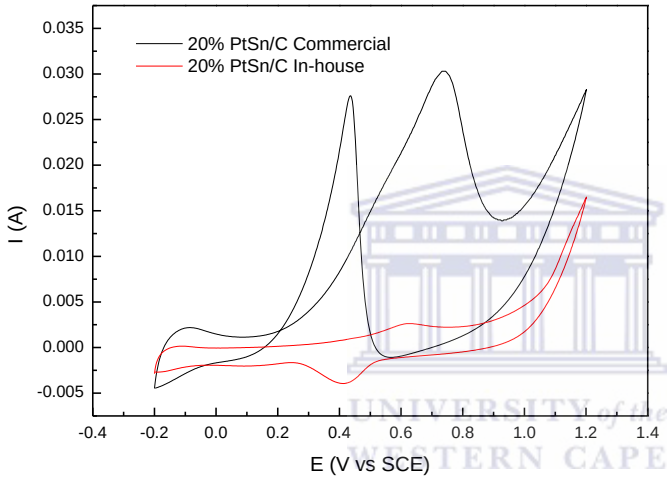

Figure 4.86: Cyclic voltammograms for MOR of 20%PtSn/C Commercial and 20%PtSn/C In-house electro-catalyst in N_2 saturated 0.5M H_2SO_4 at a scan rate of 20mV

Figure 4.86 shows the activity of 20%PtSn/C commercial and 20%PtSn/C in-house towards MOR. It is observed that the 20%PtSn/C commercial catalyst has a higher methanol oxidation current compared to the 20%PtSn/C in-house since it showed small methanol oxidation peak than the 20%PtSn/C commercial catalyst. The current density of the 20%PtSn/C commercial was found to be 3.04A/cm^2 and that of the in-house catalyst was found to be 0.27A/cm^2 as shown in Table 4.62. The MA of the 20%PtSn/C commercial and 20%PtSn/C in-house electro-catalysts were found to be 12.2A/g and 1.06A/g, respectively and the SA were found to be 0.049A/cm^2 and 0.004A/cm^2, respectively.

Table 4.62: Current density, mass activity and specific activity PtSn/C electro-catalysts as anode electro-catalysts for a DMFC

Catalysts	20%PtSn/C Commercial	20%PtSn/C In-house
Current density (A/cm^2)	3.04	0.27
Mass activity (A/g)	12.2	1.06
Specific activity (A/cm^2)	0.049	0.004

(a) Effect of heat treatment on the MOR activity of the 20%PtCo/C Commercial and 30%PtCo/C In-house electro-catalysts

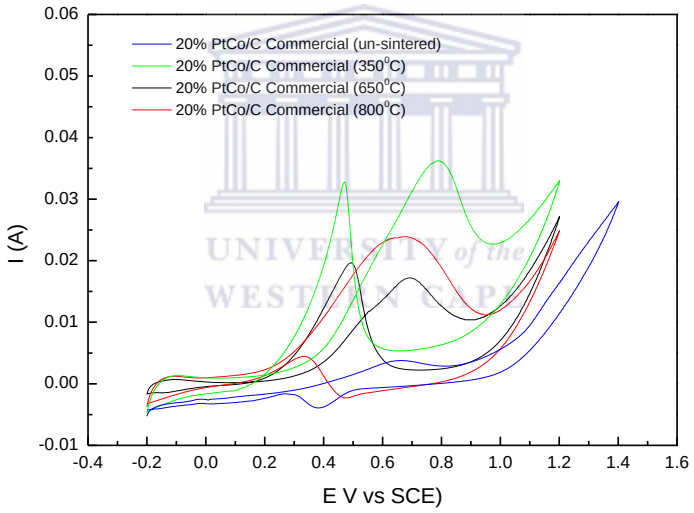

Figure 4.87: Cyclic voltammograms for MOR of 20%PtCo/C Commercial (un-sintered), 20%PtCo/C Commercial (350^0C), 20%PtCo/C Commercial (650^0C), and 20%PtCo/C Commercial (800^0C) electro-catalysts in N_2 saturated 0.5M H_2SO_4 at a scan rate of 20mV

Figure 4.87 reveals that the 20%PtCo/C commercial (350^0C) catalyst has the highest methanol oxidation current. This means that the catalyst heat treated at this temperature is the most active in the presence of methanol with a current density of $5.18A/cm^2$. The 20%PtCo/C commercial (650^0C) and 20%PtCo/C commercial (800^0C) were found to have current densities of $2.38A/cm^2$ and $3.62\ A/cm^2$, respectively (see Table 4.63). The 20%PtCo/C commercial (350^0C) was found to be a better anode catalyst for a DMFC compared to other

heat treated electro-catalysts. The MA of the 20%PtCo/C commercial (350^{0}C), 20%PtCo/C commercial (650^{0}C), and 20%PtCo/C commercial (800^{0}C) electro-catalysts were found to be 20.7A/g, 9.50A/g and 14.5A/g, respectively and the SA were found to be 0.083A/cm2, 0.038A/cm^2 and 0.058A/cm^2, respectively.

Table 4.63: Current density, mass activity and specific activity of heat treated PtCo/C commercial electro-catalysts as anode electro-catalysts for a DMFC

Catalysts	20%PtCo/C Commercial (Un-sintered)	20%PtCo/C Commercial (350^{0}C)	20%PtCo/C Commercial (650^{0}C)	20%PtCo/C Commercial (800^{0}C)
Current density (A/cm^2)	0.66	5.18	2.38	3.62
Mass activity (A/g)	0.31	20.7	9.50	14.5
Specific activity (A/cm^2)	0.023	0.083	0.038	0.058

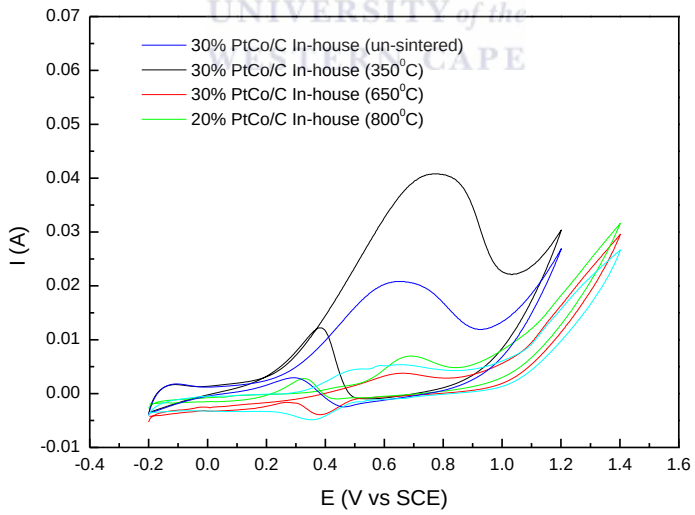

Figure 4.88: Cyclic voltammograms for MOR of 30%PtCo/C In-house (un-sintered), 30%PtCo/C In-house (350^{0}C), 30%PtCo/C In-house (650^{0}C), 30%PtCo/C In-house (800^{0}C) and 20%PtCo/C In-house (800^{0}C) electro-catalysts in N_2 saturated 0.5M H_2SO_4 at a scan rate of 20mV

The 30%PtCo/C in-house (350^0C) catalyst is observed to have higher methanol oxidation current than the 30%PtCo/C in-house (650^0C) and 30%PtCo/C in-house (800^0C) catalysts which implies that these electro-catalysts are not active in the presence of methanol therefore they are not good anode electro-catalysts for a DMFC. The 30%PtCo/C in-house (350^0C) and 20%PtCo/C in-house (800^0C) were found to have current densities of 4.08A/cm^2 and 4.00A/cm^2 and the current densities of the 30%PtCo/C in-house (650^0C), 30%PtCo/C in-house (800^0C) electro-catalysts were found to be 2.04A/cm^2 and 2.87A/cm^2, respectively. The MA of the 30%PtCo/C in-house (350^0C), 30%PtCo/C in-house (650^0C), 30%PtCo/C in-house (800^0C) and 20%PtCo/C in-house (800^0C) catalysts were found to be 16.3A/g, 1.60A/g, 8.16A/g and 11.5A/g, respectively and the SA was found to be 0.065A/cm^2, 0.006A/cm^2,0.033A/cm^{2}and 0.046A/cm^2, respectively as shown in Table 4.64.

Table 4.64: Current density, mass activity and specific activity of heat treated PtCo/C in-house electro-catalysts as anode electro-catalysts for a DMFC

Catalysts	**30%PtCo/C In-house (Un-sintered)**	**30%PtCo/C In-house (350^0C)**	**30%PtCo/C In-house (650^0C)**	**30%PtCo/C In-house (800^0C)**	**20%PtCo/C In-house (800^0C)**
Current density (A/cm^2)	0.53	4.08	2.04	2.87	4.00
Mass activity (A/g)	0.12	16.3	1.60	8.16	11.5
Specific activity (A/cm^2)	0.008	0.065	0.006	0.033	0.046

4.5.3 Summary of the study of DMFC electro-catalysts

From the study of the cathode catalysts of a DMFC above it is observed that the catalysts with higher methanol tolerance were found to be 20%PtCo/C commercial, 30%PtCo/C in-house catalyst and 20%PtSn/C in-house catalysts. They are considered to be good cathode catalysts for a DMFC however, when the 20%PtCo/C commercial catalyst and the 30%PtCo/C in-house catalyst were heat treated it was observed that they are active in the presence of methanol. The 30%PtCo/C in-house catalyst was active in the presence of methanol when it was heat treated at 800^0C and 350^0C. The 20%Pt/C in-house catalyst was

observed to have the highest methanol oxidation current followed by the 20%Pt10%Ru/C commercial catalyst. It was also observed from the study of anode catalysts that the 20%PtCo/C commercial, 30%PtCo/C in-house and 20%PtSn/C in-house electro-catalysts have very small methanol oxidation peak currents compared to 20%Pt/C in-house catalyst which have higher methanol oxidation peak current. The 20%Pt/C in-house was found to be a better anode catalyst.

CHAPTER 5

CONCLUSION

Fuel cells are one of the technologies as energy devices that can meet the energy demand facing the world because of several advantages that they possess. For example they are environmentally friendly but their use is hindered by the disadvantages that are encountered in the course of their operation such as; (1) the slow kinetics of the oxygen reduction reaction occurring at the cathode, (2) the effect of the methanol crossover from the anode to the cathode of a direct methanol fuel cell which interferes with the activity of the cathode catalyst, and (3) the poisoning of the anode catalyst by the carbon monoxide a by-product of the methanol oxidation which affects the methanol oxidation reaction activity of the anode catalyst.

This study was based on finding the best cathode catalyst for a PEMFC and DMFC, methanol tolerant cathode catalyst for a DMFC and best anode catalysts for a DMFC by determining the electro-catalytic activities using the cyclic voltammetry technique and rotating disk electrode. From the CV analysis (section 4.3) the 20%Pt/C in-house catalyst was found to be the best cathode catalyst as it showed higher ORR activities compared to the other electro-catalysts. The ORR study using the RDE (section 4.4) technique also showed that the 20%Pt/C in-house catalyst is the best cathode catalyst for ORR due to its current density and this is in good agreement with the cyclic voltammetry study that found this catalyst to be the best cathode catalyst. In the methanol oxidation studies, study of anode electro-catalysts (Section 4.5.2), 20%Pt/C In-house was observed to be a better anode catalyst for a DMFC as it gave the highest methanol oxidation current peak followed by the 20%Pt10%Ru/C commercial. From the study of cathode electro-catalysts (section 4.5.1) for a DMFC it was observed that the 20%PtCo/C commercial, 30%PtCo/C in-house and 20%PtSn/C in-house electro-catalysts showed no methanol oxidation peaks meaning that these electro-catalysts are the best cathode electro-catalysts for a DMC. The 20%Pt/C in-house was observed not be a good cathode catalyst since the methanol oxidation peak current density was high as well as the methanol oxidation peak current for the 20%Pt10%Ru/C commercial catalyst was also high. The Pt/C catalysts having higher activity than Pt binary catalysts could be attributed to the preparation method of the binary catalysts as they did not give better activity compared to the Pt/C catalysts.

The effect of heat treatment on the activity and morphology of the 20%PtCo/C commercial and 30%PtCo/C in-house catalyst was studied. It was found that the ORR activity increased after heat treatment for the 20%PtCo/C commercial catalyst using both the rotating disk electrode and cyclic voltammetry techniques. The ORR activity for the 30%PtCo/C in-house catalyst activity increased when the catalyst was heat treated at 350^0C and was better than the un-sintered 20%PtCo/C commercial and 30%PtCo/C in-house catalysts. The XRD and HRTEM analysis showed that the particle size increased as the heat treatment increased for the 20%PtCo/C commercial. It also increased for the 30%PtCo/C in-house catalyst but decreased when the catalyst was heat treated at 350^0C.

The 20%PtCo/C commercial after heat treatment was observed not to be a good cathode catalyst for a DMFC but a good anode catalyst for a DMFC after heat treatment as it gave higher MOR peaks compared to the un-sintered 20%PtCo/C commercial catalyst. When the 30%PtCo/C in-house catalyst was heat treated at 650^0C and 800^0C it was observed to be a good cathode catalyst as no MOR peaks were observed and when heat treated at 350^0C MOR peaks were observed therefore it was considered to be a better anode catalyst.

Although the 20%Pt/C in-house was found to be the most active catalyst for ORR it is not methanol tolerant and so cannot be used as a cathode catalyst for a DMFC. The 20%PtCo/C commercial (with specific activity of 0.036A/cm^2 towards ORR) showed that it could be a better cathode electro-catalysts as the activity was about half that of the 20%Pt/C (with a specific activity of 0.085A/cm^2 towards ORR) in-house and the use of the 20%PtCo/C commercial catalyst would be advantageous as it contains a second metal reducing the amount of Pt which is expensive that is used for the electro-catalysts. The 20%Pt/C in-house catalyst (with specific activity of 0.202A/cm^2 towards MOR) was observed to be the best anode catalyst for a DMFC but the 20%Pt10%Ru/C (with specific activity of 0.169A/cm^2 towards MOR) could be used as the anode catalyst as it showed higher methanol oxidation current not much different from that obtained for the 20%Pt/C in-house and also this would reduce the amount of the metal that is used due to the second metal that is used. This would lead to less loss of fuel cell efficiency and also cut the cost of fuel cells due to less Pt used of the catalyst (Pt-M) and lower the cost. From the physical characterization it was observed that XRD data for particle size determination was in good agreement with the HRTEM results with particle size ranging from 2.72nm and 4.18nm.

REFERENCES

1) Natural gas and technology, *Natural.org. (2004-2011)* www.naturalgas.org/environment/technology.asp

2) Advantages and benefits of hydrogen and fuel cell technologies, *Fuel cell Markets.* (2002-2012) www.fuelcellmarkets.com/fuel_cell_markets/5,1,1,663.html

3) C. Rayment and S. Sherwin, *Introduction to fuel cell technology*, Department of aerospace and mechanical engineering University of Norte Dame, Notre Dame, IN 46556, USA. (2003): p.12-13

4) N.M. Markovic and P.N. Ross, , *Surf Sci Rep*. **45**, (2002): p.117-229

5) R.S. Khurmi and R.S. sedha, *Material Science*, Ed. 4, ISBN 8121901464. (2008): p. 18

6) W.R. Grove, On a gaseous voltaic battery, *Philosophical magazine and journal of science*. **101**, (1842): p.417-420

7) A.B. Stambouli and E. Traversa, *Renewable and sustainable energy reviews*. **6**, (2002): p.433-455

8) N.P. Brandon, P. Aguiar and C.S. Adjiman, *Journal of power sources*. **147**, (1-2) (2005): p.136-147

9) S.C. Singhal, *Solid State Ionics*. **135**, (2000): p.305-313

10) International energy agency, *Hydrogen and fuel cells-Review of national R&D programs*. (2004): p.25

11) B. Sorensen, *Hydrogen and fuel cells*. (2005): p.64

12) R. L. Busby, *Hydrogen and fuel cells-A comprehensive guide*. (2005): p.100

13) S. Basu, *Recent trends in fuel cell science and technology*, ISBN 1441922563. (2010): p. 60

14) J.E. Larminie and A. Dicks, *Fuel Cell Systems Explained.* (2000)

15) F. Maillard, G. Lu, A. Wieckowski and U. Stimming, *Journal of Physical Chemsitry*. **B 109**, (2005): p.16230-16243

16) Acres, G.J.K.et.al, *Catal today.* **38**, (1997): p.393

17) M Cell, *MCEL.Technology/Technology advantages.* (2005)

18) Mobiletrax, *Fuel cells: The Nirvana of portable systems*. (2003)

19) Johnsson-Matthey, *ETSU Direct Methanol Fuel Cell Review*, Tech. rep.UK Department of Trade & Industry. (1995)

20) K. Ley, R. Liu, C. Pu, Q. Fan, N. Leyarovska, C. Segre and E. Smotkin,Electrochim. *Acta.* **144**, (1997): p.1543-1548

21) D. Lee, S. Hwang and I. Lee, , *Journal of Power Sources*. **145**, (2005): p.147-153

22) A. Hamnett, B.J. Kennedy, and S.A. Weeks, Base metal oxides as promotors for the electrochemical oxidation of methanol, *J. Electroanal. Chem*. **240**, (1988): p.349-353

23) N. Munichandraiah, K. McGrath, G.K. Prakash, S. Aniszfeld, R. George and A. Olah, *Journal of Power Sources.***117**, (2003):p.98–101

24) E.V. Anslyn and D.A. Dougherty, *Modern Physical organic chemistry*. **490**, (2006)

25) A. Fullick and P. Fullick. *Chemistry for AQA.*(2001), ISBN 0 435 583913, p.9.3

26) M. Wilson and S. Gottesfeld, Thin-film catalyst layers for polymer electrolyte fuel cell electrodes. *J. Appl. Electrochem*. **22**, (1992): p.7

27) Y. Takasu, T. Fujiwara and Y. Murakami, *J. Electrochem*. Soc. **147**, (2000): p.4421

28) A.J. Dickinson, L.P.L. Carrette, J.A. Collins, K.A. Friedrich andU. Stimming, *Electrochim.Acta*. **47**, (2002): p.3733

29) K.A. Friedrich, K.P. Geyzers, A.J. Dickinson andU. Stimming, *J. Electroanal. Chem*. **261**, (2002): p.524–525

30) K. Machida, A. Fukuoka, M. Ichikawa and M. Enyio, *J. electrochem. Soc*.**138**, (1991): p.1958

31) A.J. DukinsonJ, L.P.L. Carrette, J.A. Collins, K.A. Friedrich and U Stimming, *Electrochem.Acta*. **47**, (2002): p.3733

32) N. Alonso-Vanta, *Fuel cells*. **6**, (2006): p.182

33) T. Teranishi, M. Hosoe, T. Tanaka and M. Mayaka, *J. Phys. Chem*. **B103**, (1999): p.3818

34) L.M. Bronstein, *Top Curr. Chem*. **226**, (2003): p.55

35) H. Bonnemann and R.M.R. Eur, J. *Inorg. Chem*. **10**, (2001): p.2455

36) A. Roucoux, J. Schulz andH. *Patin, Chem. Rev*. **102**, (2002):p.3757

37) L. Xiong andA. Menthiram, *Solid state Ionics*. **176**, (2005): p.385

38) D.R.M. Godoi, J. Perez and H.M. Villullas, *J. Electrochem. Soc*. **B474**, (2007): p.154

39) H. Liu, C. Song, L. Zhang, J. Zhang, H. Wang andD. Wilkinson.et. al, *J. Power sources*.**155**, (2006): p.95

40) S. Griksson, U. Nylen, S. Rojas and M. Boutonnet, *Appl. Catal.* **A207**, (2004): p.265

41) Y. Gong, (2008): p.17-20

42) A. Appleby and F. Foulkes, *Fuel cell handbook,* Van Nostrand Reinhold, New York, USA. (1989): p.762

43) J. Zhang, *PEM fuel cell electro-catalysts and catalyst layers-Fundamentals and applications*. (2008): p.50

44) K. Kinoshita, *Electrochemical oxygen technology*. John Wiley& sons. 1992

45) Y. Ernest, *Journal of molecular catalysis*. **38**, (1986): p.5-25

46) R. Adzic, "Recent advances in the kinetics of oxygen reduction, "electrocatalysis. *Wiley-VCH*., (1998)

47) S. Gottesfeld, T.A. Zawodzinski, R.C. Alkire, H. Gerischer, D.M. Kolb and C.W. Tobias, Polymer electrolyte fuel cells. In advances in electrochemical Science and Engineering, vol. 5, 1st ed., *Wiley-VCH*, Weinheim. (1997): p.195

48) T. Gale, *Chemistry foundation and applications*, Lagowski, J.J., ed. ISBN 0-02-865724-1, (2004): p.267-268.

49) M. Schwarts, *CRC press encyclopedia of materials and finishes*, 2nd edition.(2002)

50) M. Hill, J. Vaccari, *Materials handbook*. Fifteenth edition.(2002)

51) I. Lide andR. David, *CRC Handbook of chemistry and physics*, 4 New York: CRC Press. CRC contributors. ISBN 978-0-8493-0488-0, (2007-2008): p. 26.

52) C. Bruce, D. Anderson and S. David, International, A.S.M. "Platinum", *Handbook of corrosion data*. ISBN 978-0-87170-518-1, (1995-01): p.8-9

53) R.H. Petrucci, *General chemistry: Principles & modern applications*, Prentice Hall. ISBN 0-13-149330-2, (2007): p. 606.

54) C. He, S. Desai, G. Brown and S. Bollepalli, PEM fuel cell electro-catalysts: Cost, performance, and durability, *The electrochemical society Interface*. (2005): p.41-44

55) I.E. Santiago, C.L. Varanda, and H. Mercedes Villullas, *J. Phys. Chem*. **C 111**, (2007): p.3146-3151

56) R.C. Koffi, C. Coutanceau , E. Garnier, J.-M. L´eger and C. Lamy1**,** *Electrochimica Acta* **50**, (2005): p.4117–4127

57) S. Thanasilp, M.Hunsom, S. Thanasilp and M. Hunsom, *Renewable Energy.* **36**, (2011): p.1795-1801

58) S. Siracusanoa, A. Stassi, V. Baglioa, A.S. Aricòa, F. Capitaniob and A.C. Tavares, *Electrochimica Acta.* **54**, (2009): p.4844–4850

59) M. Nie, P.K. Shen, M. Wu, Z. Wei and H. Meng, *Journal of Power Sources*. **162**, (2006):p.173–176

60) W. Li, Q. Xin and Y. Yan, *International journal of hydrogen energy*. **35**, (2010): p.2530-2538

61) W.M. Martínez, T. T. Thompson and A.M. Smit, *Int. J. Electrochem. Sci*. **5**, (2010)

62) Q. He, S. Mukerjee, Q. He and S. Mukerjee, *Electrochimica Acta* **55**, (2010): p.1709–1719

63) Yan Zhuo, T.L.U. Hong, C. Peng and Y.W. Wei, *Chinese Chemical Letters.* **16**, 9, (2005): p.1252-1254

64) A.K. Shukla, R.K. Raman, N.A. Choudhury, K.R. Priolkar, P.R. Sarode, S. Emura and R. Kumashiro, *Journal of Electroanalytical Chemistry*. **563**, (2004): p.181–190

65) K. Park, D. Hanb and Y. Sung, *Journal of Power Sources*. **163**, (2006): p.82–86

66) G. Selvarani, S. Vinod Selvaganesh, S. Krishnamurthy, G. V. M. Kiruthika, P. Sridhar, S. Pitchumani, and A. K. Shukla, *DFT.J. Phys. Chem*. **C 113**, (2009): p.17

67) H. Meng and P.K. Shen, *Chem. Commun*. (2005): p.4408–4410

68) J. Yang, W. Zhou, C.H. Cheng, J.Y. Lee and Z. Liu, *Applied material and interfaces*. **2**, 1, (2010): p.119–126

69) A. M. Remona1 and K. L.N, Phani, *Fuel cells*. **11**, (2011): p.385–393

70) K.S. Han, Y.S. Moon, O.H. Han, K.J. Hwang, I. Kim and H. Kim, *Electrochem. Commun*. **9**, (2007): p.317–324

71) H. Wang, H. Li, X. Yan, *PEM fuel cell failure made analysis.* (2012): p.53

72) S. Ang, A.D. Walsh, *Applied Catalysis B: Environmental*.**98**, (2010): p.49–56

73) C. Jeyabharathia, P. Venkateshkuma, J. Mathiyarasua and K.L.N. Phani, *Electrochimica Acta* **54**, (2008):p.448–454

74) J. Kim, A. Ishihara, S. Mitsushima, N. Kamiya, K.I. Ota, *Electrochimica Acta*. **52**, (2007): p.2492–2497

75) S. Li, L. Zhanga, J. Kima, M. Panb, Z. Shia, J. Zhanga, *Electrochimica Acta*. **55**, (2010): p.7346–7353

76) W.B.C. Bezerraa, L. Zhanga, K. Lee, H. Liu, J. Zhang, Z. Shi, L.B. Aldale, M. Edmar, P. Marques, S. Zhang, *Electrochimica Acta*. **53**, (2008): p.7703–7710

77) I. Do, (2006): p.21-24

78) K. Kinoshita, J. *Electrochem. Soc*. **137**, (1990): p.845

79) S. Mukerjee, *J. Appl. Electrochem*. **20**; (1990): p.537

80) A. Kabbabi, F. Gloaguen, F. Andolfatto and R. Durand, J. *Electroanal. Chem*. **373**, (1994):p.251

81) T. Frelink, W. Visscher, J.A.R. van Veen, *J. Electroanal. Chem*. **382**, (1995): p.65

82) A. Gamez, D. Richard, P. Gallezot, F. Gloaguen, R. Faure and R.Durand, *Electrochim. Acta* **41**, (1996): p.307

83) L. Genies, R. Faure and R. Durand, *Electrochim. Acta*. **44**, (1998): p.1317

84) S. Mukerjee and J. McBreen, *J. Electroanal. Chem*. **448**, (1998): p.163

85) S.L. Gojkovic and T.R. Vidakovic, *Electrochim. Acta*. **47**, (2001): p.633

86) T. Frelink, W. Visscher and J.A.R. van Veen, *J. Electroanal. Chem*. **382**, (1995): p.65

87) F. Gloaguen, J.-M. Leger and C. Lamy, *J. Appl. Electrochem*. **27**, (1997): p.1052

88) F. Maillard, M. Martin, F. Gloaguen and J.-M.Le´ger, *Electrochimica Acta*. **47**, (2002): p.3431-3440

89) A.N. Frumkin, O.A. Petrii, B.B. Damaskin, J.O.M. Bockris, B.E. Conway and E.B. Yeager, *Plenum Press*, New York. **1**, (1980): p. 221

90) K. Kinoshita, *J. Electrochem. Soc*. **137**, (1990): p.845-848

91) M. Min, J. Cho, K. Cho, H. Kim, *Electrochimica Acta*. **45**, (2000): p.4211–4217

92) Y.Y. Shao,J. Liu, Y. Wang, Y.H. Lin, *J. Mater Chem*. **19**, (2009): p.46-59

93) S. Wang, Nanostructured electro-catalysts for proton exchange membrane fuel cells (PEMFC), Phd thesis, Nanyang Technological University, Singapore. (2010)

94) Y. Takasu, T. Kawaguchi, W. Sugimito, Y. Murakami, *Electrochim. Acta*. **48**, (2003): p.3861

95) A.S. Arico, S. Srinivasan and V. Antonucci, *Fuel cells*. **2**, (2001): p.133

96) A. Arico, S. Srinivasan, V. Antonucci , *Fuel cells*. **2**, (2001): p.1

97) M.K. Ravikumar, and A.K. Shukla, *J. Electrochem. Soc*. **143**, (1996): p.2601

98) G. Wu, L. Li, J.H. Li, B.Q. Xu, Carbon. **43**, (2005): p.2579

99) M. Uchida, Y. Fukuoka, Y. Sugawara, H. Ohara, A. Ohta, *J. Electrochem. Soc*. **145**, (1998): p.3708

100) M.L. Anderson, R.M. Stroud, D.R. Rolison, *Nano Lett*. **2**, (2002): p.235

101) M. Mastragostino, A. Mossiroli, F. Soavi, *J. Electrochem. Soc*. **151**, (2004): p.1919

102) Y.H. Pai, J.H. Ke, C.C. Chou, J.J. Lin,J.M. Zen, F.S. Shieu, *J. Power source*

103) P. Stonehardt, B. Bunsen-Ges, *Phys Chem*. **94**, (1990):913

104) P. Sotelo-Mazón, R.G. González-Huerta, J. G. Cabañas-Moreno and O. Solorza-Feria, *Int. J. Electrochem. Sci*.**2**, (2007): p.523 - 533

105) A.J. Bard, L.R. Faulkner, Electrochemical methods: fundamentals and applications. New York: Wiley, (1980).

106) D. Andrienko, *Cyclic Voltammetry*. (2008): p.11

107) J. L. Fernandez, D. A. Walsh and A. J. Bard, *J. Am. Chem. Soc*.**127**, (2005):p.358.

108) S. Fukuzumi, K. Okamoto, C. P. Gros and R. Guilard, *J. Am. Chem. Soc*, **126**, (2004): p.10441.

109) T. A. Nissinen, Y. Kiros, M. Gasik and M. Leskela, *Chem. Mater*. **15**, (2003): p.4974.

110) F. Jaouen, S.Marcotte, J. P. Dodelet and G. Lindbergh, *J. Phys. Chem*. **B 107**, (2003): p.1376.

111) S. Srinivasan, Fuel cells: *Fundamentals to applicatios.* p. 299

112) W.B. Cicero, B.L. Zhanga, K. Leea, H. Liua, J. Zhanga, Z. Shi, A.L.B. Marques , E.P. Marques , S. Wua, J. Zhanga, *Electrochimica Acta*. **53**, (2008): p.7703–7710

113) A.J. Bard, L. Faulkner, *Electrochemical methods. 2nd ed*. NJ: Wiley & Sons. (2001): p.331.

114) C. Couteanceau, P. Crouigneau, J.M. Le´ger, C. Lamy, *J Electroanal Chem*. **379**, (1994): p.389-97.

115) A.J. Bard, L.R. Faulkner, Electrochemical methods: *fundamentals and applications*. 2nd ed. New York: John Willey & Sons. (2001) [chapters 3 and 9]

116) G. Selvarani, S. Vinod Selvaganesh, S. Krishnamurthy, G. V. M. Kiruthika, P. Sridhar, S. Pitchumani, and A. K. Shukla, *DFT.J. Phys. Chem*. **113**, (2009): p.7461–7468

117) H. Schulenburg, E. Müller, G. Khelashvili, T. Roser, H. Bünnemann, A. Wokaun and G.G. Scherer, *J. Phys. Chem.* ***C*****113**, (2009): p. 4069-4077.

118) J. Perez, E.R. Gonzalez and E.A. Ticianelli, *Electrochimica Acta*. **44**, (1998): p.1329±1339

119) M. Ciureanu, H. Wang, *J. Electrochem*. Soc. **146**, (1999) p.4031

120) K. Senevirathne, *Electrochemica Acta*, **59**, (2012): p.538-540

121) T. Matsui, K. Fujiwara, T. Okanishi, R. Kikuchi and T. Fakeguchi, K. Eguchi , *Journal of Power sources*, **155**, (2006): p.152-156

122) S.E. Guterman, S.V. Belenov, T.A. Lastovina, E.P. Fokina, N.V. Prutsakova, Ya. B. Konstonti, *Russian Journal of electrochemistry,* **47**, (2011) 8

123) J. Zhang, *PEM fuel cell electrocatalysts and catalyst layers Fundamentals and applications*, **XXII**, (2008): p.1137, 489 illus., ISBN 978-1-8400-935-6

124) Q. He, S. Mukerjeem, *Electrochimica Acta*, **55**: (2010) p.1709–1719